A DISSERTATION
FOR THE DEGREE OF DOCTOR OF PHILOSOPHY

The influence of photic stimuli on regulation of neuroendocrine-reproductive system in eel, *Anguilla japonica*

Ji-Yeon Hyeon

Department of Biology
GRADUATE SCHOOL
JEJU NATIONAL UNIVERSITY

August, 2022

뱀장어의 신경내분비-생식계 조절에 대한 광 신호의 영향

지도교수 김 세 재

현 지 연

이 논문을 이학 박사학위 논문으로 제출함

2022년 8월

현지연의 이학 박사학위 논문을 인준함

심사위원장 허 성표

위 원 송 우람

위 원 김 종 덕

위 원 김 진 형

위 원 김 세 재

제주대학교 대학원

2022년 8월

The influence of photic stimuli on regulation of neuroendocrine-reproductive system in eel, *Anguilla japonica*

Ji-Yeon Hyeon

(Supervised by professor Se-Jae Kim)

A thesis submitted in partial fulfillment of the requirement for the degree of Doctor of Philosophy

August, 2022

This thesis has been examined and approved.

Hur, Sung-Pyo

Thesis director, Sung-Pyo Hur, Prof. of Ocean Science

Uh-Ram Song, Prof. of Biology

Jong-Myoung Kim, Prof. of Fisheries Biology

Jin-Hyoung Kim, Prof. of Polar Science

Se Jae Kim

Se-Jae Kim, Prof. of Biology

August, 2022
Date

Department of Biology
GRADUATE SCHOOL
JEJU NATIONAL UNIVERSITY

Table of Contents

Contents **page**

국문 요약

어류의 생체 리듬은 광주기, 달주기와 같은 광 조건에 의해 조절된다. 어류는 생체 리듬을 조절하는 환경 요인을 감지하고 이로 인해 자극 받은 내분비 시스템의 작용으로 종 특이적인 번식 생리 및 행동을 갖는다. 뱀장어는 야행성이며 강하성 어종으로 일반적인 주행성 어류와 다른 생체 리듬을 갖는 것으로 추측된다. 이 연구는 야행성 뱀장어의 종 특이적인 산란 생태에 따른 광전달 인식 기전 및 생체시계 발현 패턴을 통해 뱀장어의 산란생태와의 연관성을 조사하였다.

1. 뱀장어(*Anguilla japonica*) 수컷의 성 성숙도에 따른 opsin family의 유전자 발현 패턴 비교

이 연구는 RNA-Seq transcriptome 방법으로 극동산 뱀장어의 망막과 전뇌에 존재하는 새로운 type의 opsin subfamily를 동정하고 생리적 기능을 추측하고자 하였다. RNA-seq을 통해 총 18 종의 opsin subfamily가 동정되었다. 시각 opsin family는 Rh2, SWS2, FWO, DSO, Exo-Rhod를 포함하며 비시각 opsin family는 4종의 melanopsin subfamily (Opn4x1, Opn4x2, Opn4m1, Opn4m2), peropsin, 2종의 neuropsin subfamily (Opn5-like, Opn5), Opn3, 3종의 TMT subfamily(TMT1, 2, 3), VA-opsin, parapinopsin이 확인되었다. 뱀장어의 망막에서 성 성숙도에 따른 광수용체 유전자 발현 변화를 관찰한 결과, 성숙한 뱀장어에서 DSO mRNA 발현이 증가하였다. 뇌에서 광수용체 유전자 발현은 시각 opsin인 DSO와 SWS2 mRNA 발현이 성숙한 뱀장어에서 증가하였다. 비시각 opsin에서는 fore-brain에서 parapinopsin mRNA 발현이 성숙한 뱀장어에서 증가한 반면에 TMT2 mRNA 발현은 감소하였다. 성숙한 뱀장어에서는 미성숙한 뱀장어보다 mid-brain에서 parapinopsin mRNA, hind-brain에서 TMT1, TMT3 mRNA 발현이 증가하였다. 미성숙한 뱀장어보다 성숙한 뱀장어의 망막에서 DSO mRNA, 모든 부위의 뇌에서 DSO, SWS2 mRNA 발현이 증가한 것으로 보아 DSO와 SWS2가 뱀장어 성 성숙에 밀접한 관련이 있을 것으로 추정된다.

2. 광 신호에 따른 멜라토닌 분비 변화가 뱀장어(*Anguilla japonica*)의 정소 발달에 미치는 영향

멜라토닌은 생체 리듬을 조절하는 인돌아민호르몬으로 야간에 분비되며 주로 송과체와 망막에서 합성되고 분비된다. 이 연구는 뱀장어 수컷의 정소가 발달하는 동안 멜라토닌 분비 변화가 광 신호를 전달하는 역할을 하는지 조사하였다. 뱀장어의 눈과 혈중 멜라토닌 분비 변화는 일주기[12시간 명기:12시간 암기(12L12D), 24시간 명기(LL), 24시간 암기(DD)], 광주기[장주기(15L9D), 단주기(9L15D)], 달주기[new moon (NM), full moon (FM)]와 같은 여러 조건에서 조사하였다. 눈과 혈중 멜라토닌 농도는 12L12D와 DD 조건에서 야간에 증가하는 양상을 보였으나 LL 조건에서는 멜라토닌이 증가하는 양상을 보이지 않았다. 단주기 조건에서 눈 멜라토닌 분비는 12L12D 패턴과 유사하였다. 혈장 멜라토닌 레벨이 장주기 조건에서 주야간 리듬이 없는 반면 단주기 조건에서는 야간에 멜라토닌 분비가 증가하였다. human chorionic gonadotropin (hCG)을 1주일 간격으로 총 8회 복강 주사하여 성 성숙을 유도한 뱀장어의 눈과 혈중 멜라토닌 농도는 FM에 노출된 뱀장어보다 NM에 노출된 뱀장어에서 유의하게 높았다. 이 결과를 통해 뱀장어의 눈과 혈장 멜라토닌 분비는 반복적인 일광 리듬에 의해 조절되며 성 성숙한 뱀장어는 야간의 월광에 의해 멜라토닌 분비가 억제되는 것을 확인하였다. 뱀장어에 있어 일광과 월광의 광 조건은 정소 발달과 산란을 포함한 야간 행동 반응과 상관 관계가 있을 수 있음을 시사한다.

3. 광 신호에 따른 뱀장어(*Anguilla japonica*) 망막과 뇌에서 시계유전자 발현 특성

이 연구는 RNA-Seq transcriptome 방법으로 뱀장어의 망막과 전뇌에 존재하는 per(period)와 cry(cryptochrome)를 동정하고 생리적 기능을 추측하고자 하였다. RNA-seq을 통해 per와 cry 각각 3 종이 동정되었다. per는 per1, 2, 3, cry는 cry2, 3, 4가 확인되었다. 뱀장어의 망막과 뇌에서 각 시계유전자의 리듬을 관찰하기 위해 일주기(LD; 12L(light)12D(dark), DD; 암기, LL; 명기), 광주기(SP; 단주기 (9L15D), 장주기(LP; 15L9D)), 달주기(NM; 삭, FM; 보름) 조건에서 실험을 수행하였다. 일주기 조건에서는 망막에서 per1, 2, cry3, 4의 mRNA 발현 리듬이 LD와 DD 조건에서 비슷한 패턴을 보였다. 광주기 실험에서는 망막에서 per1, 2, cry3, 4의 mRNA 발현 리듬이 SP 조건에서 LD와 DD 조건과 유사한 패턴을 보였다. 달주기 조건에서 NM 조건에서의 망막 per1, 2, cry3, 4의 mRNA 발현 리듬이 LD, SP 조건과 비슷한 패턴을 관찰하였다. 이러한 결과를 종합해보면 뱀장어의 망막이 생체리듬을 조절하는 핵심기관 역할을 하는 것을 시사하고 달빛에 의한 시계유전자들의 동기화에 의해 회유를 개시할 것으로 추측할 수 있다. 더 나아가 자기장 수용체 기능을 하는 cry4가 달빛에 의해 발현 패턴이 달라지는 것으로 보아 뱀장어의 회유와 밀접한 관계가 있음을 시사한다.

Author's publication List

1. Hyeon JY, Hur SP, Kim BH, Byun JH, Kim ES, Lim BS, Lee BI, Takemura A, Kim SJ. 2019. Involvement of estrogen and its receptors in morphological changes in the eyes of the Japanese eel, *Anguilla japonica*, in the process of artificially-induced maturation. Cells. 8:310. DOI 10.3390/cells8040310.
2. Byun JH, Hyeon JY, Kim ES, Kim SK, Hur SP, Kim SJ, Takemura A. 2020. Daily variation of D2 dopamine receptor transcription in the brain of the Japanese eel *Anguilla japonica* and its regulation with dopamine and melatonin. Comparative Biochemistry and Physiology A. 240:110581. DOI 10.1016/j.cbpa.2019.110581.
3. Byun JH, Hyeon JY, Kim ES, Kim BH, Lim BS, Kim SK, Kagawa H, Takeuchi Y, Kim SJ, Takemura A, Hur SP. 2020. Gene expression patterns of novel visual and non-visual opsin families in immature and mature Japaense eel males. PeerJ. 8:e8326. DOI 10.7717/peerj.8326.
4. Kim BS, Hur SP, Hyeon JY, Yamashina F, Takemura A, Lee YD. 2020. Annual patterns of ocular melatonin level in the female grass puffer, Takifugr alboplumbeus: possible involvement in seasonal reproductive response. Fish Physiology and Biochemistry. 46:787-801. DOI 10.1007/s10695-019-00749-9.
5. Hyeon JY, Byun JH, Kim ES, Heo YS, Fukunaga K, Kim SK, Imamura S, Kim SJ, Takemura A, Hur SP. 2021. Testis development in the Japanese eel is affected by photic signals through melatonin secretion. PeerJ. 9:e12289. DOI 10.7717/peerj.12289.
6. Hettiarachchi SA, Hyeon JY, Mahardini A, Kim HS, Byun JH, Kim HJ, Jeong JG, Yeo JK, Kim SK, Kim SJ, Heo YS, Sathyadith J, Kang DH, Hur SP. 2022. DNA barcoding and morphological identification of spiny lobsters in South Korean waters: a new record of *Panulirus longipes* and *Panulirus homarus homarus*. PeerJ. 10:e12744. DOI 10.7717/peerj.12744.

List of Figures

Chapter Ⅰ. Gene expression patterns of opsin families in immature and mature Japaense eel males

General Conclusion

List of Tables

General Introduction

Living organisms receive various environmental cues (light, water temperature, and salinity, etc.) that direct their evolution. Organisms perceive the external environment through light, transmit signals to the brain, synchronize the biological clock to activate metabolism, and control physiological and ecological functions by inducing the secretion of endocrine hormones, such as melatonin (Benoit, 1978; Falcón, 1999; Campbell, Murphy & Suhner, 2001; Falcón et al., 2007).

Seasonal variation in photoperiod is a stimulus for teleosts, and the variation mainly affects growth, reproduction, and spawning (Polat et al., 2021). Photoperiod-mediated intrinsic rhythms and synthesis and secretion of sex hormones regulate fish reproduction (Shahjahan et al., 2020). Most fish inhabiting temperate regions with distinct seasonal changes have a clear seasonal light response and seasonal cycle of reproduction (Ikegami & Yoshimura, 2016). Organisms recognize the lengths of the day and night by receiving external light signals, such as seasonal changes in photoperiod, through light-sensory organs in the body. Photoperiod is considered to be a major environmental factor affecting the puberty and sexual maturity of some fish species (El-Sayed & Kawanna, 2007; Carrillo et al., 2010; Worrall et al., 2011). The regulation of photoperiod is involved in gonad maturation and reproductive timing in fishes, such as red sea bream (*Pagrus major*; Biswas et al., 2010), rainbow trout (*Oncorhynchus mykiss*; Pavlidis et al., 1992), European sea bass (*Dicentrarchus labrax*; Rodríguez, Zanuy & Carrillo, 2001), and topmouth gudgeon (*Pseudorasbora parva*; Zhu et al., 2014). Besides photoperiod, specific wavelengths of light also affect the sexual maturation in fish (Volpato, Duarte & Luchiari, 2004; Bapary et al., 2011). However, in places with limited seasonal variation, such as in the tropics, reproduction, and spawning are affected by external environments, such as moonlight and lunar cycle changes, tides, and tropical rains

(Falcón et al., 2010; Takemura, Rahman & Park, 2010; Takeuchi et al., 2018; Fukunaga et al., 2022). The periodic changes in the moonlight signal are presumed to have significant influence in the tropics, where the changes in photoperiod and water temperature are not evident (Johannes, 1978). The Moon orbits the Earth in a cycle of 27.3 days, where the lunar cycle induces various periodicities in the Earth's environment that affect biological activities of organisms. The lunar cycle drives moonlight intensity, tidal amplitude, and periodic changes in the geomagnetic field. These factors can affect reproduction in organisms. Marine organisms that are affected by the lunar cycle have evolved survival strategies such as spawning mainly at night to avoid the effects of tide in coastal waters. Changes in moonlight intensity affect gonadal development and gamete release during a specific lunar phase (Takemura, Rahman & Park, 2010). The periodic change in moonlight also affects the spawning migration of some teleosts. For example, the European eel, *Anguilla anguilla*, begin downstream migration for spawning (Miyai et al., 2004), or swims from the bottom with cold-water layers to the top with warm water layers of the ocean in the presence or absence of moonlight during the migratory process. Eels are more sensitive to moonlight than to temperature during spawning migration (Tesch, 1978). Most studies on synchronization of gonadal development or spawning by moonlight in marine species have focused on subtropical or tropical species such as the *Siganus* species (Hoque et al., 1999; Rahman, Takemura & Takano, 2000; Harahap et al., 2001; Park, Takemura & Lee, 2006). This species has probably adapted to the lunar signal because of external environmental information in the tropical regions, where seasonal changes are not evident or relatively less abundant than those in the temperate regions.

In marine organisms, the sensory organ retina conducts several important visual processes, including the detection of food, predators, and attractants. In addition, the retina acts as a medium to transmit light information to the body through photoreceptors. As an organ that recognizes light signals, the retina receives incoming

light signals and transmits the information to the nervous and peripheral tissues to induce physiological changes (visual sensitivity: Storch et al., 2007; Cameron, Barnard & Lucas, 2008; dopamine and melatonin levels: Doyle et al., 2002; Garbarino-Pico et al., 2004; circadian-dependent light damage: Organisciak et al., 2000; gene expression: Bailey et al., 2004; Mure et al., 2018). The mechanisms underlying the ability of marine species to adapt to different dynamic marine environments is still unclear. In the marine environment, 99% of natural light is absorbed within 150 m of the water column. However, in clear waters, fish living at a depth of up to 1,000 m can recognize day and night. The lack of perceived light in deep water requires visual adaptation to improve light sensitivity. Since all organisms adapt to the light environment, the type, shape, and spatial arrangements of photoreceptors differ from species to species (Newman, Marshall & Collin, 2013). Light intensities and spectral compositions change depending on the depth of the ocean. In shallow water, the spectrum has wavelengths in the range of 300−800 nm; however, as the depth increases, light becomes scattered and absorbed, and the intensity rapidly decreases and only light of cyan wavelength (approximately 480 nm) remains (Busserolles et al., 2002). Light is sensed by rod and cone photoreceptors in the outer retina and through the expression of photopigment melanopsin in the inner retina. Rod and cone photoreceptors act as visual opsins, whereas melanopsin acts as a non-visual opsin (van Diepen, Foster & Meijer, 2015). Non-visual photopigments regulate a variety of subconscious and reflex functions such as biological clock setting, pupillary light reflexes, pineal melatonin production, sleep patterns, and mood (Guido et al., 2022). In addition, the light-sensing systems in the pineal gland and retina activate the brain-pituitary-gonad (BPG) axis by converting incident light into a physiological signal (Boeuf & Le Bail, 1999; Plant, 2015). To date, many types of photoreceptors have been reported, and studies are being conducted to understand their functions. However, the process of converting photic information into physiological functions and the different functions of a photoreceptor in marine organisms living in various environments should be explored in detail.

Environmental signals synchronize the circadian system that regulates the physiological, metabolic, and behavioral activities of an organism. Light information, such as the light–dark (LD) cycle, is the most important external time period in the circadian system of vertebrates (Hastings, O'Neill & Maywood, 2007; Albrecht, 2012; Schibler et al., 2015). Biological time is a time-dependent adaptation that lasts for seconds or minutes, repeated throughout the day (ultradian) or lasting for days or months (infradians). This phenomenon allows organisms to adapt to endogenous (molecular and cellular) and external stimuli or temporal changes (i.e., zeitogeber; Andreani et al., 2015; López-Olmeda, Sánchez-Vázquez & Fortes-Silva, 2021). These environmental factors are considered the 'input' of the circadian system and the generated rhythm is called the 'output'. This 24-h period system consists of a third element, the core clock that is synchronized by the input and drives the output (Hastings, O'Neill & Maywood, 2007; Albercht, 2012). Clock genes regulate each other through an interconnected negative feedback mechanism that self-transcribes and translates the circadian clock at the molecular level, known as the 'transcription-translation feedback loop' (Albercht, 2004). In vertebrates, this regulatory loop consists of positive elements (Clock and Bmal) that induce the expression of negative elements [Period (per) and cryptochrome (cry)], which in turn through feedback. It downregulates the expression itself and consists of a 24-h cycle. Clock and Bmal, the bHLH PAS domain transcriptional activators, induce transcription by binding to the heterodimeric E-box elements located at the promoters of per and cry. Per and Cry interact to inhibit the transcriptional activation driven by the Clock–Bmal complex after translation, dimerization, and translocation to the nucleus. Stability, turnover, subcellular localization, translational control, and post-translational modifications contribute to the timing of this feedback loop. Moreover, the presence of an additional feedback loop directing the rhythmic expression of the Bmal transcript confers stability and robustness to the core loop (Emery & Reppert, 2004). In teleosts, the central clock is assumed to be located in the pineal gland and retina

(Falcón. 1999). The circadian system of fish is more complex because thay are more dynamic than terrestrial organisms and inhabit ocean territories with complex environments that are still unexplored (light conditions, the influence of food time, tidal differences, and water temperature; López-Olmeda, 2017). In addition, the lunar cycle and moonlight influence the expression of several clock genes in the pineal organs of fish (Ikegami, Takeuchi & Takemura. 2014). The correlation between the circadian rhythms of clock genes and endocrine control in marine species remains unclear. For example, whether the oscillation of clock genes in the peripheral or nervous tissues is precisely connected to the endocrine rhythm, and changes in transcriptomes of clock genes induced by the endocrine hormone affect the accompanying molecular core need to be clarified. In addition, given the diverse habitats of the ocean, various circadian systems in fish need a detailed understanding.

Melatonin plays an important role in the circadian system of vertebrates. The melatonin rhythm was first reported in the retina of vertebrates (Besharse & Iuvone, 1983; Tosini & Menaker, 1996). Melatonin is an indoleamine hormone synthesized by the pineal gland and retina and secreted at night and regulates circadian rhythms. Once secreted from the pineal gland, melatonin is transported via the bloodstream and cerebrospinal fluid to the central and peripheral tissues, where it regulates physiological, biochemical, and behavioral processes (Klein et al., 1997; Falcón et al., 2010). In contrast, melatonin secreted from the retina influences retinomotor movement, neurotransmitter release, and neuronal electrical activity (Besseau et al., 2006; Siu et al., 2006; Ping et al., 2008; Sauzet et al., 2008; Falcón et al., 2010). Photosensors in the retina and pineal gland sense photic cues through common photoreceptor cells, thereby directly participating in melatonin production (Cahill, Grace & Besharse, 1991; Falcón & Collin, 1991). Photic signals are involved in light sensing and melatonin production and secretion in both the retina and pineal gland (Iigo et al., 1994; Ekstrzm & Meissl, 1997; Falcón, 1999; Iigo et al., 2007). However, the mechanisms that regulate photic signal-induced melatonin secretion from

the eye remain largely unexplored.

The Japanese eels (*Anguilla japonica*) were used in this study. The Japanese eels have a catadromous lifecycle. Glass eels that transform from the leptocephalus stage live in regions of northeast Asia after migrating to freshwater areas, where they spend most of their lives (approximately 5−17 y; Kotake et al., 2007). The yellow eels also exhibit lunar cycle-based locomotor behavior at sexually immature stages (Baras et al., 1998). The Japanese silver eels begin spawning migration between September and November when their puberty is initiated (Tsukamoto, 2009). In addition to changes in body color from yellow (sexually immature) to silver (sexually mature), sexual maturation of eels is accompanied by an increase in the eye size (Pankhurst, 1982; Beullens et al., 1997; Han et al., 2003; Okamura et al., 2007; Okamura et al., 2008), suggesting photic perception and adaptation during spawning migration. This morphological change may be influenced by reproduction-related hormones (Hyeon et al., 2019). Anguillids are nocturnal species whose locomotor activity increases at night (Japanese eel: Aoyama et al., 2002; European eel: Tesch, 1978; Tesch, 1989; American eel *A. rostrata*: Helfman et al., 1983; shortfinned eel *A. australis* and longfin eel *A. dieffenbachii*: Jellyman & Sykes, 2003). The spawning period was suggested to be regulated by the lunar cycle in studies conducted at a site close to the West Mariana Ridge, where spawning occurred during the last days of the lunar month (Tsukamoto et al., 2003; Sudo & Tsukamoto, 2015). The Japanese eels have a high commercial value in east Asian countries, where efficient aquaculture is currently under research and development. Eels have recently been listed on the International Union for Conservation of Nature Red List (2014) owing to a drastic decrease in their natural population. In this regard, the entire process of reproduction can be replicated using immature eels, as their sexual maturation can be induced by prolonged treatment with salmon pituitary extract on females and human chorionic gonadotropin on males (Kagawa, 2013).

Although the induction of sexual maturation in eels has been attempted, applying

the techniques of reproduction of general saltwater fish to eels suffers from several limitations. Reproductive control of teleosts is synchronized by photoperiod; however, little is known regarding the relationship between photic signals and reproduction in eels. Eels do not respond to seasonal changes until they begin spawn migration. Based on this information, we assessed the relation between photic signals (circadian, photoperiodic change, and moonlight) and the habitat and spawning ecology of eels to investigate the yet unknown spawning migration and reproductive mechanisms of eels. The purpose of this study was to assess the possibility of inducing reproduction in eels by controlling artificial environmental factors. Therefore, the following three objectives were undertaken to investigate the mechanism of light-induced activation of the reproductive endocrine system in eels.

In Chapter 1, photoreceptors were investigated in eels using RNA sequencing, and photo-recognition pathways were investigated by comparing photoreceptor expression between sexually mature and immature individuals.

In Chapter 2, the correlation between melatonin secretion and spawning migrations of eels was investigated by assessing the responses to circadian rhythms, photoperiod, and moonlight.

Finally, in Chapter 3, the effects of external photic stimuli (daily, circadian, photoperiod, and moonlight) on the expression of genes of the biological clock in eels were investigated.

References

Albrecht U. 2004. The mammalian circadian clock: a network of gene expression. Front Bioscience. 9:48-55.

Albrecht U. 2012. Timing to perfection: the biology of central and peripheral circadian clocks. Neuron. 74:246-260. DOI 10.1016/j.neuron.2012.04.006.

Andreani TS, Itoh TQ, Yildirim E, Hwangbo DS, Allada R. 2015. Genetics of circadian rhythms. Sleep medicine clinics. 10(4):413-21. DOI 10.1016/j.jsmc.2015.08.007.

Aoyama J, Sasai S, Miller MJ, Shinoda A, Nakamura A, Kawazu K, Tsukamoto K. 2002. A preliminary study of the movements of yellow and silver eels, *Anguilla japonica*, in the estuary of the Fukui River, Japan, as revealed by acoustic tracking. Hydrobiologia. 470:31-36. DOI 10.1023/A:1015604906154.

Bailey MJ, Beremand PD, Hammer R, Reidel E, Thomas TL, Cassone VM. 2004. Transcriptional profiling of circadian patterns of mRNA expression in the chick retina. Journal of Biological Chemistry. 279:52247-52254. DOI 10.1074/jbc.M405679200.

Bapary MAJ, Amin MN, Takeuchi Y, Takemura A. 2011. The stimulatory effects of long wavelengths of light on the ovarian development in the tropical damselfish, *Chrysiptera cyanea*. Aquaculture. 314:188-192. DOI 10.1016/j.aquaculture.2011.02.006.

Baras E, Jeandrain D, Serouge B, Philippart JC. 1998. Seasonal variations in time and space utilization by radio-tagged yellow eels *Anguilla anguilla* (L.) in a small stream. Hydrobiologia. 371:187-198.

Benoit JM. 1978. Chronobiologic study in the domestic duck. II. Physiological mechanism of the chronobiologic action of visible light on the gonads of the male duck. Chronobiologia. 5:158-168.

Besharse JD, Iuvone PM. 1983. Circadian clock in *Xenopus* eye controlling retinal

serotonin N-acetyltransferase. Nature. 305:133-135. DOI 10.1038/305133a0.

Besseau L, Benyassi A, Møller M, Coon SL, Weller JL, Boeuf G, Klein DC, Falcón J. 2006. Melatonin pathway: breaking the 'high-at-night' rule in trout retina. Experimental Eye Research. 82:620-627. DOI 10.1016/j.exer.2005.08.025.

Beullens K, Eding EH, Gilson P, Ollevier F, Komen J, Richter CJJ. 1997. Gonadal differentiation, intersexuality and sex ratios of European eel (*Anguilla anguilla* L.) maintained in captivity. Aquaculture. 153:135-150. DOI 10.1016/S0044-8486(97)00018-5.

Boeuf G, Le Bail PY. 1999. Does light have an influence on fish growth? Aquaculture. 199:129-152. DOI 10.1016/S0044-8486(99)00074-5.

Biswas A, Seoka M, Inagaki H, Takii K. 2010. Reproduction, growth and stress response in adult red sea bream, *Pagrus major* (Temminck & Schlegel) exposed to different photoperiods at spawning season. Aquaculture Research. 41:519-527. DOI 10.1111/j.1365-2109.2009.02341.x.

Busserolles FD, Fogg L, Cortesi F, Marshall J. 2002. The exceptional diversity of visual adaptations in deep-sea teleost fishes. Seminars in Cell & Developmental Biology. 106:20-30. DOI 10.1016/j.semcdb.2020.05.027.

Cahill GM, Grace MS, Besharse JC. 1991. Rhythmic regulation of retinal melatonin: Metabolic pathways, neurochemical mechanisms, and the ocular circadian clock. Cellular and Molecular Neurobiology. 11(5):529-560. DOI 10.1007/BF00734814.

Cameron MA, Barnard AR, Lucas RJ. 2008. The electroretinogram as a method for studying circadian rhythms in the mammalian retina. Journal of Genetics. 87:459-466. DOI 10.1007/s12041-008-0068-5.

Campbell SS, Murphy PJ, Suhner AG. 2001. Extraocular phototransduction and circadian timing systems in vertebrates. Chronobiology International. 18:137-172. DOI 10.1081/CBI-100103183.

Carrillo M, Begtashi I, Rodríguez L, Marin MC, Zanuy S. 2010. Long photoperiod on sea cages delays timing of first spermiation and enhances growth in male European sea bass (*Dicentrarchus labrax*). Aquaculture. 299:157-164. DOI

10.1016/j.aquaculture.2009.11.024.

Doyle SE, Grace MS, McIVOR W, Menaker M. 2002. Circadian rhythms of dopamine in mouse retina: the role of melatonin. Visual Neuroscience. 19:593-601. DOI 10.1017/s0952523802195058.

Ekstrzm P, Meissl H. 1997. The pineal organ of teleost fishes. Reviews in Fish Biology and Fisheries. 284:199-284.

El-Sayed AFM, Kawanna M. 2007. Effects of photoperiod on growth and spawning efficiency of Nile tilapia (*Oreochromis niloticus* L.) broodstock in a recycling system. Aquaculture Research. 38:1242-1247. DOI 10.1111/j.1365-2109.2007.01690.x.

Emery P, Reppert SM. 2004. A rhythmic Ror. Neuron. 43:443-446.

Falcón J, Besseau L, Sauzet S, Boeuf G. 2007. Melatonin effects on the hypothalamopituitary axis in fish. Trends in Endocrinology and Metabolism. 18:81-88. DOI 10.1016/j.tem.2007.01.002.

Falcón J, Collin JP. 1991. Pineal-retinal relationships: rhythmic biosynthesis and immunocytochemical localization of melatonin in the retina of the pike (*Esox luxius*). Cell and Tissue Research. 265(1991):601-609. DOI 10.1007/BF0034 0884.

Falcón J. 1999. Cellular circadian clocks in the pineal. Progress in Neurobiology. 58(2):121-162. DOI 10.1016/S0301-0082(98)00078-1.

Falcón J, Migaud H, Muñoz Cueto JA, Carrillo M. 2010. Current knowledge on the melatonin system in teleost fish. General and Comparative Endocrinology. 165(3):469-482. DOI 10.1016/j.ygcen.2009.04.026.

Fukunaga K, Takeuchi Y, Yamauchi C, Takemura A. 2022. Induction of spawning under artificial moonlight in the honeycomb grouper *Epinephelus merra*, a lunar-synchronized spawner. Biological Rhythm Research. Latest article. DOI 10.1080/09291016.2022.2046416.

Garbarino-Pico E, Carpentieri AR, Contin MA, Keller Sarmiento MI, Brocco MA, Panzetta P, Rosenstein RE, Caputto BL, Guido ME. 2004. Retinal ganglion cells

are autonomous circadian oscillators synthesizing N-acetylserotonin during the day. Journal of Biological Chemistry. 279:51172-51181. DOI 10.1074/jbc.M309248200.

Guido ME, Marchese NA, Rios MN, Morera LP, Diaz NM, Garbarino-Pico E, Contin MA. 2022. Non-visual opsins novel photo-detectors in the vertebrate inner retina mediate light responses within the blue spectrum region. Cellular and Molecular Neurobiology. 42:59-83. DOI 10.1007/s10571-020-00997-x.

Han YS, Liao IC, Huang YS, He JT, Chang CW, Tzeng WN. 2003. Synchronous change of morphology and gonadal development of silvering Japanese eel *Anguilla japonica*. Aquaculture. 219:783-796. DOI 10.1016/S0044-8486(02)00578-1.

Harahap AP, Takemura A, Nakamura S, Rahman MS, Takano K. 2001. Histological evidence of lunar-synchronized ovarian development and spawning in the spiny rabbitfish *Siganus spinus* (Linnaeus) around the Ryukyus. Fisheries Science. 67:888-893. DOI 10.1046/j.1444-2906.2001.00337.x.

Hastings M, O'Neill JS, Maywood ES. 2007. Circadian clocks: regulators of endocrine and metabolic rhythms. Journal of Endocrinology. 195:187-198. DOI 10.1677/JOE-07-0378.

Helfman GS, Stoneburner DL, Bozeman EL, Christian PA, Whalen R. 1983. Ultrasonic telemetry of American eel movements in a tidal creek. Transactions of the American Fisheries Society. 112:105-110. DOI 10.1577/1548-8659(1983)112<105:UTOAEM>2.0.CO;2.

Hoque MM, Takemura A, Matsuyama M, Matsuura S, Takano K. 1999. Lunar spawning in *Siganus canaliculatus*. Journal of Fish Biology. DOI 10.1111/j.1095-8649.1999.tb02071.x.

Iigo M, Kezuka H, Suzuki T, Tabata M, Aida K. 1994. Melatonin signal transduction in the goldfish, *Carassius auratus*. Neurosci Biobehavio Reviews. 18(4):563-569. DOI 10.1016/0149-7634(94)90012-4.

Iigo M, Abe T, Kambayashi S, Oikawa K, Masuda T, Mizusawa K, Kitamura S,

Azuma T, Takagi Y, Aida K, Yanagisawa T. 2007. Lack of circadian regulation of in vitro melatonin release from the pineal organ of salmonid teleosts. General and Comparative Endocrinology. 154:91-97. DOI 10.1016/j.ygcen.2007.06.013.

Ikegami K, Takeuchi Y, Takemura A. 2014. Lunar clock in fish reproduction. Annual, Lunar, and Tidal Clocks. p.163-178. DOI 10.1007/978-4-431-55261-1_9.

Ikegami K, Yoshimura T. 2016. Comparative analysis reveals the underlying mechanism of vertebrate seasonal reproduction. General and Comparative Endocrinology. 227:64-68. DOI 10.1016/j.ygcen.2015.05.009

Jellyman DJ, Sykes JRE. 2003. Diel and seasonal movements of radio-tagged freshwater eels, *Anguilla* spp. in two New Zealand streams. Environmental Biology of Fishes. 66:143-154. DOI 10.1023/A:1023691604088.

Johannes RE. 1978. Reproductive strategies of coastal marine fishes in the tropics. Environmental Biology of Fishes. 3:65-84. DOI 10.1007/BF00006309.

Kagawa H. 2013. Oogenesis in Teleost Fish. Aqua-Bioscience Monographs. 6:99-127.

Kotake A, Arai T, Okamura A, Yamada Y, Utoh T, Oka HP, Miller MJ, Tsukamoto K. 2007. Ecological aspects of the Japanese eel, *Anguilla japonica*, collected from coastal areas of Japan. Zoological Science. 24:1213-1221. DOI 10.2108/zsj.24.1213.

Klein DC, Coon SL, Roseboom PH, Weller JL, Bernard M, Gastel JA, Zatz M, Iuvone PM, Rodriguez IR, Begay V, Falcón J, Cahill GM, Cassone VM, Baler R. 1997. The melatonin rhythm-generating enzyme: molecular regulation of serotonin N-acetyltransferase in the pineal gland. Recent Progress in Hormone Research. 52:307-356.

López-Olmeda JF. 2017. Nonphotic entrainment in fish. Comparative Biochemistry and Physiology. 203:133-143. DOI 10.1016/j.cbpa.2016.09.006.

López-Olmeda JF, Sánchez-Vázquez FJ, Fortes-Silva R. 2021. Taylor & Francis Ltd, London, UK.

Newman AS, Marshall JN, Collin SP. 2013. Visual eyes: a quantitative analysis of the photoreceptor layer in deep-sea sharks. Behavior and Evolution. 82:237-249.

DOI 10.1159/000355370.

Miyai T, Aoyama J, Sasai S, Inoue JG, Miller MJ, Tsukamoto K. 2004. Ecological aspects of the downstream migration of introduced European eels in the Uono river, Japan. Environmental biology of Fishes. 71:105-114. DOI 10.1023/B:EBFI.0000043178.50750.18.

Mure LS, Le HD, Benegiamo G, Chang MW, Rios L, Jillani N, Ngotho M, Kariuki T, Dkhissi-Genyahya O, Cooper HM, Panda S. 2018. Diurnal transcriptome atlas of a primate across major neural and peripheral tissues. Science. 359. DOI 10.1126/science.aao0318.

Okamura A, Yamada Y, Yokouchi K, Horie N, Mikawa N, Utoh T, Tanaka S, Tsukamoto K. 2007. A silvering index for the Japanese eel Anguilla japonica. Environmental Biology of Fishes. 80:77-89. DOI 10.1007/s10641-006-9121-5.

Okamura A, Yamada Y, Horie N, Utoh T, Mikawa N, Tanaka S, Tsukamoto K. 2008. Effects of silvering state on induced maturation and spawning in wild female Japanese eel *Anguilla japonica*. 2008. Fisheries Science. 74:642-648. DOI 10.1111/j.1444-2906.2008.01569.x.

Organisciak DT, Darrow RM, Barsalou L, Kutty RK, Wiggert B. 2000. Circadian-dependent retinal light damage in rats. Investigative Ophthalmology and Visual Science. 41:3694-3701.

Pankhurst NW. 1982. Relation of visual changes to the onset of sexual maturation in the European eel *Anguilla anguilla* (L.). Journal of Fish Biology. 21:127-140. DOI 10.1111/j.1095-8649.1982.tb03994.x.

Park YJ, Takemura A, Lee YD. 2006. Annual and lunar-synchronized ovarian activity in two rabbitfish species in the Chuuk lagoon, Micronesia. Fisheries Science. 72:166-172. DOI 10.1111/j.1444-2906.2006.01131.x.

Pavlidis M, Theochari V, Paschos J, Dessypris A. 1992. Effect of six photoperiod protocols on the spawning time of two rainbow trout, *Oncorhynchus mykiss* (Walbaum), populations in north-west Greece. Aquaculture Research. 23:431-441. DOI 10.1111/j.1365-2109.1992.tb00787.x.

Ping Y, Huang H, Zhang XJ, Yang XL. 2008. Melatonin potentiates rod signals to ON type bipolar cells in fish retina. Journal de Physiologie. 586:2683-2694. DOI 10.1113/jphysiol.2008.152959.

Plant TM. 2015. 60 Years of neuroendocrinology: the hypothalamo-pituitary-gonadal axis. Journal of Endocrinology. 226:T41-T54. DOI 10.1530/JOE-15-0213.

Polat H, Ozturk RC, Terzi Y, Aydin I, Kucuk E. 2021. Effect of photoperiod manipulation on spawning time and performance of turbot (*Scophthalmus maximus*). Aquaculture Studies. DOI 10.4194/2618-6381-v21_3_03.

Rahman MS, Takemura A, Takano K. 2000. Lunar synchronization of testicular development and plasma steroid hormone profiles in the golden rabbitfish. Journal of fish Biology. 57:1065-1074. DOI 10.1111/j.1095-8649.2000.tb02212.x.

Rodŕıguez L, Zanuy S, Carrillo M. 2001. Influence of daylength on the age at first maturity and somatic growth in male sea bass (*Dicentrarchus labrax*, L.). Aquaculture. 196:159-175. DOI 10.1016/S0044-8486(00)00555-X.

Sauzet S, Besseau L, Perez PH, Covès D, Chatain B, Peyric E, Boeuf G, Muñoz-Cueto JA, Falcón J. 2008. Cloning and retinal expression of melatonin receptors in the European sea bass, *Dicentrarchus labrax*. General and Comparative Endocrinology. 157(2):186-195. DOI 10.1016/j.ygcen.2008.04.008.

Schibler U, Gotic I, Saini C, Gos P, Curie T, Emmenegger Y, Sinturel F, Gosselin P, Gerber A & Fleury-Olela F, Rando G, Demarque M Franken P. 2015. Clock-talk: interactions between central and peripheral circadian oscillators in mammals. Cold Spring Harbor Symposia on Quantitative Biology. 80:223-232. DOI 10.1101/sqb.2015.80.027490.

Shahjahan M, Al-Emran M, Islam SMM, Baten SMA, Rashid H, Haque MM. 2020. Prolonged photoperiod inhibits growth and reproductive functions of rohu *Labeo rohita*. Aquaculture Reports. 16:100272. DOI 10.1016/j.aqrep.2019.100272.

Siu AW, Maldonado M, Sanchez-Hidalgo M, Tan DX, Reiter RJ. 2006. Protective effects of melatonin in experimental free radical-related ocular diseases. Journal of Pineal Research. 40(2):101-109. DOI 10.1111/j.1600-079X.2005.00304.x.

Storch KF, Paz C, Signorovitch J, Raviola E, Pawlyk B, Li T, Weitz CJ. 2007. Intrinsic circadian clock of the mammalian retina: importance for retinal processing of visual information. Cell. 130:730-741. DOI 10.1016/j.cell.2007.06.045.

Sudo R, Tsukamoto K. 2015. Migratory restlessness and the role of androgen for increasing behavioral drive in the spawning migration of the Japanese eel. Scientific Reports. 5:17430. DOI 10.1038/srep17430.

Takemura A, Rahman MS, Park YJ. 2010. External and internal controls of lunar-related reproductive rhythms in fishes. Journal of Fish Biology. 76:7-26. DOI 10.1111/j.1095-8649.2009.02481.x.

Takeuchi Y, Kabutomori R, Yamauchi C, Miyagi H, Takemura A, Okano K, Okano T. 2018. Moonlight controls lunar-phase-dependency and regular oscillation of clock gene expressions in a lunar-synchronized spawner fish, Goldlined spinefoot. Scientific Reports. 8:6208. DOI 10.1038/s41598-018-24538-1.

Tesch FW. 1978. Telemetric observations on the spawning migration of the eel *Anguilla anguilla* west of the European continental shelf. Environmental Biology of Fishes. 3:203-209. DOI 10.1007/BF00691944.

Tesch FW. 1989. Changes in swimming depth and direction of silver eels (*Anguilla anguilla* L.) from the continental shelf to the deep sea. Aquatic Living Resources. 2:9-20. DOI 10.1051/alr:1989002.

Tosini G, Menaker M. 1996. Circadian rhythms in cultured mammalian retina. Science. 272:419-421. DOI 10.1126/science.272.5260.419.

Tsukamoto K. 2009. Oceanic migration and spawning of anguillid eels. Journal of Fish Biology. 74(9):1833-1852. DOI 10.1111/j.1095-8649.2009.02242.x.

Tsukamoto K, Otake T, Mochioka N, Lee TW, Fricke H, Inagaki T, Aoyama J, Ishikawa S, Kimura S, Miller MJ, Hasumoto H, Oya M, Suzuki Y. 2003. Seamounts, new moon and eel spawning: the search for the spawning site of the Japanese eel. Environmental Biology of Fishes. 66(3):221-229. DOI 10.1023/A:1023926705906.

van Diepen HC, Foster RG, Meijer JH. 2015. A colourful clock. PLoS Biology. 13(5): e1002160. DOI 10.1371/journal.pbio.1002160.

Volpato GL, Duarte CRA, Luchiari AC. 2004. Environmental color affects Nile tilapia reproduction. SciELO Brasil. 37:479-483. DOI 10.1590/S0100-879X2004000400004.

Worrall KL, Carter CG, Wilkinson RJ, Porter MJR. 2011. The effects of continuous photoperiod (24L: 0D) on growth of juvenile barramundi (*Lates calcarifer*). Aquaculture International. 19:1075-1082. DOI 10.1007/s10499-011-9425-0.

Zhu D, Yang K, Gul Y, Song W, Zhang X, Wang W. 2014. Effect of photoperiod on growth and gonadal development of juvenile Topmouth Gudgeon *Pseudorasbora parva*. Environmental Biology of Fishes. 97:147-156. DOI 10.1007/s10641-013-0133-7.

Chapter Ⅰ

Gene expression patterns of opsin families in immature and mature Japanese eel males

Abstract

This study was carried out to identify and estimate physiological function of a new type of opsin subfamily present in the retina and whole brain tissues of Japanese eel using RNA-Seq transcriptome method. A total of 18 opsin subfamilies were identified through RNA-seq. The visual opsin family included Rh2, SWS2, FWO, DSO, and Exo-Rhod. The non-visual opsin family included four types of melanopsin subfamily (Opn4x1, Opn4x2, Opn4m1, and Opn4m2), peropsin, two types of neuropsin sub-family (Opn5-like, Opn5), Opn3, three types of TMT opsin subfamily (TMT1, 2, 3), VA-opsin, and parapinopsin. In terms of changes in photoreceptor gene expression in the retina of sexually mature and immature male eels, DSO mRNA increased in the maturation group. Analysis of expression of opsin family gene in male eel brain before and after maturation revealed that DSO and SWS2 expression in terms of visual opsin mRNA increased in the sexually mature group. In terms of non-visual opsin mRNA, parapinopsin mRNA increased whereas that of TMT2 decreased in the fore-brain of the sexually mature group. The mRNA for parapinopsin increased in the mid-brain of the sexually mature group, whereas those of TMT1 and TMT3 increased in the hind-brain of the sexually mature group. DSO mRNA also increased in the retina after sexual maturation, and DSO and SWS2 mRNA increased in whole brain part, suggesting that DSO and SWS2 are closely related to sexual maturation.

1. Introduction

Mammals have two types of photoreceptor proteins (rhodopsin, cone-opsin) that perceive light in the retina of the eye, and different types of photoreceptors recognize the signals of light (wavelength of light, intensity of light, direction of light, and periodicity) (Hastings & Maywood, 2000; Tada, Altun & Yokoyama, 2009). A photoreceptor is a visual sensory cell capable of recognizing light of a specific wavelength. Photoreceptors also refer to an opsin protein receptor that actually absorbs light and converts it into chemical energy. Vertebrate photoreceptors are regulated by opsin, a superfamily of G-protein-coupled receptor (GPCR), opsin, with an inverse agonist 11–*cis* retinal chromophore, covalently bound. Indeed, retinal molecules selectively absorb various spectrum of light depending on the formation of binding with the opsin protein (reviewed in Pugh & Lamb, 2000). Absorption of light at a specific wavelength leads to conversion into all-*trans* form that binds the opsin and transducing proteins, thereby activating a series of visual sensitive-related cellular signal transduction processes (Terakita, 2005). Opsin superfamily is broadly divided into visual and non–visual opsins. There have been extensive studies on vision function of opsin-based photopigment. However, when the opsin was found in tissues such as avian pineal and amphibian skin, opsins were unofficially divided into visual and non–visual groups (Okano, Yoshizawa & Fukada, 1994; Kojima & Fukada, 1999; Van Gelder, 2001). As extra-ocular tissues cannot form images, this classification was suggested. Visual opsin initiates the visual transduction cascade, whereas non-visual opsin is involved in circadian entrainment (Doyle et al., 2008) and retinal metabolism (Bellingham et al., 2003).

The habitats of marine organisms, especially fish, vary in depth and region, ranging from freshwater to brackish areas. The light conditions of these habitats are different in terms of turbidity, color, and brightness (Bowmaker et al., 1994; Bowmaker, 2008). For example, in the case of deep-sea snailfish inhabiting relatively

deep-water areas, the spectral sensitivities of the rod and cone photoreceptors react to the blue light (Sakata et al., 2015). In contrast, in the case of black bream, shallow-sea fish, cone photoreceptors (Rh2 or MWS), have maximal light absorbance wavelength (λmax) at 545 to 575 nm, which is the dominant light in their habitat (Shand et al., 2002). Thus, it is presumed that animals have obtained a unique visual system that have made them adapt to the light environment of their habitats in the process of evolution.

To date, photoreceptor studies on Anguillid have identified fresh water rhodopsin (FWO) (Zhang et al., 2000), deep-sea rhodopsin (DSO) (Zhang et al., 2000), Rh1d (European eel, *A. anguilla* and Japanese eel, *A. japonica* and giant mottled eel, *A. marmorata*) (Wang et al., 2014), Rh2 (European eel and giant mottled eel) (Cottrill et al., 2009), and SWS2 (European eel and giant mottled eel) (Wang et al., 2014). Molecular biological studies on photo sensitivities of these visual pigments and studies on the expression mechanism of photoreceptors according to ecological stages (glass eel, yellow eel, and silver eel) have been actively conducted. However, the presence or function of a subfamily other than the above-mentioned four types of visual opsin or non-visual opsin subfamily in *Anguilla* species has not been reported yet. Physiological studies of photoreceptors in vertebrate animals have reported that pinopsin and VA-opsin (Okano, Yoshizawa & Fukada, 1994; Soni & Foster, 1997) in the brain of birds and exo-rhodopsin in the pineal gland of zebrafish directly affect body color change and reproductive physiology (Kojima, Mano & Fukada, 2000; Collin et al., 2009). Thus, it is considered that other types of photoreceptors, except for the previously reported opsins, may play an important reproductive physiological role in Japanese eel but there has been no further investigation into it.

In this study, we investigated the opsin subfamily present in the retina and whole brain tissues of Japanese eel inhabiting Northeast Asia using the RNA-Seq transcriptome. In addition, we examined the opsin subfamily mRNA levels in sexually immature and mature eels using qPCR method. These results identify the physiological role of photoreceptors in the maturation process of Japanese eels and,

thus, can be used as a basic material for studies on photoreceptor mechanisms including the effect of environmental factors on maturation and visual adaptation.

2. Materials and Methods

2.1. Experimental fish

We purchased Japanese eels, *A. japonica,* inhabiting brackish water at Hadori, Gujwaeup, Jejusi, Jeju, South Korea in September at 2016. The wild fish were kept in Lava seawater center in Jeju Techno-park, Jeju, South Korea (33°N, 126°E). The fish were reared for 1 weeks in acryl tank (800 L/capacity) with recirculation system (natural photoperiod = approximately 12L12D, water temperature 20 ± 1 °C). for the study of the maturation induction of the Japanese eel, males were purchased from an eel aquafarm (Hanwool aquafarm, Gwangju, South Korea). The obtained eels were acclimated in the freshwater round acrylic tank (1 ton/capacity) for at least one week. Light conditions were maintained at 12L12D using fluorescent bulbs (10W, 600 lx, PPFD = 10.0 μmol $m^{-2}s^{-1}$, λp = 545 nm) light on at 06:00 and light off at 18:00, and the temperature of the water was maintained at 20 ± 1 °C. All experiments were conducted in compliance with the guidelines of Institutional Animal Care and Experimental Committee of Korea Institute of Ocean Science and Technology. The protocol was approved by the Animal care and use committee of the Korea Institute of Ocean Science and Technology (KIOST 2021-0001).

For the retina and whole brain RNA-transcriptome analysis (Figure 1.1), wild caught Japanese eels (body weight: 233−726 g and body length: 55.3−80.7 cm) were reared for 1 weeks in acryl tank. For the sampling of experimental fish, the retina and the brain were isolated from Japanese eels at 12:00 h and 24:00 h (n = 12, six females and six males) after anesthesia with tricaine methanesulfonate (MS-222, Sigma-Aldrich, ST., USA). The collected tissues were frozen using liquid nitrogen and stored at −80 °C until used for analysis.

For maturation artificially induction of Japanese eels, only males (initial body weight: 186.1 ∼227.1 g, n = 6) were selected and reared in the freshwater tank for

at least one week. Later, the water was replaced with sea water for one week, and the fish were reared for eight weeks and intraperitoneally injected with human chorionic gonadotropin (n = 6, hCG, 1 IU/g^{-1}) dissolved in saline (150 mM NaCl) at one-week intervals for sexually maturation. During the maturation induction, photoperiod of 12L12D (lights on = 07:00, lights off = 19:00) and water temperature of 20 ± 1 °C were maintained, and a complete recirculating aquaculture system (800 L/capacity). Fluorescent bulbs (20W, approximately 600 lx, 10.0 μmolm^{-2}s^{-1} at 545 nm) were situated above on the tank to provide an illuminance at water surface of 600 lx. After eight weeks of intraperitoneal injection, maturation was determined by the presence or absence of spermiation and histological observation of the testis. For analysis of opsin family genes mRNA level changes in the retina and brain part of Japanese eels before and after maturation, the brain was dissected into the fore-brain, mid-brain, and hind-brain (Figure 1.2). The extracted tissues were frozen using liquid nitrogen and stored at −80 °C until used for analysis.

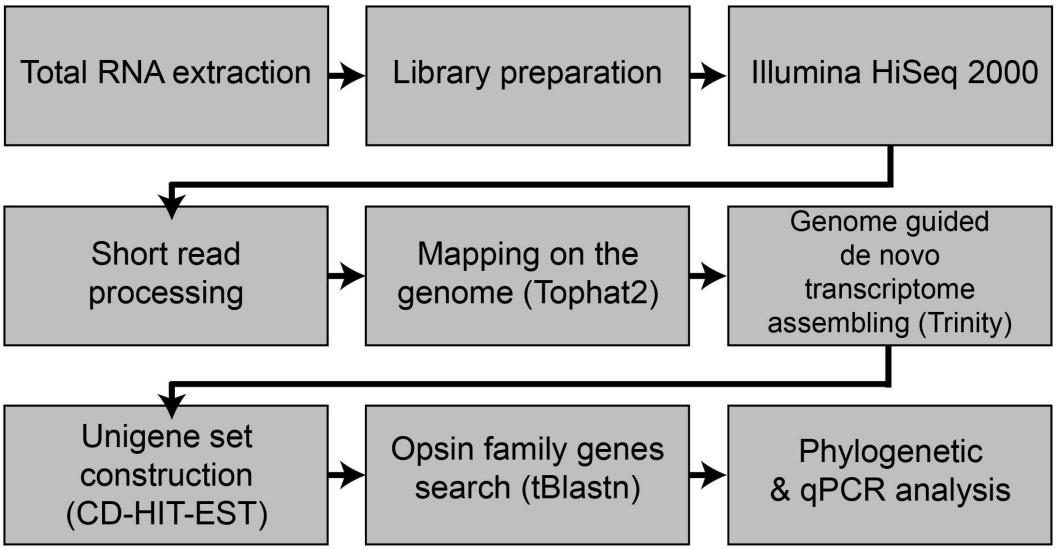

Figure 1.1. Flowchart of the present study.

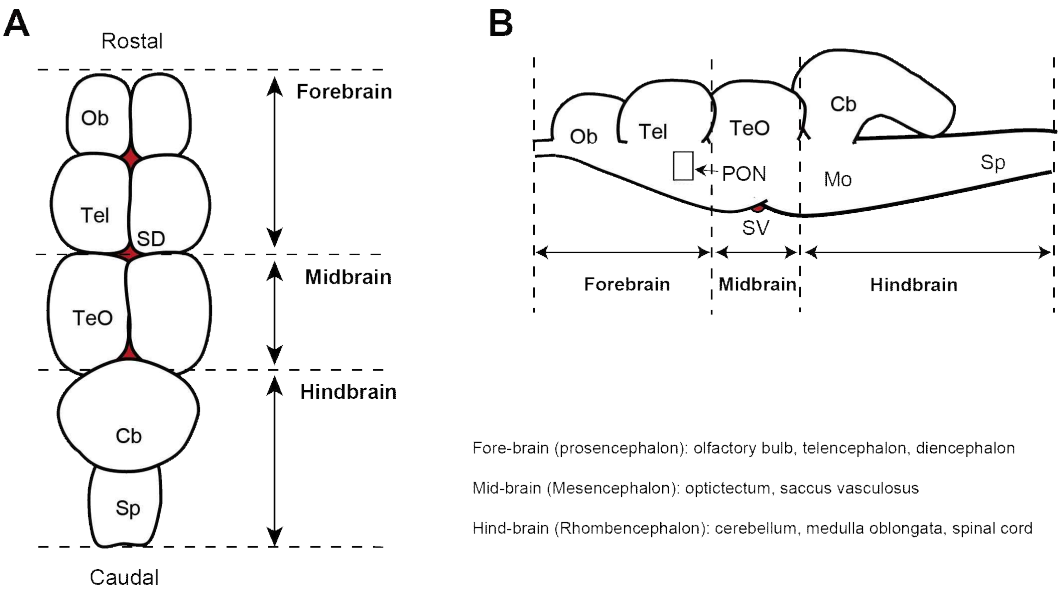

Figure 1.2. Diagram showing the dosal view (A) and sagittal plane (B) of the eel brain. Ob, olfactory bulb; Tel, telencephalon; TeO, optictectum; Cb, cerebellum; Mo, medulla oblongata; P, pineal gland; SD, saccus dorsalis; PON, preoptic nucleus; SV, saccus vasculosus.

2.2. Total RNA isolation and cDNA synthesis

Total RNA was isolated from the retina and three parts of the brain (fore-, mid-, and hind-) using RNA-iso plus (Takara-Bio, Otsu, Japan) according to the manufacturer's protocol. After isolated the total RNA, quality, and amount-checked on a 2100 bioanalyzer RNA 6000 NANO chip (Bio-Rad, Hercules, CA, USA) and electrophoresis. cDNA was synthesized using the Transcriptor High Fidelity cDNA Synthesis kit (Roche-diagnostics, Indianapolis, IN, USA) by following the manufacturer's protocol.

2.3. cDNA library construction and massively parallel sequencing

RNA-Seq paired end libraries were prepared using the Illumina TruSeq RNA Sample Preparation Kit v2 (catalog #RS-122-2001, Illumina, San Diego, CA). Total RNA was isolated from the retina and brain, respectively. After removal of genomic DNA contamination, RNA quality and quantity were assessed by 2100 bioanalyzer RNA 6000 NANO chip (Bio-Rad). High quality total RNA extracted from retina and brain of X individuals were then pooled, respectively. Starting with total RNA, mRNA purified using poly (A) selection was chemically fragmented and converted into single-stranded cDNA using random hexamer priming. Next, the second strand is generated to create double-stranded cDNA. Library construction begins with generation of blunt-end cDNA fragments from ds-cDNA. Then A-base added to the blunt-end in order to make them ready for ligation of sequencing adapters. After the size selection of ligates, the ligated cDNA fragments which contain adapter sequences are enhanced via PCR using adapter specific primers. The library was quantified with KAPA library quantification kit (Kapa biosystems KK4854) following the manufacturer's instructions. Each library is loaded on Illumina Hiseq2000 platform, and we performed high-throughput sequencing (read length 2 × 100) to ensure that each sample meets the desired average sequencing depth.

2.4. Preprocessing and *de novo* reconstruction of transcriptome

The bases from 5^{r} end and 3^{r} end of each read with low quality and adapter sequences were trimmed using Trimmomatic (ver. 0.3.6 Bolger, Lohse & Usadel, 2014), then low averaged quality (Q < 25) were removed by PRINSEQ lite (ver. 0.20.4 Schmieder & Edwards, 2011). Cleaned raw reads from retina and brain RNA were pooled, then mapped to the *Anguilla japonica* draft genome sequence (Ref) using tophat2 (ver.2.1.0, Kim et al., 2013), then *de novo* transcriptome reconstruction was performed by a genome-guided Trinity (ver. 2.3.2 Grabherr et al., 2011) with bam mapping result. To remove redundant contigs and create an unigene set, the assembled contigs were clustered and filtered using cd-hit-est with default parameters (CD-HIT package, Li & Godzik, 2006).

2.5. Analysis of the opsin DNA sequence

To search opsin family genes from the assembled transcriptome sequences of Japanese eel, the tBlastn program was utilized (*E*-value < 0.01) on zebrafish opsin protein sequences as queries.

The ORF regions of Japanese eel opsin candidates were found through ORF Finder (http://www.ncbi.nlm.nih.gov/gorf/gorf.html), then presumed protein sequences were aligned with teleost opsin family proteins. A phylogenetic tree was constructed by the maximum-likelihood algorithm using RAxML (Stamatakis, 2014). For quantifying the identified opsin family genes expressions, cleaned reads were mapped on reconstructed contigs by Bowtie2 (Langmead & Salzberg, 2012), then the expression levels were estimated using Tigar2 (Nariai et al., 2014).

2.6. Quantitative real-time RT-PCR (qRCR)

Real-time qPCR reactions were performed using the Dice real time thermal cycler (TaKaRa- Bio) and SYBR Premix Ex Taq^{TM} II (TaKaRa-Bio). Gene specific primers used for qPCR were designed using Primer3 plus (Primer Biosoft) and are provided in Table 1.1. Each PCR reaction mix contained 50% of SYBR Premix, 0.2 μM of each forward and reverse primer, and 2 μl of diluted cDNA template by nuclease-free water. The initial 1 min denaturation was followed by 40 cycles of denaturation for 5 s at 95 °C, annealing and extension for 1 min at 60 °C. To ensure the specificity of the PCR amplicons, the temperature of the sample was gradually raised from 60 to 95 °C as the last step of the PCR reaction and a melting curve analyzed. The primers were successfully tested in the different cDNA samples of the Japanese eel, evaluating that each primer should amplify a single product, reflected as a single peak in the melting curve analysis. The relative mRNA expression levels of target genes were calculated using the $\Delta\Delta$Ct method, and the reference gene was virtually defined as the average of the threshold cycles (Ct) for EF1*α*.

Table 1.1. Primer sets in this study.

Gene ID	Oligo ID	Sequence	Product size (bp)
EF1α	Forward	5′–TCACCCTGGGAGTAAAGCAG–3′	222
	Reverse	5′–TCCATCCCTTGAACCAGGAC–3′	
Opn4x1	Forward	5′–GGATCACCTCCATGATCACC–3′	189
	Reverse	5′–GGCCCTCTGGAATGTATGAA–3′	
Opn4x2	Forward	5′–GAGTGGGTGTTCGGTGAACT–3′	191
	Reverse	5′–GAGTACAGCCACACCAGCAG–3′	
Opn4m1	Forward	5′–AATTCCACCGCATGAAGAAC–3′	197
	Reverse	5′–GATTATGGGGTTGTGGATGG–3′	
Opn4m2	Forward	5′–ACTGCAACGGGACATTTAGG–3′	226
	Reverse	5′–CAGAACGCGTAGATCACCAG–3′	
Peropsin	Forward	5′–ATGTCTGTGATTGCGGTGAA–3′	212
	Reverse	5′–AGGCACACAATGGAGTAGGG–3′	
Opn5–like	Forward	5′–CCAGCCGAGTTCTTCATTGT–3′	177
	Reverse	5′–TGTGAGGTTGGTCAGACTGC–3′	
Opn5	Forward	5′–GCCTCCAAATTGTCGAAAGA–3′	191
	Reverse	5′–GGCTTCCCTGTGACTGTGAT–3′	
Opn3	Forward	5′–TTGCCTTCACTATCGGAACC–3′	194
	Reverse	5′–TATCCACCCTCCTTTGATGC–3′	
TMT1	Forward	5′–TTGGAACTCCGTTCAGCTTT–3′	161
	Reverse	5′–GGAGGCCATCATGGTACAGT–3′	
TMT2	Forward	5′–GCTGGGCTGGAGTAGTTACG–3′	187
	Reverse	5′–GATCTTCCCCACCTGTTTGA–3′	
TMT3	Forward	5′–TTCGTCTTCTGCCTGTTCCT–3′	161
	Reverse	5′–AGCAGGTAGCAGGACACCAT–3′	
VA–opsin	Forward	5′–CAGCTACACCACCAGCAAGA–3′	205
	Reverse	5′–CGGTTTCCTGGCATTACCTA–3′	
Parapinopsin	Forward	5′–CTGGAGGGGGTAAAGACCTC–3′	227
	Reverse	5′–ACAATTACCATGCGGGCTAC–3′	
SWS2	Forward	5′–AGATGGTGGTGGTGATGGT–3′	169
	Reverse	5′–GACGTAGATGACGGGGTTG–3′	
Rh2	Forward	5′–CACCCAGAAAGCAGAGAAGG–3′	173
	Reverse	5′–ACGCTGAGCTCTTGGAGAAG–3′	
Exo–Rhod	Forward	5′–GTGGCTGACCTCTTCATGGT–3′	189
	Reverse	5′–CACAGGCTTGCAGACCACTA–3′	
DSO	Forward	5′–TCACCATCGAGCACAAGAAG–3′	206
	Reverse	5′–AACCAGAGACCAGAGCGAAA–3′	
FWO	Forward	5′–CGATGTACACCTCCATGCAC–3′	185
	Reverse	5′–CATGATGGCATGGTTCTCAC–3′	

2.7. Histological anaysis

The eel testis was fixed in Bouin's fluid. Fixed testis samples were dehydrated through an ethanol series, embedded in paraffin wax, and sectioned to 7–8 μm thickness. Sectioned tissues were stained with Mayer's hematoxylin and eosin. State of the sexual maturation was classified into the following 2 stages: immature stage (spermatogonia and spermatocyte; Figure 1.3A) and maturation stage (fully spermatozoa; Figure 1.3B).

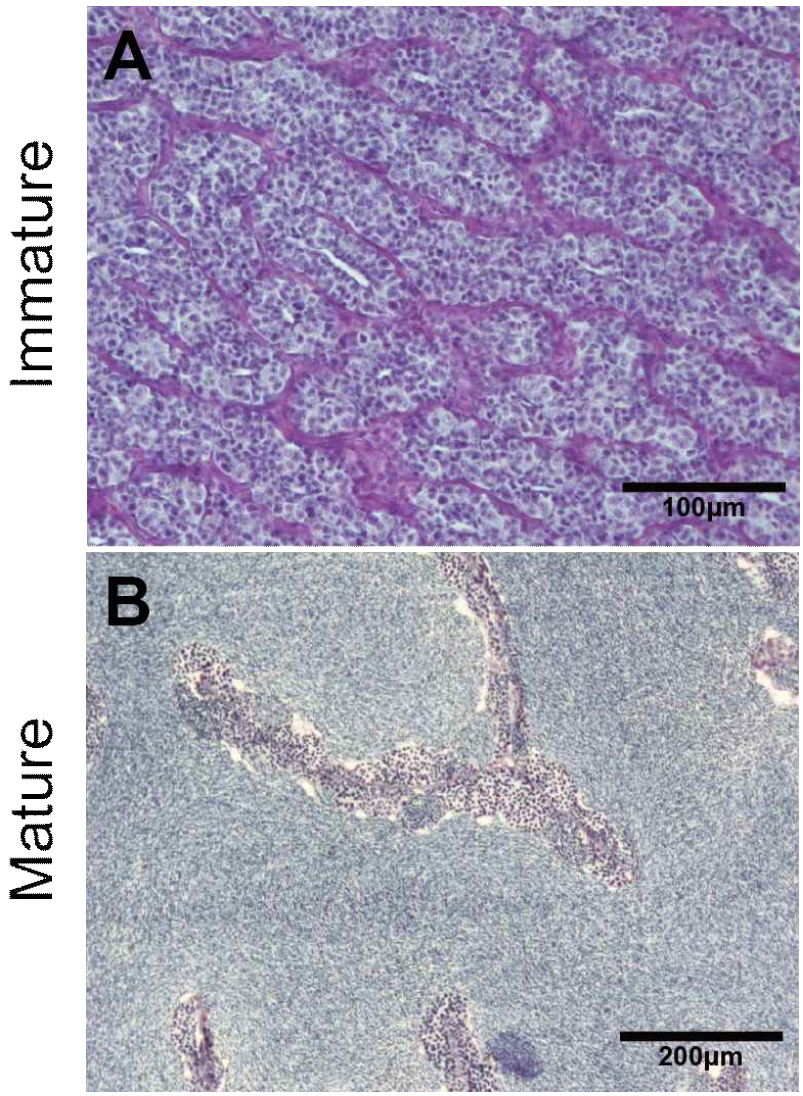

Figure 1.3. Microphotographs of histological sections of different stages of eel testis after hormonally induced sexual maturation. (A) immature testis, (B) mature testis.

2.8. Statistics

All statistical analyses were performed using GraphPad Prism 8.0.2 Software. Comparisons of opsin genes expression levels between sexually immature and mature group were performed by the Unparied t test. In the present study, $P < 0.05$ was accepted as statistically significant.

3. Results

3.1. RNA-Seq transcriptome analysis

Total RNA extracted from the whole brain and retinal tissues of Japanese eels were analyzed using the NGS method. After the adapter trimming and quality filtering, 150,898,925 paired-end reads were survived and used for *de novo* transcriptome reconstruction. As a result of cd-hit-est clustering, a total of 313,671 contigs (N50 = 965) were obtained. tBlastn and phylogenetic analysis revealed that a total of 18 opsin subfamilies were identified in the retina and the whole brain through RNA–seq (Figure 1.4). Among them, the visual opsin families of Japanese eels included rhodopsin2 or middle wave sensitive pigment (Rh2 or MWS), short wavelength-sensitive opsin 2 or blue light sensitive opsin (SWS2), fresh water rhodopsion (FWO), deep–sea water rhodopsin (DSO), and exo-rhodopsion (Exo–Rhod). The non-visual opsin families included four types of melanopsin subfamily (Opn4x1, Opn4x2, Opn4m1, and Opn4m2), peropsin, two types of neuropsin (Opn5-like, Opn5), Opn3 (encephalopsin), three types of teleost multiple tissue opsin (TMT1, TMT2, and TMT3), VA-opsin (vertebrate ancient opsin) and parapinopsin.

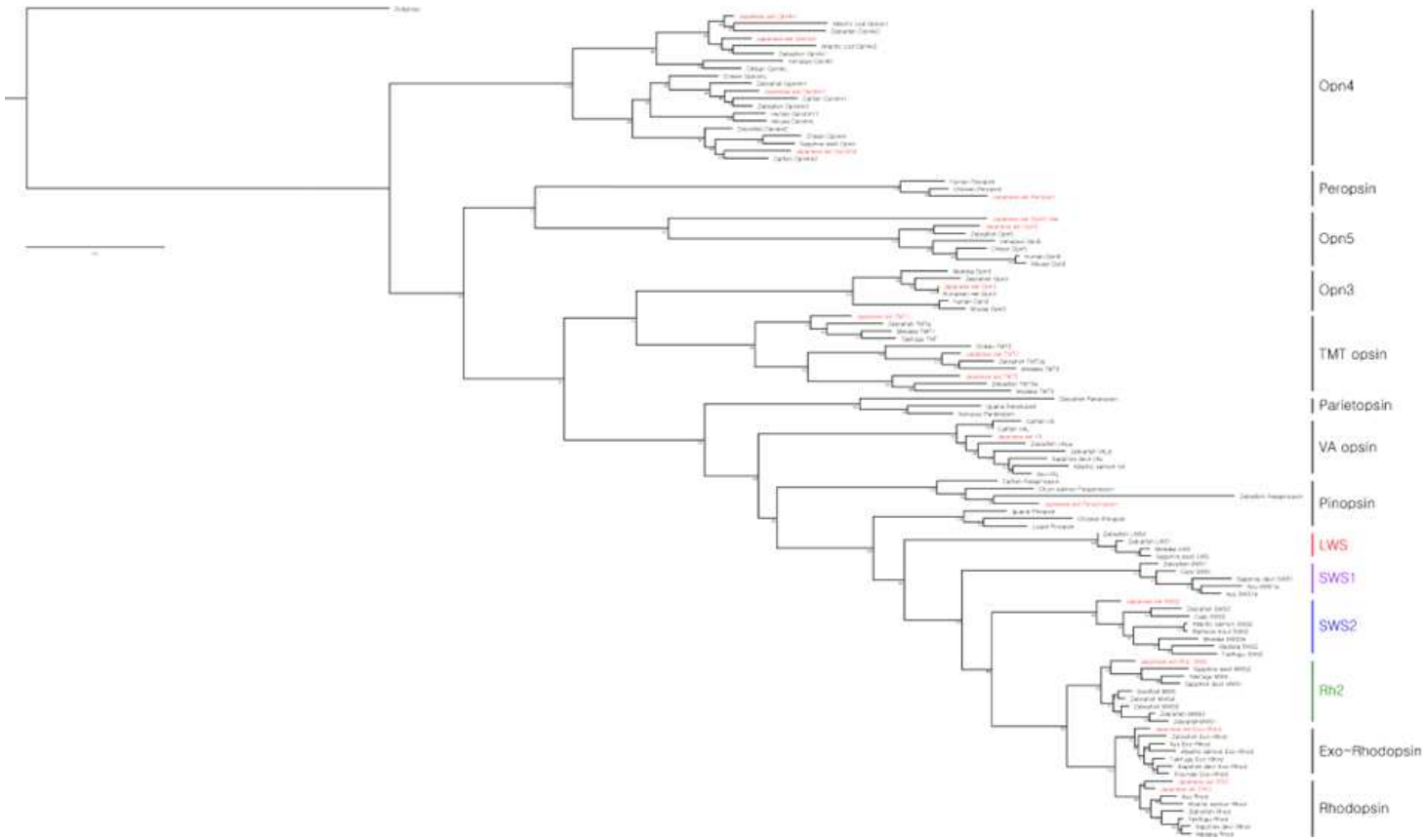

Figure 1.4. Phylogeny of vertebrate visual and non-visual opsins. One thousand bootstrap repetitions were performed and values are shown at the inner nodes. The zebrafish beta 1 adrenergic receptor was used as an outgroup to root the tree. Analysis was performed with multiple alignments from the amino acid sequence by using ClustalW program. Bold is indicated the visual and non-visual opsin families of Japanese eel, *A. japonica*.

3.2. Changes of GSI

Sexually immature and mature eels were classified based on the histological observation of testis before and after hCG treatment. In the beginning, spermatogonia was mostly observed in the testis of eel males. After eight weeks of hCG injection, spermiation was found in most of male eels, and spermatozoa was mostly observed in lobules. The gonadosomatic index (GSI) was 0.20 ± 0.01 at the beginning and was 25.7 ± 1.4 after maturation, showing a significant difference ($P > 0.0001$, Figure 1.5)

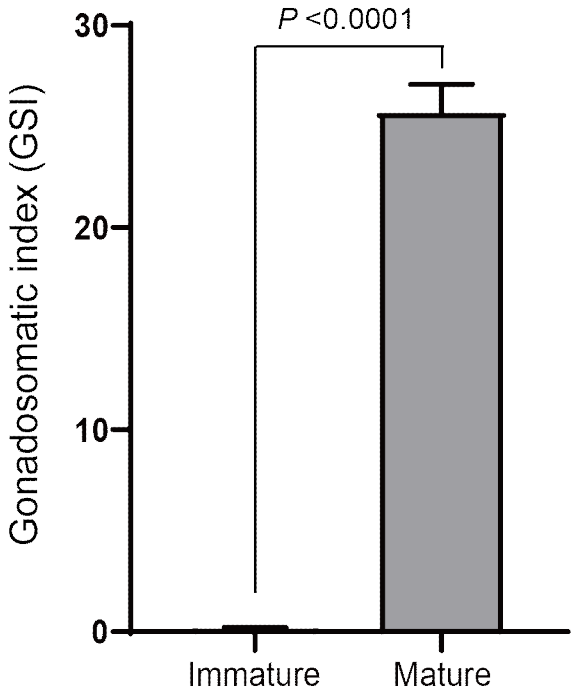

Figure 1.5. Changes of gonadosomatic index (GSI) after hormonally induced sexual maturation.

3.3. Changes in opsin family gene expression in the retina between sexually immature and mature eels

Eighteen opsin families identified using the RNA-Seq method were divided into visual opsin (Figure 1.6) and non-visual opsin (Figure 1.7) families. Then, the mRNA abundance in the retina of sexually immature and mature eels was analyzed using qPCR. In terms of visual opsin expression, the mRNA abundance of DSO increased in the sexually mature group (Figure 1.6B), whereas those of FWO and Rh2 were low in the sexually mature group (Figure 1.6C and 1.6D). Non-visual opsin mRNA showed no significant difference between sexually immature and mature groups (Figure 1.7).

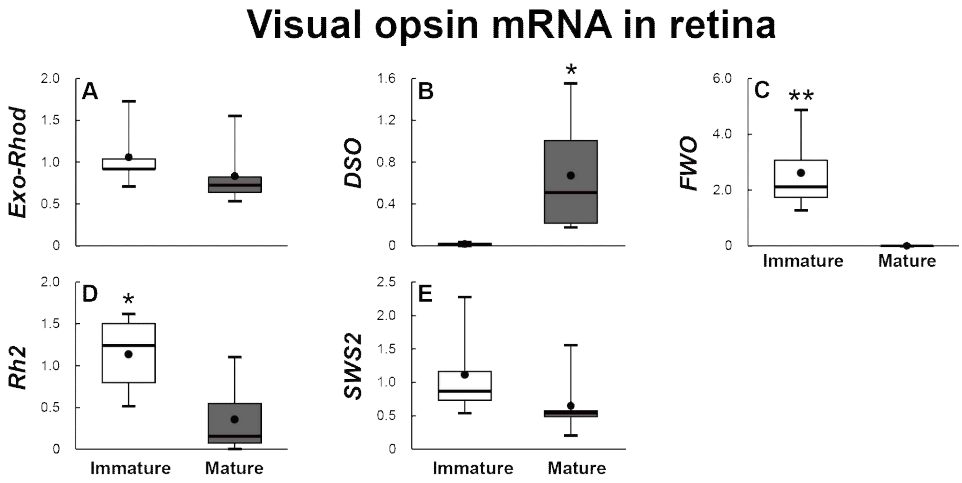

Figure 1.6. Visual opsin mRNA level in the retina of sexually immature and mature male Japanese eel. For the artificially induced sexual maturation, hCG was intraperitoneally injected to the experimental fish group (n = 6) at a concentration of 1 IU/g body weight. Immature fish was sampled before hCG injection (n = 6). Eight weeks after injection, retina was sampled and used for total RNA extraction and cDNA synthesis. The mRNA expression of visual opsin (A⁻E) in each sample was measured real-time qPCR. Box plots show min and max values (whiskers), first and third quartiles (box limits), and median (box inner line) of mRNA levels. The asterisk above each bar indicates significant differences according to the unpaired t test (*P < 0.05, **P < 0.01).

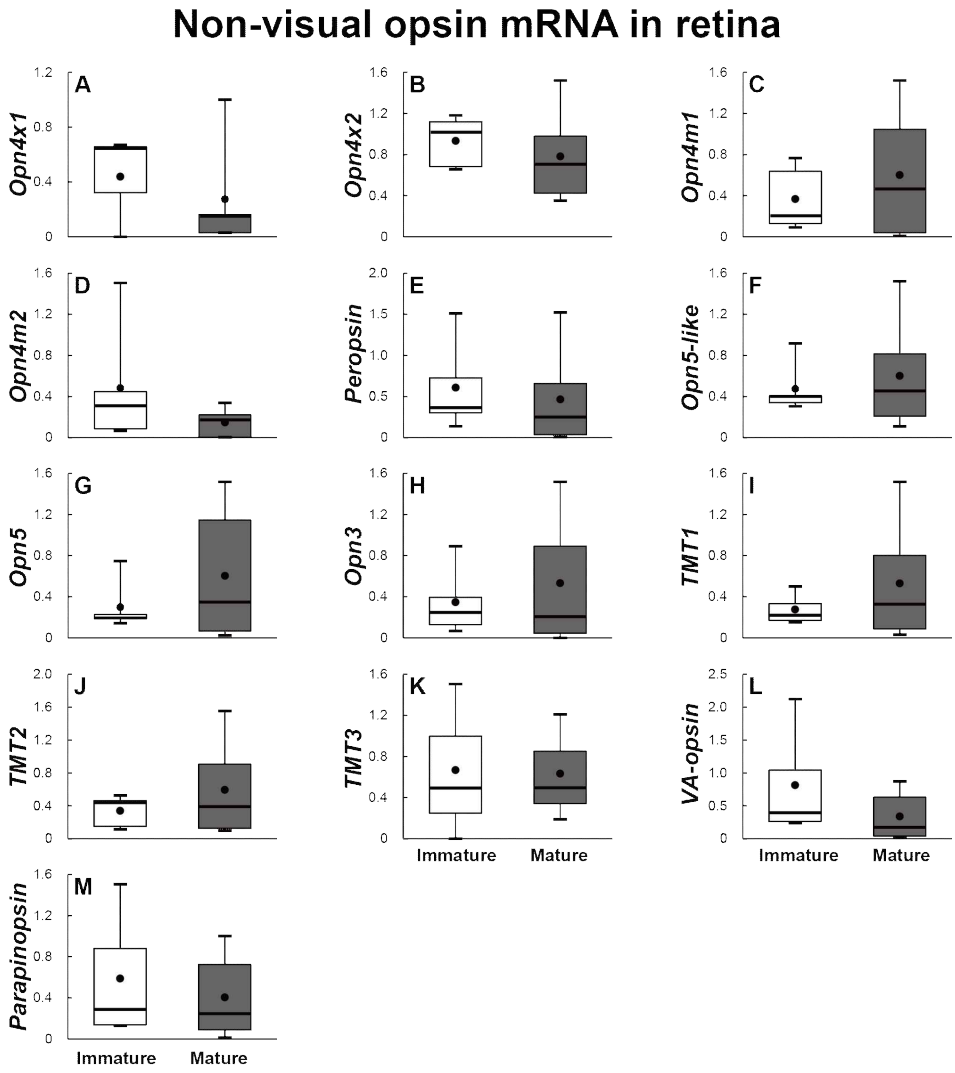

Figure 1.7. Non-visual opsin mRNA level in the retina of sexually immature and mature male Japanese eel. For the artificially induced sexual maturation, hCG was intraperitoneally injected to the experimental fish group (n = 6) at a concentration of 1 IU/g body weight. Immature fish was sampled before hCG injection (n = 6). Eight weeks after injection, retina was sampled and used for total RNA extraction and cDNA synthesis. The mRNA expression of non-visual opsin (A–M) in each sample was measured real-time qPCR. Box plots show min and max values (whiskers), first and third quartiles (box limits), and median (box inner line) of mRNA levels. The asterisk above each bar indicates significant differences according to the unpaired t test (*P < 0.05, **P < 0.01).

3.4. Changes in opsin family gene expression in brain of sexually immature and mature eels

The brains of the sexually immature and mature eels were dissected into the fore-brain, mid-brain, and hind-brain. Then, the opsin families that showed significant differences were investigated as in the retina ($P < 0.05$). In terms of visual opsin expression in the brain, DSO and SWS2 mRNA abundance increased in the fore-brain, mid-brain, and hind-brain of the mature group. Other visual opsin mRNAs did not show significant differences in whole brain part (Figure 1.8, 1.9, and 1.10). In terms of non-visual opsin expression in the brain, mRNA abundance of parapinopsin and Opn4m2 increased in the fore-brain of the mature group (Figure 1.11D), whereas that of TMT2 was low in the mature group (Figure 1.11J). Opn4m2 and parapinopsin mRNA abundance increased in the mid-brain (Figure 1.12D and 1.12F). TMT1 and TMT3 mRNA abundance increased in the hind-brain of the mature group (Figure 1.13I and 1.13K).

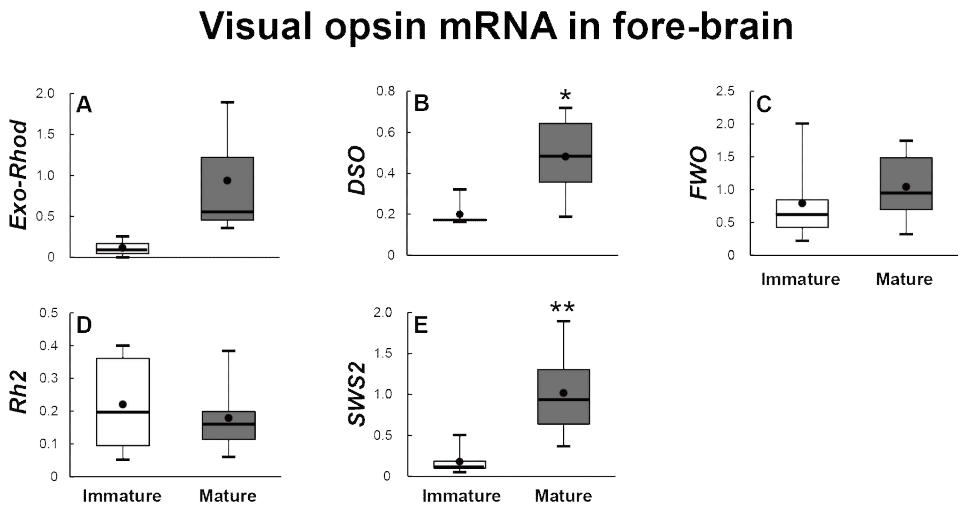

Figure 1.8. Visual opsin mRNA level in fore-brain of sexually immature and mature male Japanese eel. For the artificially induced sexual maturation, hCG was intraperitoneally injected to the experimental fish group (n = 6) at a concentration of 1 IU/g body weight. Immature fish was sampled before hCG injection (n = 6). Eight weeks after injection, brain was sampled and used for total RNA extraction and cDNA synthesis. The mRNA expression of visual opsin (A⁻E) in each sample was measured real-time qPCR. Box plots show min and max values (whiskers), first and third quartiles (box limits), and median (box inner line) of mRNA levels. The asterisk above each bar indicates significant differences according to the unpaired t test (*$P < 0.05$, **$P < 0.01$).

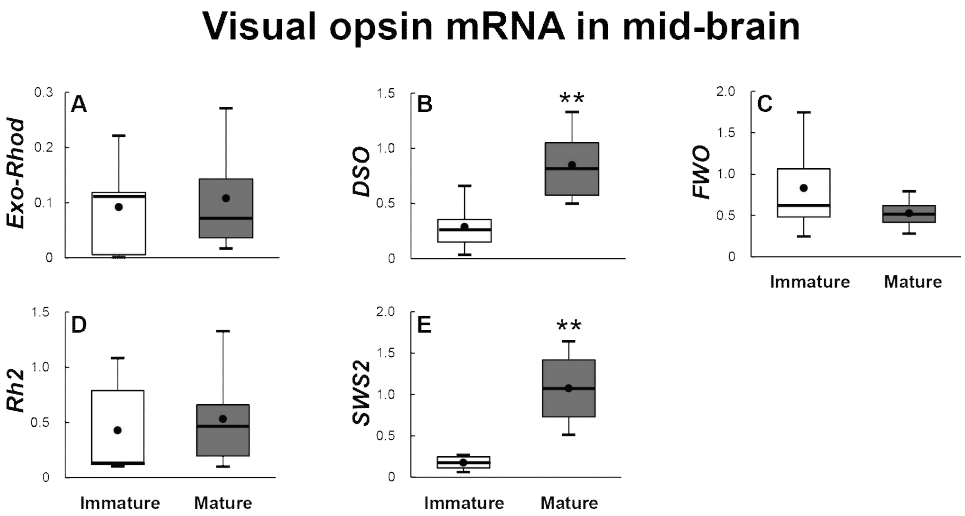

Figure 1.9. Visual opsin mRNA level in mid-brain of sexually immature and mature male Japanese eel. For the artificially induced sexual maturation, hCG was intraperitoneally injected to the experimental fish group (n = 6) at a concentration of 1 IU/g body weight. Immature fish was sampled before hCG injection (n = 6). Eight weeks after injection, brain was sampled and used for total RNA extraction and cDNA synthesis. The mRNA expression of visual opsin (A⁻E) in each sample was measured real-time qPCR. Box plots show min and max values (whiskers), first and third quartiles (box limits), and median (box inner line) of mRNA levels. The asterisk above each bar indicates significant differences according to the unpaired t test (*P < 0.05, **P < 0.01).

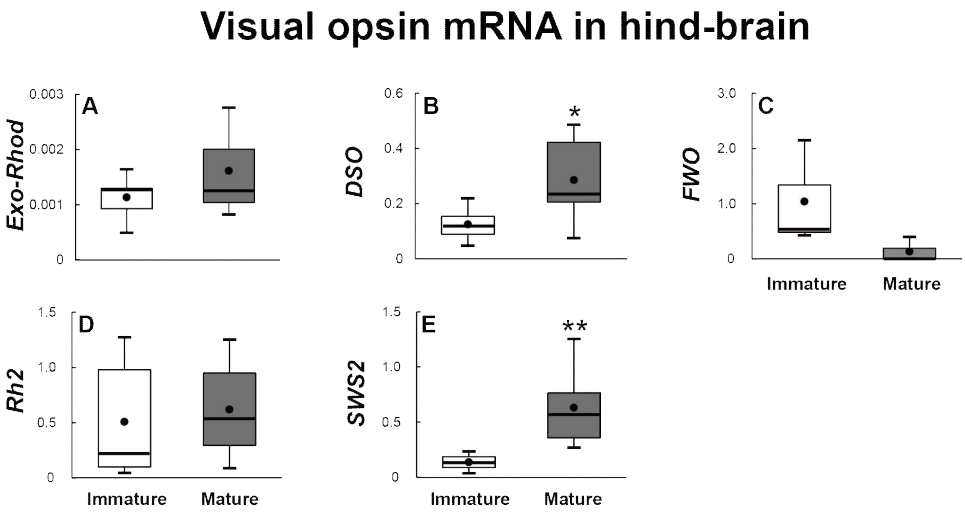

Figure 1.10. Visual opsin mRNA level in hind-brain of sexually immature and mature male Japanese eel. For the artificially induced sexual maturation, hCG was intraperitoneally injected to the experimental fish group (n = 6) at a concentration of 1 IU/g body weight. Immature fish was sampled before hCG injection (n = 6). Eight weeks after injection, brain was sampled and used for total RNA extraction and cDNA synthesis. The mRNA expression of visual opsin (A–E) in each sample was measured real-time qPCR. Box plots show min and max values (whiskers), first and third quartiles (box limits), and median (box inner line) of mRNA levels. The asterisk above each bar indicates significant differences according to the unpaired t test (*P < 0.05, **P < 0.01).

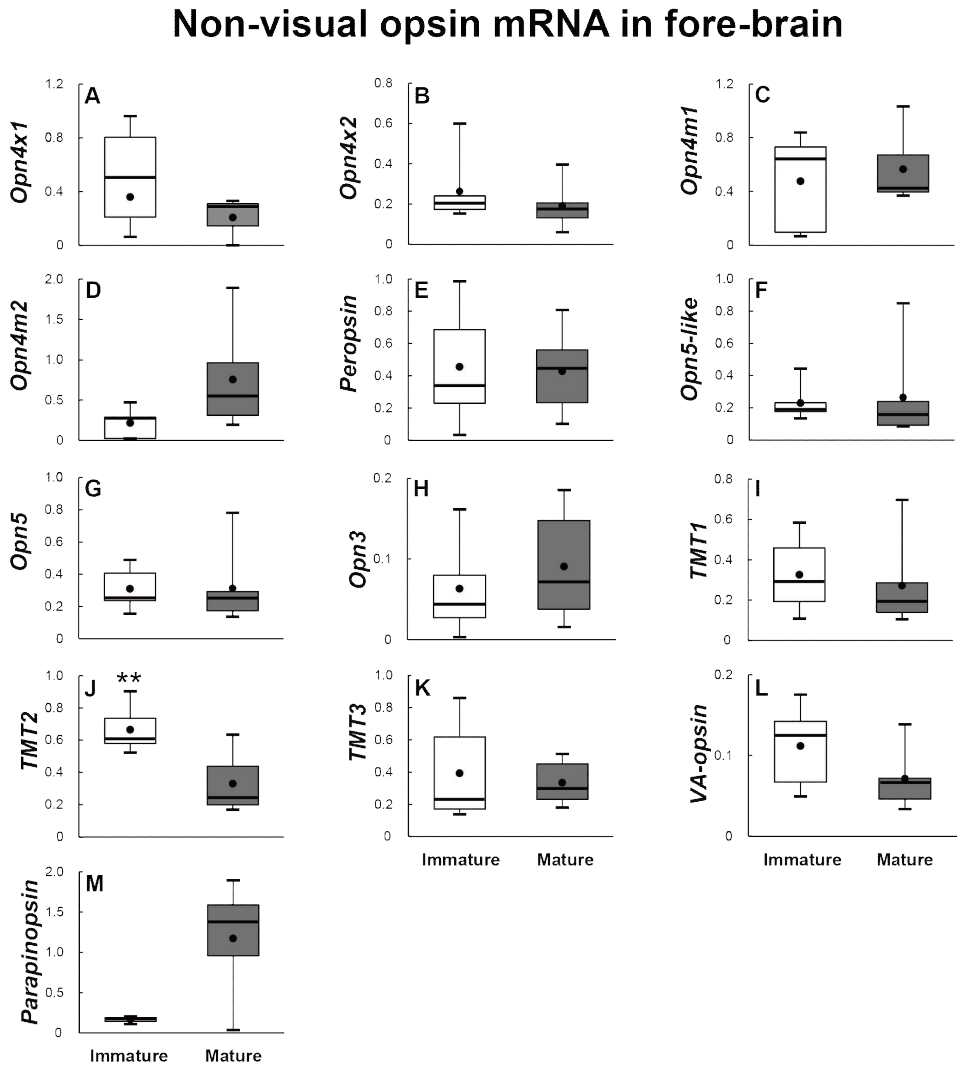

Figure 1.11. Non-visual opsin mRNA level in fore-brain of sexually immature and mature male Japanese eel. For the artificially induced sexual maturation, hCG was intraperitoneally injected to the experimental fish group (n = 6) at a concentration of 1 IU/g body weight. Immature fish was sampled before hCG injection (n = 6). Eight weeks after injection, brain was sampled and used for total RNA extraction and cDNA synthesis. The mRNA expression of non-visual opsin (A⁻M) in each sample was measured real-time qPCR. Box plots show min and max values (whiskers), first and third quartiles (box limits), and median (box inner line) of mRNA levels. The asterisk above each bar indicates significant differences according to the unpaired t test (*P < 0.05, **P < 0.01).

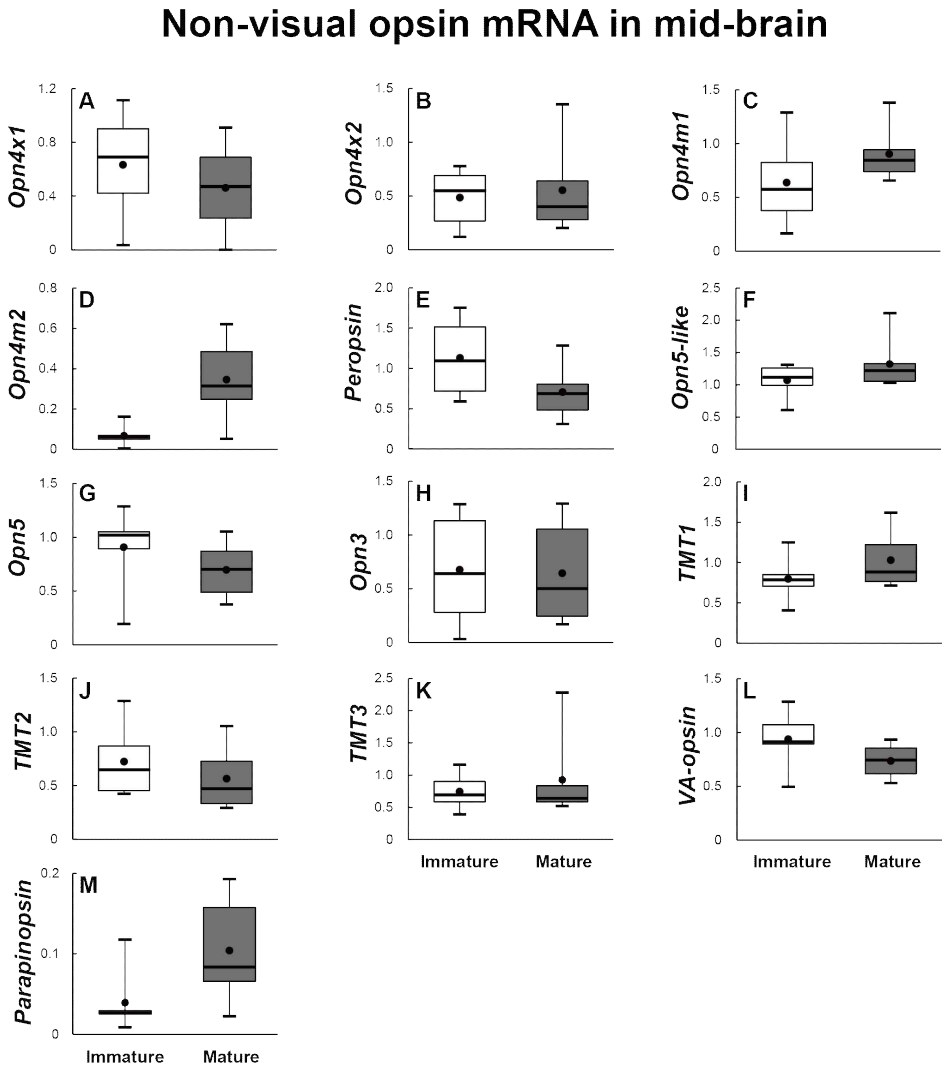

Figure 1.12. Non-visual opsin mRNA level in mid-brain of sexually immature and mature male Japanese eel. For the artificially induced sexual maturation, hCG was intraperitoneally injected to the experimental fish group (n = 6) at a concentration of 1 IU/g body weight. Immature fish was sampled before hCG injection (n = 6). Eight weeks after injection, brain was sampled and used for total RNA extraction and cDNA synthesis. The mRNA expression of non-visual opsin (A⁻M) in each sample was measured real-time qPCR. Box plots show min and max values (whiskers), first and third quartiles (box limits), and median (box inner line) of mRNA levels. The asterisk above each bar indicates significant differences according to the unpaired t test (*P < 0.05, **P < 0.01).

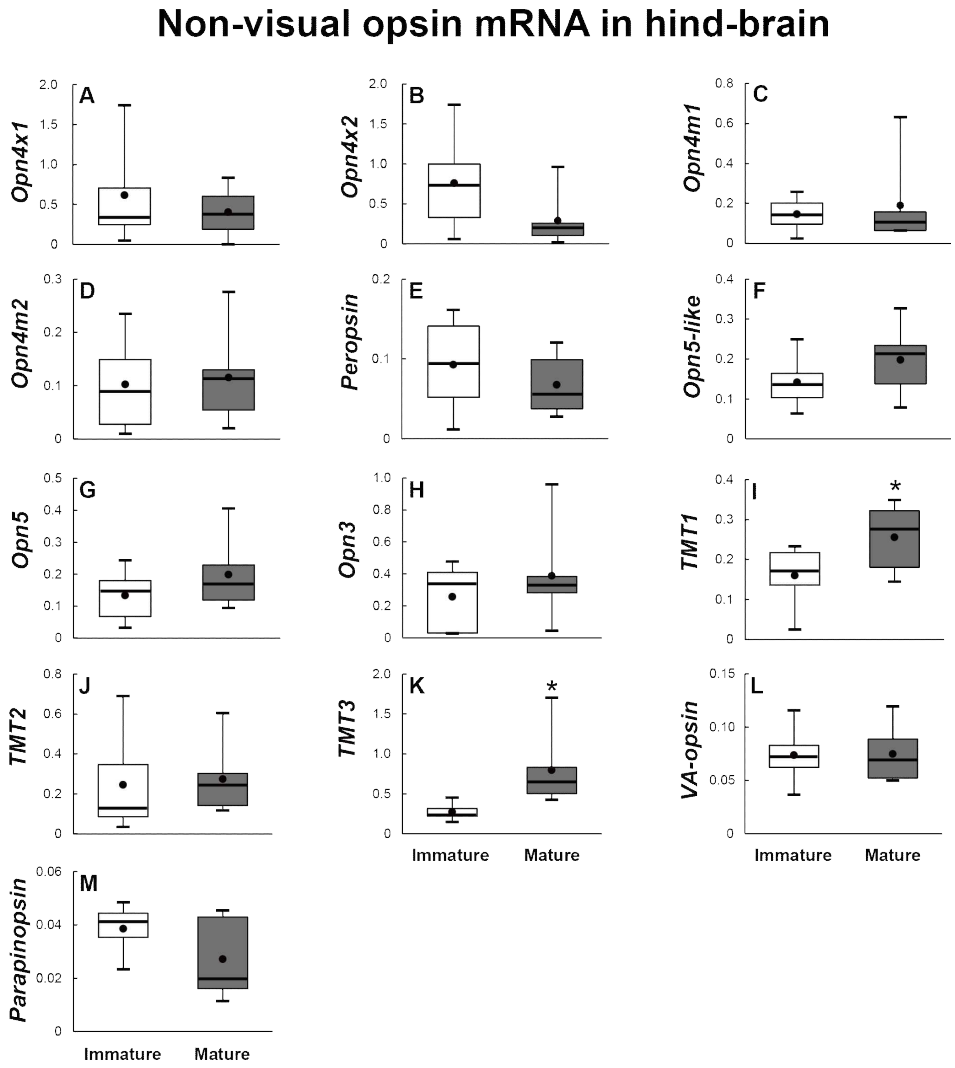

Figure 1.13. Non-visual opsin mRNA level in hind-brain of sexually immature and mature male Japanese eel. For the artificially induced sexual maturation, hCG was intraperitoneally injected to the experimental fish group (n = 6) at a concentration of 1 IU/g body weight. Immature fish was sampled before hCG injection (n = 6). Eight weeks after injection, brain was sampled and used for total RNA extraction and cDNA synthesis. The mRNA expression of non-visual opsin (A⁻M) in each sample was measured real-time qPCR. Box plots show min and max values (whiskers), first and third quartiles (box limits), and median (box inner line) of mRNA levels. The asterisk above each bar indicates significant differences according to the unpaired t test (*P < 0.05, **P < 0.01).

4. Discussion

RNA-Seq transcriptome analysis was performed to examine 18 photoreceptor genes in the retina and whole brain of Japanese eels. As a result, two types of cone opsin (SWS2, Rh2) were identified. However, the presence of a long wavelength-sensitive pigment (LWS) in the long wavelength region was not confirmed in this study. In general, organisms must have at least two cone opsin with different spectra to distinguish colors. Species with one type of cone opsin are considered as ‘‘monochromatic vision’’ or color-blind (Bowmaker et al., 1994). Eels have two or more cone opsin, so they can recognize colors. However, they recognize the wavelength of the narrower region compared with other animals or other fish species. A study suggested that the European eel has two types of cone opsin subfamily, Rh2 (or MWS) and SWS2 cones, so it can distinguish colors (Cottrill et al., 2009). However, the giant mottled eel showed only one type of cone cell that detected a limited range of the optical spectrum (λmax) of 500 nm to 535 nm (Wang et al., 2014). Japanese eels are genetically and ecologically similar European eels; thus, it is presumed that they can recognize colors through two types of cone opsin. In addition, Japanese eels are nocturnal fish and have evolved in a way that they have adapted to dark habitat and/or nocturnal habits. Thus, it is considered that their photoreceptors recognizing the light spectrum of the long wavelength band region may have been functionally atrophied or photoreceptor may have not existed. Similarly, species living in deep-sea or those evolved to adapt to dark environments have been reported to have fewer cone opsins (Mas-Riera, 1991; Pankhurst & Conroy, 1987). SWS1 and LWS gene expression levels were higher in fresh water fish than those in fish inhabiting seawater (Lin et al., 2017). This is because in most freshwater environments, most of the ultraviolet rays penetrating the water surface can be recognized by organisms because of low water depth, while the fish living in deep-sea (50 m or more) tend to lose the LWS gene because the long wavelength

(red) is not transmitted to deep-sea regions (Lin et al., 2017).

Japanese eel, which was investigated in this study, live in a shallow freshwater region during most of their life span except for spawning. This eel will migrate to deep-sea area of at least 100 m (Cottrill et al., 2009; Tsukamoto, 1992). Regarding this, they may share some genetic characteristics with the deep-sea fish and in this study cone opsin was predicted to be one of the possible genes. The distribution and physiological function of cone opsin appear to be different depending on the level of ecological evolution. In Anguillid sp., only four types opsins (DSO, FWO, Rh2 and SWS2) (Cottrill et al., 2009; Zhang et al., 2000) were studied. Therefore, it is necessary to carry out additional molecular biological and biochemical studies on the range of recognition of color in eels. In this study, opsin families were identified through RNA-seq method, and then highly expressed genes in the retina and brain were analyzed by qPCR. As a result, Parapinopsin mRNA was predominantly expressed in the whole brain, but peropsin and Opn5 were relatively highly expressed in the retina. According to previous studies on opsin expression, the expression of rhodopsin genes in the retina and brain in the ayu (Masuda et al., 2003; Minamoto & Shimizu, 2003), Atlantic salmon (Philp et al., 2000), Japanese eel (Zhang et al., 2000), and percomorph fishes (Cortesi et al., 2015), showed different photoreceptor types and expression sites. However, only the limited physiological function of opsin has been reported.

Non-visual opsin was named in the 1990s, and it has been known to affect circadian rhythms in mammals, reproduction in birds, light avoidance in amphibian larvae, and neural development during egg development in fish (Beaudry et al., 2017). A study on non-visual opsin showed Opn4 expression in the retinal ganglion in mammals, but Opn4 gene was expressed in the retina, brain and skin in non-mammals (Bellingham et al., 2006). In addition, VA-opsin is known to be expressed in the hypothalamus and gonads in birds and fish, and it directly stimulates GnRH in the hypothalamus by recognizing wavelength changes due to photoperiod changes (Davies, Hankins & Foster, 2010; Grone et al., 2007). TMT

opsin is expressed in most tissues and embryos in the case of zebrafish. In case of medaka, TMT and Opn3 are expressed in nerve tissues (retina and brain) (Sato, Nwe & Ohuchi, 2021). In particular, TMT opsin is expressed in cell lines associated with light entrain able clock (Moutsaki et al., 2003).

In this study, DSO expression increased, and FWO, Opn4m2, VA-opsin, SWS2 and Rh2 expression decreased in the retina during sexual maturation. All of the three brain areas showed the increased DSO and SWS2 expressions. Consistent with the results of this study, a previous study on the photoreceptors of the Japanese eel, reported that DSO expression increased and FWO expression decreased in silver eels (Zhang et al., 2000). In the case of European eel, DSO expression also increased to make eels adapt to the environment before the spawning migration in the early sexual maturation stage. In the late sexual maturation stage, European eels enter deep-sea beyond 100 m depth to spawn, thereby showing a decrease in FWO expression (Zhang et al., 2000). In addition, Japanese conger eel changes its habitat environment from fresh water to open sea while moving from juvenile stage to sexual maturation. To adapt to the changed environment, FWO was mainly expressed in the retina during the juvenile stage, and then DSO expression started to be increased during sexual maturation (Zhang et al., 2002). This may have resulted from Japanese conger eel's adaptation to the environmental change related to light in the process of migrating to the spawning ground. Also, incase of deep-sea fishes, adult rely on rod-dominated or rod-only visual system (Lupše et al., 2021). Analysis of opsin family gene mRNA levels in the Japanese eel brain before and after maturation showed that DSO and SWS2 expressions increased after maturation in all three areas of brain. In addition, DSO expression increased in the retina after maturation, suggesting that DSO is closely related to maturation. However, it is unclear whether the increase in DSO and SWS2 expressions in the brain affects maturation.

In recent years, there have been some studies on the reproductive physiological function of VA-opsin belonging to the non-visual opsin (deep brain photoreceptor) family in the brain. VA opsin was identified from Atlantic salmon (Soni & Foster,

1997), Crimson snapper (Liang et al., 2022), and VA-long (VAL-opsin) was discovered in zebra fish (Kojima, Mano & Fukada, 2000). Immunohistochemistry studies on Atlantic salmon have reported the existence of opsin-like protein in the hypothalamic nucleus magnocellularis preopticus, suggesting its potential gonadal development control function. There have been few studies on non-visual opsin in the brain, especially its relevance to gonadal development. However, photoperiod action did not influence the gonadal development in ayu without both eyes and pineal gland (Suzuki, 1975), and opsin immune-positive fibers passing through basal hypothalamus were observed in the hypothalamus of Atlantic salmon (Philp et al., 2000). These results suggest that the opsin present in the brain directly affects gonadal development. The level of expression of GnRH located at the top of the BPG axis directly affects reproduction. It is unclear as to whether VA-opsin regulates the expression level of GnRH in the hypothalamus of Japanese quail, but VA-opsin, which affected GnRH expression, was identified in GnRH cells (García-Fernández et al., 2015). Other opsin subfamilies other than VA-opsin may also affect the reproduction system in the hypothalamus, but more research is needed to investigate this hypothesis.

5. References

Beaudry FEG, Iwanicki TW, Mariluz BRZ, Darnet S, Brinkmann H, Schneider P, Taylor JS. 2017. The non-visual opsins: eighteen in the ancestor of vertebrates, astonishing increase in ray-finned fish, and loss in amniotes. Journal of Experimental Zoology Part B: Molecular and Developmental Evolution. 328(7):685–696. DOI 10.1002/jez.b.22773.

Bellingham J, Chaurasia SS, Melyan Z, Liu C, Cameron MA, Tarttelin EE, Iuvone PM, Hankins MW, Tosini G, Lucas RJ. 2006. Evolution of melanopsin photoreceptors: discovery and characterization of a new melanopsin in nonmammalian vertebrates. PLOS Biology. 4(8):e254. DOI 10.1371/journal. pbio.0040254.

Bellingham J, Tarttelin EE, Foster RG, Wells DJ. 2003. Structure and evolution of the Teleost extraretinal rod-like opsin (errlo) and ocular rod opsin (rho) genes: is teleost rho a retrogene? Journal of Experimental Zoology Part B: Molecular and evelopmental Evolution. 297(1):1–10.

Bolger AM, Lohse M, Usadel B. 2014. Trimmomatic: a flexible trimmer for Illumina sequence data. Bioinformatics. 30:2114–2120. DOI 10.1093/bioinformatics/btu170.

Bowmaker JK. 2008. Evolution of vertebrate visual pigments. Vision Research. 48(20):2022–2041. DOI 10.1016/j.visres.2008.03.025.

Bowmaker JK, Govardovskii VI, Shukolyukov SA, Zueva LV, Hunt DM, Sideleva VG, Smirnova OG. 1994. Visual pigments and the photic environment: the Cottoid fish of Lake Baikal. Vision Research. 34(5):591–605. DOI 10.1016/0042-6989(94)90015-9.

Collin SP, Davies WL, Hart NS, Hunt DM. 2009. The evolution of early vertebrate photoreceptors. Philosophical Transactions of the Royal Society B: Biological Sciences. 364(1531):2925–2940. DOI 10.1098/rstb.2009.0099.

Cortesi F, Musilová Z, Stieb SM, Hart NS, Siebeck UE, Malmstrøm M, Tørresen

OK, Jentoft S, Cheney KL, Marshall NJ, Carleton KL, Salzbuger W. 2015. Ancestral duplications and highly dynamic opsin gene evolution in percomorph fishes. Proceedings of the National Academy of Sciences of the United States of America. 112(5):1493–1498. DOI 10.1073/pnas.1417803112.

Cottrill PB, Davies WL, Semo M, Bowmaker JK, Hunt DM, Jeffery G. 2009. Developmental dynamics of cone photoreceptors in the eel. BMC Developmental Biology. 9(1):71. DOI 10.1186/1471-213X-9-71.

Davies WL, Hankins MW, Foster RG. 2010. Vertebrate ancient opsin and melanopsin: divergent irradiance detectors. Photochemical & Photobiological Sciences. 9(11): 1444–1457. DOI 10.1039/c0pp00203h.

Doyle SE, Yoshikawa T, Hillson H, Menaker M. 2008. Retinal pathways influence temporal niche. Proceedings of the National Academy of Sciences of the United States of America. 105(35):13133–13138. DOI 10.1073/pnas.0801728105.

García-Fernández JM, Cernuda-Cernuda R, Davies WI, Rodgers J, Turton M, Peirson SN, Follett BK, Halford S, Hughes S, Hankins MW, Foster RG. 2015. The hypothalamic photoreceptors regulating seasonal reproduction in birds: a prime role for VA opsin. Frontiers in Neuroendocrinology. 37:13–28. DOI 10.1016/j.yfrne.2014.11.001.

Grabherr MG, Haas BJ, Yassour M, Levin JZ, Thompson DA, Amit I, Adiconis X, Fan L, Raychowdhury R, Zeng Q, Chen Z, Mauceli E, Hacohen N, Gnirke A, Rhind N, Palma FD, Birren BW, Nusbaum C, Lindblad-Toh K, Friedman N, Regev A. 2011. Full-length transcriptome assembly from RNA-Seq data without a reference genome. Nature Biotechnology. 29(7):644–652. DOI 10.1038/nbt. 1883.

Grone BP, Zhao S, Chen CC, Fernald RD. 2007. Localization and diurnal expression of melanopsin, vertebrate ancient opsin, and pituitary adenylate cyclase-activating peptide mRNA in a teleost retina. Journal of Biological Rhythms. 22(6):558–561. DOI 10.1177/0748730407308285.

Hastings M, Maywood ES. 2000. Circadian clocks in the mammalian brain.

Bioessays. 22:23−31. DOI 10.1002/(SICI)1521-1878(200001)22:1<23::AID-BIES6>3.0.CO;2-Z.

Kim D, Pertea G, Trapnell C, Pimentel H, Kelley R, Salzberg SL. 2013. TopHat2 accurate alignment of transcriptomes in the presence of insertions, deletions and gene fusions. Genome Biology. 14:R36. DOI 10.1186/gb-2013-14-4-r36.

Kojima D, Fukada Y. 1999. Non-visual photoreception by a variety of vertebrate opsins. Rhodopsin and Phototransduction. 224:265−282.

Kojima D, Mano H, Fukada Y. 2000. Vertebrate ancient-long opsin: a green-sensitive photoreceptive molecule present in zebrafish deep brain and retinal horizontal cells. Journal of Neuroscience. 20:2845−2851. DOI 10.1523/JNEUROSCI.20-08-02845.2000.

Langmead B, Salzberg SL. 2012. Fast gapped-read alignment with Bowtie 2. Nature Methods. 9:357−359. DOI 10.1038/nmeth.1923.

Li W, Godzik A. 2006. Cd-hit: a fast program for clustering and comparing large sets of protein or nucleotide sequences. Bioinformatics. 22:1658−1659. DOI 10.1093/bioinformatics/btl158.

Liang Q, Afriyie G, Chen Z, Xu Z, Dong Z, Guo Y, Wang Z. 2022. Analysis of opsin gene family of Crimson snapper (*Lutjanus erythropterus*). Gene. 807:145960. DOI 10.1016/j.gene.2021.145960.

Lin JJ, Wang FY, Li WH, Wang TY. 2017. The rises and falls of opsin genes in 59 rayfinned fish genomes and their implications for environmental adaptation. Scientific Reports. 7:15568. DOI 10.1038/s41598-017-15868-7.

Lupše N, Cortesi F, Freese M, Marohn L, Plhlmann JD, Wysujack K, Hanel R, Musilova Z. 2021. Visual gene expression reveals a cone-to-rod developmental progression in deep-sea fishes. Molecular Biology and Evolution. 38:566-5677. DOI 10.1093/molbev/msab281.

Mas-Riera J. 1991. Changes during growth in the retinal structure of three hake species, *Merluccius* spp. (Teleostei: Gadiformes), in relation to their depth distribution and feeding. Journal of Experimental Marine Biology and Ecology.

152(1):91−104. DOI 10.1016/0022-0981(91)90137-L.

Masuda T, Iigo M, Mizusawa K, Aida K. 2003. Retina-type rhodopsin gene expressed in the brain of a teleost, ayu (*Plecoglossus altivelis*). Zoological Science. 20:989−997. DOI 10.2108/zsj.20.989.

Minamoto T, Shimizu I. 2003. Molecular cloning and characterization of rhodopsin in a teleost (*Plecoglossus altivelis*, Osmeridae). Comparative Biochemistry and Physiology Part B: Biochemistry and Molecular Biology. 134:559−570. DOI 10.1016/S1096-4959(03)00030-7.

Moutsaki P, Whitmore D, Bellingham J, Sakamoto K, David-Gray ZK, Foster RG. 2003. Teleost multiple tissue (tmt) opsin: a candidate photopigment regulating the peripheral clocks of zebrafish? Molecular Brain Research. 112(1-2):135−145. DOI 10.1016/S0169-328X(03)00059-7.

Nariai N, Kojima K, Mimori T, Sato Y, Kawai Y, Yamaguchi-Kabata Y, Nagasaki M. 2014. TIGAR2: sensitive and accurate estimation of transcript isoform expression with longer RNA-Seq reads. BMC Genomics. 15:S5. DOI 10.1186/1471-2164-15-S10-S5.

Okano T, Yoshizawa T, Fukada Y. 1994. Pinopsin is a chicken pineal photoreceptivemolecule. Nature. 372:94−97. DOI 10.1038/372094a0.

Pankhurst NW, Conroy AM. 1987. Seasonal changes in reproductive condition and plasma levels of sex steroids in the blue cod, *Parapercis colias* (Bloch and Schneider) (Mugiloididae). Fish Physiology and Biochemistry. 4(1):15−26. DOI 10.1007/BF02073862.

Philp AR, Garcia-Fernandez JM, Soni BG, Lucas RJ, Bellingham J, Foster RG. 2000. Vertebrate ancient (VA) opsin and extraretinal photoreception in the Atlantic salmon (*Salmo salar*). Journal of Experimental Biology. 203:1925−1936.

Pugh EN, Lamb TD. 2000. Chapter 5 Phototransduction in vertebrate rods and cones: molecular mechanisms of amplification, recovery and light adaptation. Handbook of Biological Physics. 3:183−255. DOI 10.1016/S1383-8121(00)80008-1.

Sakata R, Kabutomori R, Okano K, Mitwui H, Takemura A, Miwa T, Yamamoto H,

Okano T. 2015. Rhodopsin in the dark hot sea: molecular analysis of rhodopsin in a Snailfish, *Careproctus rhodomelas*, living near the deep-sea hydrothermal vent. PLOS ONE. 10(8):e0135888. DOI 10.1371/journal.pone.0135888.

Sato D, Nwe KN, Ohuchi H. 2021. The Opsin 3/Teleost multiple tissue opsin system: mRNA localization in the retina and brain of medaka (*Oryzias latipes*). Journal of Comparative Neurology. 529:2484-2516. DOI 10.1002/cne.25106.

Schmieder R, Edwards R. 2011. Quality control and preprocessing of metagenomic datasets. Bioinformatics. 27:863–864. DOI 10.1093/bioinformatics/btr026.

Shand J, Hart NS, Thomas N, Partridge JC. 2002. Developmental changes in the cone visual pigments of black bream *Acanthopagrus butcheri*. Journal of Experimental Biology. 205:3661–3667.

Soni BG, Foster RG. 1997. A novel and ancient vertebrate opsin. FEBS Letters. 406:279–283. DOI 10.1016/S0014-5793(97)00287-1.

Stamatakis A. 2014. RAxML version 8: a tool for phylogenetic analysis and post-analysis of large phylogenies. Bioinformatics. 30:1312–1313. DOI 10.1093/bioinformatics/btu033.

Suzuki K. 1975. The significance of photoperiod on the gonadal development of ayu *Plecoglossus altivelis*. K Suzuki Doctral dissertation, University of Tokyo, Tokyo.

Tada T, Altun A, Yokoyama S. 2009. Evolutionary replacement of UV vision by violet vision in fish. Proceedings of the National Academy of Sciences of the United States of America. 106(41):17457–17462. DOI 10.1073/pnas.0903839106.

Tatsukawa K. 2003. Eel resources in East Asia. In: Eel Biology. Tokyo: Springer Japan, 293–298. DOI 10.1007/978-4-431-65907-5_20.

Terakita A. 2005. The opsins. Genome Biology. 6:213. DOI 10.1186/gb-2005-6-3-213.

Tsukamoto K. 1992. Discovery of the spawning area for Japanese eel. Nature. 356:789–791. DOI 10.1038/356789a0.

Van Gelder RN. 2001. Non-visual ocular photoreception. Ophthalmic Genetics. 22(4):195–205. DOI 10.1076/opge.22.4.195.2215.

Wang FY, Fu WC, Wang IL, Yan HY, Wang TY. 2014. The giant Mottled Eel, *Anguilla marmorata*, used blue-shifted rod photoreceptors during upstream migration. PLOS ONE. 9(8):e103953. DOI 10.1371/journal.pone.0103953.

Zhang H, Futami K, Horie N, Okamura A, Utoh T, Mikawa N, Yamada Y, Tanaka S, Okamoto N. 2000. Molecular cloning of fresh water and deep-sea rod opsin genes from Japanese eel *Anguilla japonica* and expressional analyses during sexual maturation. FEBS Letters. 469(1):39−43. DOI 10.1016/S0014-5793(00) 01233-3.

Zhang H, Futami K, Yamada Y, Horie N, Okamura A, Utoh T, Mikawa N, Tanaka S, Okamoto N, Oka HP. 2002. Isolation of freshwater and deep-sea type opsin genes from the common Japanese conger. Journal of Fish Biology. 61:313−324. DOI 10.1111/j.1095-8649.2002.tb01568.x.

Chapter Ⅱ

Testis development in the Japanese eel is affected by photic signals through melatonin secretion

Abstract

According to reported spawning characteristics of Japanese eel, *Anguilla japonica*, which exhibit spawning and migration patterns that are synchronized with lunar cycles and photoperiod, we hypothesized that a close association exists between specific photic signals (daylight, daylength, and moonlight) and endocrinological regulation. Given the photic control in melatonin secretion, this hypothesis was tested by investigating whether melatonin signals act as mediators relaying photic signals during testis development in the eel. We examined changes in melatonin-secretion patterns using time-resolved fluorescence immunoassays in sexually immature and mature male Japanese eels under the condition of a new moon (NM) and a full moon (FM). The eye and plasma melatonin levels exhibited a nocturnal pattern under a 12-h light: dark cycle (12L12D) or under constant darkness (DD), but not with constant light (LL). Eye melatonin levels were similar under the 12L12D and short-photoperiod (9L15D) conditions. In the long-photoperiod condition (15L9D), secreted plasma melatonin levels were stable, whereas short-day melatonin secretion began when darkness commenced. Sexual maturation began at 8 weeks following intraperitoneal injection of human chorionic gonadotropin (hCG), and NM exposure led to significantly higher eye and plasma melatonin levels compared with those detected under FM exposure.

1. Introduction

Many animals sense photic cues that are used in physiological processes (Bromage, Porter & Randall, 2001). Currently, the known key aspects of photic cues include exposure time (duration) of daylight, intensity, and spectrum. Photoperiod changes occur periodically and predictably, whereas the light quality is more difficult to predict, and different organisms show varying degrees of photo-sensitivity depending on ecological conditions (Mazurais et al., 2000; Migaud et al., 2006). Effects of photoperiodic changes can be described for species inhabiting a temperate zone; however, such descriptions are limited for sub-tropical and tropical zones. However, tropical fish are considered to use relatively invariable photic signals and have different photo-sensing mechanisms from those of fish inhabiting temperate zones. Previous studies indicated that the moonlight intensity influences gonadal development and gamete release (Takemura et al., 2006; Takemura et al., 2004), along with melatonin secretion from the pineal gland and retinas (Takemura et al., 2006; Rahman et al., 2004) in goldlined spinefoot (*Siganus guttatus*) residing in sub-tropical and tropical zones. Thus, the photoperiod and water temperature function as a zeitgeber that synchronizes the reproductive rhythms of species living in aquatic environments in regions with relatively little variability.

Previous studies have illustrated the importance of environmental factors for various reproductive traits of anguillid species, such as the influence of photoperiod changes on ovarian development in European eels (Parmeggiani et al., 2015), the influence of temperature on the spawning performance of artificially matured Japanese eels (Dou et al., 2008), and the influence of swimming performance on ovarian development in European eels (Palstra et al., 2007). These findings suggest that environmental factors may also be closely correlated with endocrinological regulation in anguillids and further support the possibility of a close correlation between melatonin production and environmental cues. However, no study has yet described the mechanism whereby

environmental information is sensed, or how it might regulate melatonin secretion in eel which are catadromous fish. A study of the endogenous melatonin system based on environmental information is important for understanding how external light signals are converted internally in anguillids.

We hypothesized that a close association exists between specific photic signals and physiological regulation, regarding previously reported spawning migration of eels (Tsukamoto et al., 2003). This hypothesis could be tested by determining whether melatonin signals act as mediators relaying photic information as endocrine signals. To achieve this purpose, the following parameters were investigated: (1) examined eye and plasma melatonin levels of male Japanese eels for 24 h under conditions of a 12-h light: dark cycle (12L12D), constant light (LL), and constant darkness (DD), (2) the pattern of melatonin secretion under different photoperiod (short-day; 9L15D, long-day; 15L9D condition), and (3) examined eye and plasma melatonin levels under natural moonlight conditions [NM] and full moon [FM]) between immature and mature in Japanese eel males were comparatively analyzed.

2. Material and Methods

2.1. Animals and maintenanace

The Japanese yellow eels (n = 234, 2-years old) used in this study were cultivated males (body weight: 280–405 g) obtained from a commercial source in Gwangju Prefecture of South Korea. The eels were reared in indoor circular tanks (1-metric ton capacity) at 20 ± 1 $^{\circ}$C in the Lava-water Aquatic Animals Care Center (Jeju Techno-Park, Jeju, South Korea) with continuously running fresh water under the artificial 12L12D condition (light on at 07:00 h and light off at 19:00 h, 600 lx, PPFD = 10.0 μmol $m^{-2}s^{-1}$, λp = 545 nm) with a white light-emitting diode (LED) light (KRGB3, SS Light, Co., Seoul, South Korea). No food was given to the fish during the experiments. All experiments were conducted in compliance with the guidelines of the Animal care and use committee of the Korea Institute of Ocean Science and Technology (KIOST 2021-0001).

2.2. Experiment 1: Variations of eye and plasma melatonin levels under the 12L12D, LL, and DD conditions

To evaluate daily and circadian fluctuations in melatonin levels in the eye and plasma, fish (42 individuals per tank) were housed in three fresh water tanks (1-metric ton capacity) without a fish shelter under the 12L12D condition with a water temperature of 20 ± 1°C. Following a 1-week acclimation period, the fish were reared for 3 days under the 12L12D (light on at 07:00 h and light off at 19:00 h) or LL condition with LED lights and a water temperature of 20 ± 1°C. The light intensity at the water surface was adjusted to approximately 600 lx (10.0 μmol $m^{-2}s^{-1}$, λp = 545 nm). Fish (5 individuals per sampling time from one tank) were also held under the DD condition for comparison. Fish were anesthetized with 150 mg L^{-1} MS-222 (Sigma-Aldrich, St. Louis, MO, USA) and decapitated at 4 h intervals beginning at zeitgeber time 2(ZT; ZT0 is defined as the time when the light was on, light on= light on at 07:00 h and light off at 19:00 h) or circadian time 2(CT; CT0 is the beginning of the subjective day; CT12 is the beginning of the subjective night).

2.3. Experiment 2: Variations in eye and plasma melatonin levels under short- and long-photoperiod conditions

To examine the effects of photoperiodic changes on melatonin levels in the eyes and plasma, fish (24 per tank) were housed in two tanks (1-metric ton capacity) under the 12L12D condition with a water temperature of 20 ± 1°C for 1 week. After the 1-week acclimation period, the photoperiod in the tanks was changed to the short-phtoperiod (SP) condition (9L15D, light on at 06:00 h and light off at 15:00 h) or the long-photoperiod (LP) condition (15L9D, light on at 06:00 h and light off at 21:00 h) for 1 week. Fish (5 per sampling time from one tank) were anesthetized and decapitated at 4-h intervals beginning at ZT2.

2.4. Experiment 3: Moonlight experiments

We next compared the melatonin levels between the NM and FM periods according to testis development. A total of 71 fish were housed in an indoor tank with recirculating, aerated fresh water under the 12L12D condition at 20 ± 1 °C. Following acclimation for 1 week in fresh water, the salinity of each tank was gradually increased to the level in sea water for 1 week. After acclimation to sea water, the fish were transferred to two outdoor acryl tanks (3-metric ton capacity) to artificially induce testis development (Figure 2.1). The rearing tanks were maintained under a natural photoperiod condition (approximately 11L13D) with recirculating water (20 ±1 °C), but without a cover on the tank, until the end of the experiment. After anesthesia and weighing, the fish were intraperitoneally injected with hCG at 1 IU/g body weight (hCG+ group) or injected with 0.6% NaCl (hCG− group) once a week for a total of 8 weeks. Following initial sample collection under the fresh water condition (n = 9) and after acclimation to sea water (n = 9), the fish were randomly taken from the tank at 2400 h. Sample according to exposure to moonlight were collected around the NM (hCG+; n = 9, hCG−; n = 5) and the FM (hCG+; n = 8, hCG−; n = 5) periods. On each sampling day, the fish were taken from the tank at 2400 h, anesthetized, and then sacrificed by decapitation in accordance with the guidelines mentioned above. After weighing, the eye on the left side was immediately collected, frozen in liquid nitrogen, and stored at −80 °C until analysis. Blood was collected from the caudal vein using a heparinized syringe, transferred into a microtube on ice, and centrifuged at 8,000× g for 10 min at 4 °C to obtain plasma. The collected plasma was stored at −80 °C until performing the time-resolved fluorescence immunoassay (TR-FIA) to estimate melatonin levels. The gonads were harvested from the body cavity and weighed. Gonad sections were fixed in Bouin's solution for histological observation. All sample collections at 2400 h were carried out under dim-light conditions (1.5 lx, 0.0 μmol $m^{-2}s^{-1}$ at 670 nm) using a red-light LED module. The gonadosomatic index (GSI) and eye index (EI) (Pankhurst, 1982)

were calculated as follows:

$$GSI = (\text{gonadal mass}/\text{body mass}) \times 100$$

$$EI = \{[(A + B)/4)\ 2\times \pi\ /TL\ (mm)]\}$$

where A and B are the horizontal and vertical orbital diameter (mm), respectively.

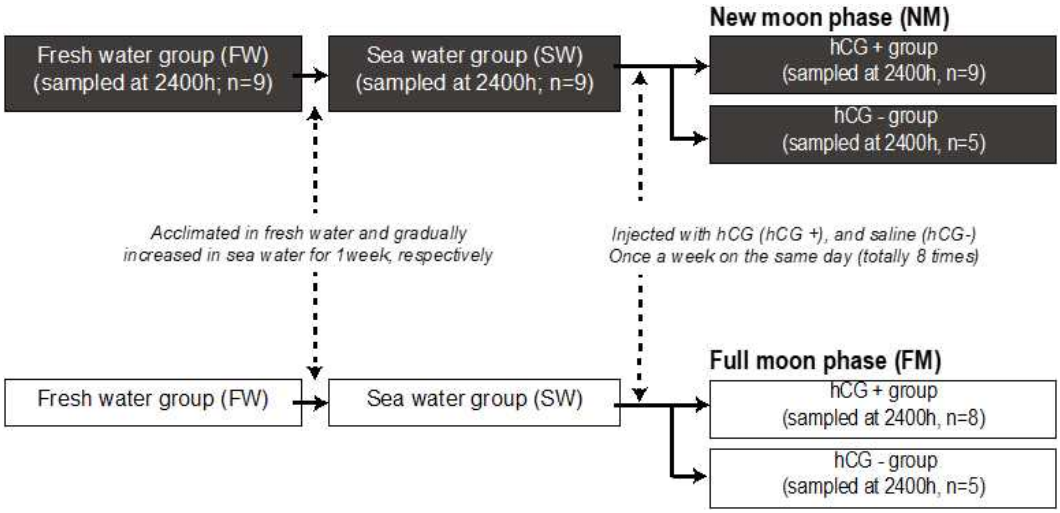

Figure 2.1. Experimental design for determining melatonin levels in ocular and plasma according to exposure to an NM or an FM. The solid and open squares represent the NM and FM groups, respectively. Following acclimation to fresh water for 1 week, the eels were gradually increased to a salinity approximating that of seawater for 1 week. After acclimation to seawater, the fish were transferred to two separate outdoor tanks for inducing sexual maturation. The fish were weighed and intraperitoneally injected with hCG (hCG+ group) or 0.6% saline (hCG− group) once a week on the same day (totally eight times) until the sampling date.

2.5. Melatonin measurements

The eyes on the left side were homogenized in 1 ml of 20 mM phosphate-buffered saline (pH 7.3) containing 0.5% bovine serum albumin (Sigma-Aldrich) and centrifuged for 15 min (10,000× g at 4 °C). Each supernatant was separated and stored on ice.

Melatonin-containing fractions were extracted from each supernatant and plasma sample using Sep-Pak Vac C18 cartridges (Waters Corporation, Milford, MA, USA), which were activated with 1 ml of 100% methanol and then with 1 ml of distilled water (DW). After applying the supernatant/plasma (500 μl) and then DW (500 μl), each cartridge was washed twice with 1 ml of 10% methanol and then with hexane. Melatonin levels were measured by the TR-FIA as described by Takeuchi et al. (2014).

2.6. Histological procedures

Testis samples were fixed in Bouin's fluid. The fixed samples were dehydrated through an ethanol series, embedded in paraffin wax (Leica Biosystems, Richmond, IL, USA), and sectioned at 8 μm. Sections were stained with Mayer's hematoxylin and eosin to study testis development.

2.7. Data analysis

All statistical analyses were performed using GraphPad Prism 8.0 Software. Daily and circadian variations of melatonin levels were compared by one-way analysis of variance (ANOVA), followed by Tukey's multiple-comparisons test. The GSI and EI values, and melatonin levels during artificially induced sex maturation under different moonlight conditions were compared by one-way ANOVA. Differences occurring under different photoperiod conditions (SD *vs.* LD) at each ZT were determined by one-way ANOVA with an unpaired *t* -test. A *P*-value < 0.05 was considered to represent a statistically significant difference.

3. Results

3.1. Experiment 1: Variation of eye and plasma melatonin levels under the 12L12D, LL, and DD conditions

Variations in circadian levels of eye and plasma melatonin are shown in Figure 2.2. A similar pattern was exhibited for both eye and plasma melatonin levels under the 12L12D and LL conditions. Both eye and plasma melatonin patterns under the 12L12D cycle showed clear day–night changes, with levels peaking at ZT18 and decreasing from ZT22 (Figure 2.2A, and 2.2D) ($P < 0.05$). In contrast, under the LL condition, eye melatonin levels were significantly higher at CT2 than at CT18 (Figure 2.2C) ($P < 0.05$), and plasma melatonin levels were significantly higher at CT18 than at CT6 (Figure 2.2F) ($P < 0.05$); however, both tissues showed lower melatonin levels under the LL condition compared with those measured under the 12L12D and DD conditions. Fundamentally, the patterns of eye and plasma melatonin levels in the 12L12D and DD conditions were similar: the levels of melatonin increased during scotophase and decreased at photophase. However, different peak times were exhibited under the DD condition in terms of the eye and plasma melatonin levels. The levels of eye melatonin peaked significantly at CT22 (Figure 2.2B) ($P < 0.01$), whereas the levels of plasma melatonin peaked significantly at CT18 (Figure 2.2E) ($P < 0.05$).

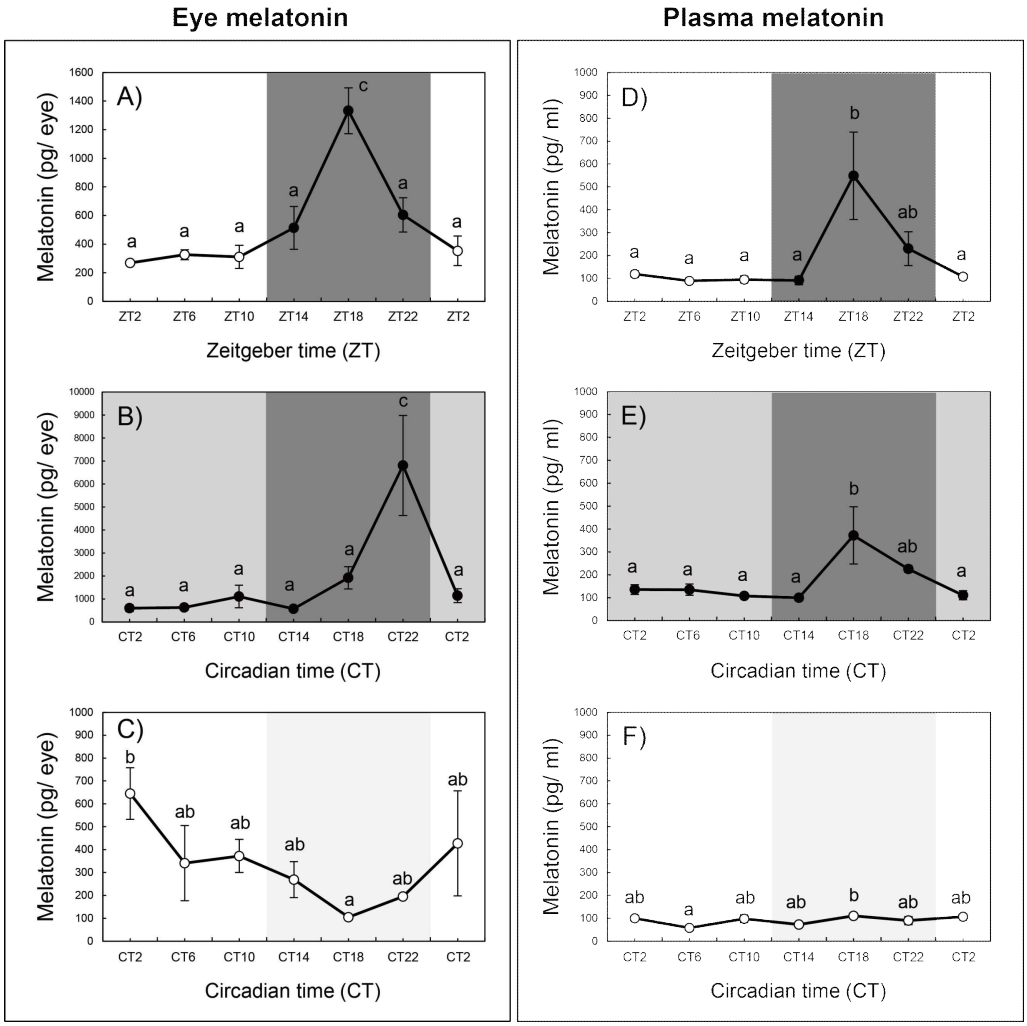

Figure 2.2. Variations of daily and circadian eye and plasma melatonin rhythms after 3 days of rearing under the 12L12D (eye; A, plasma; D), DD (eye; B, plasma; E), and LL (eye; C, plasma; F) conditions. The values shown for the melatonin levels represent the means ± standard errors of the mean (SEMs) (n = 5–6 fish per time point), where duplicate determinations were performed for each sampling time. The open and solid bars of each graph represent the scotophase and photophase, respectively. Significant differences between the means at each sampling time are indicated by different letters (one-way ANOVA, A; F = 12.22, df = 33, B; F = 6.41, df = 33, C; F = 2.456, df = 33, D; F = 5.345, df = 30, E; F = 4.583, df = 31, F; F = 2.702, df = 32, P < 0.05).

3.2. Experiment 2: Variation in eye and plasma melatonin levels under SP and LP conditions

After 1 week of rearing, the eye melatonin levels under the SP condition (9L15D) increased significantly and peaked from ZT18 to ZT22, whereas these levels peaked at ZT22 under the LP condition (15L9D) (Figure 2.3). The daily plasma melatonin levels under the SP condition increased slightly after the lights were turned off (ZT10) and peaked at ZT18, whereas low daily plasma melatonin levels were maintained under the LP condition.

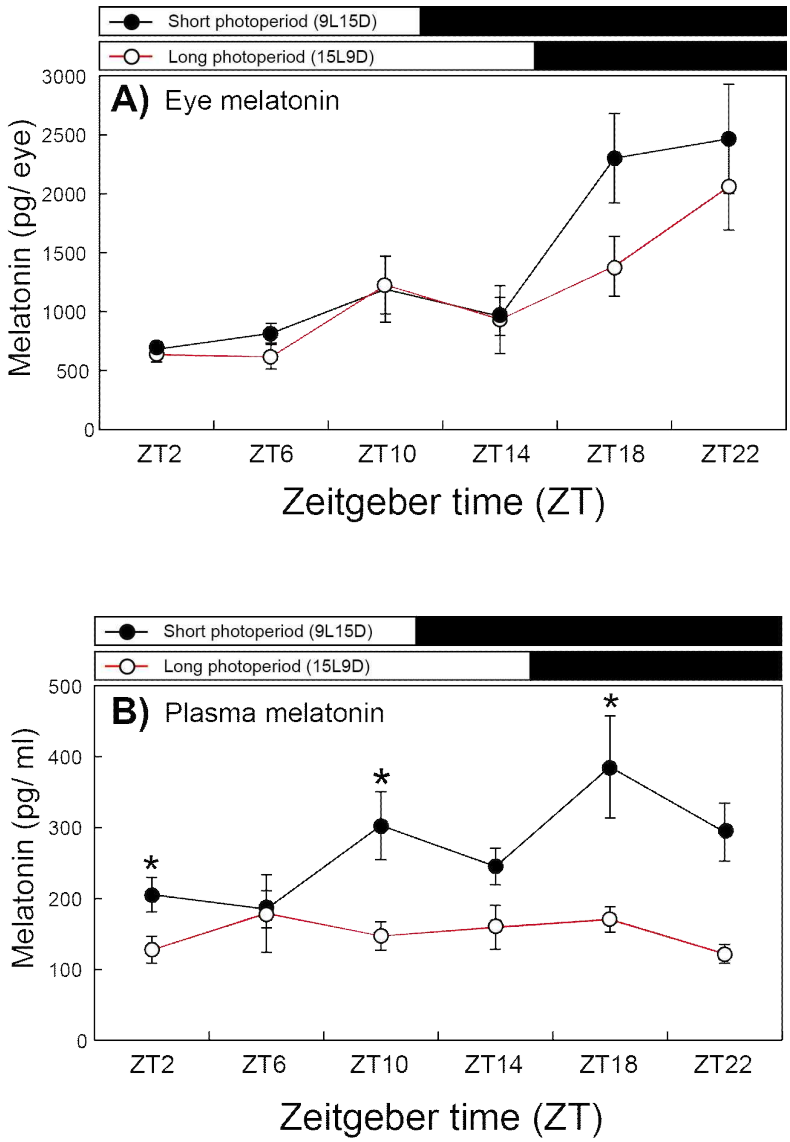

Figure 2.3. Photoperiodic changes of eye (A) and plasma (B) melatonin levels under a short-photoperiod condition (SP, 9L15D) and a long-photoperiod condition (LP, 15L9D). The values of the melatonin levels shown represent the means ± SEM (n = 5 per time point) of duplicate determinations for each sampling time. The solid and open circles indicate the SP and LP conditions, respectively. The open and solid bars at the top of each graph represent the scotophase and photophase, respectively. The asterisk indicates statistically different levels of melatonin observed between same sampling points (unpaired t -test, $P < 0.05$).

3.3. Experiment 3: Influence of moonlight in testis development and melatonin levels

3.3.1. Histological observations

Histological observations revealed that the testes of acclimated eels reared in fresh water (Figure 2.4A) and sea water (Figure 2.4B) were immature and contained both spermatogonia and spermatocytes. Histological examination of the hCG⁻ group at the FM and NM after 8 weeks revealed that the testes were still immature and contained both spermatogonia and spermatocytes (Figure 2.4C, and 2.4D). By contrast, in the hCG+ group, the testes of eels in the FM (Figure 2.4E) and NM (Figure 2.4F) groups were mature and fully contained spermatozoa after 8 weeks.

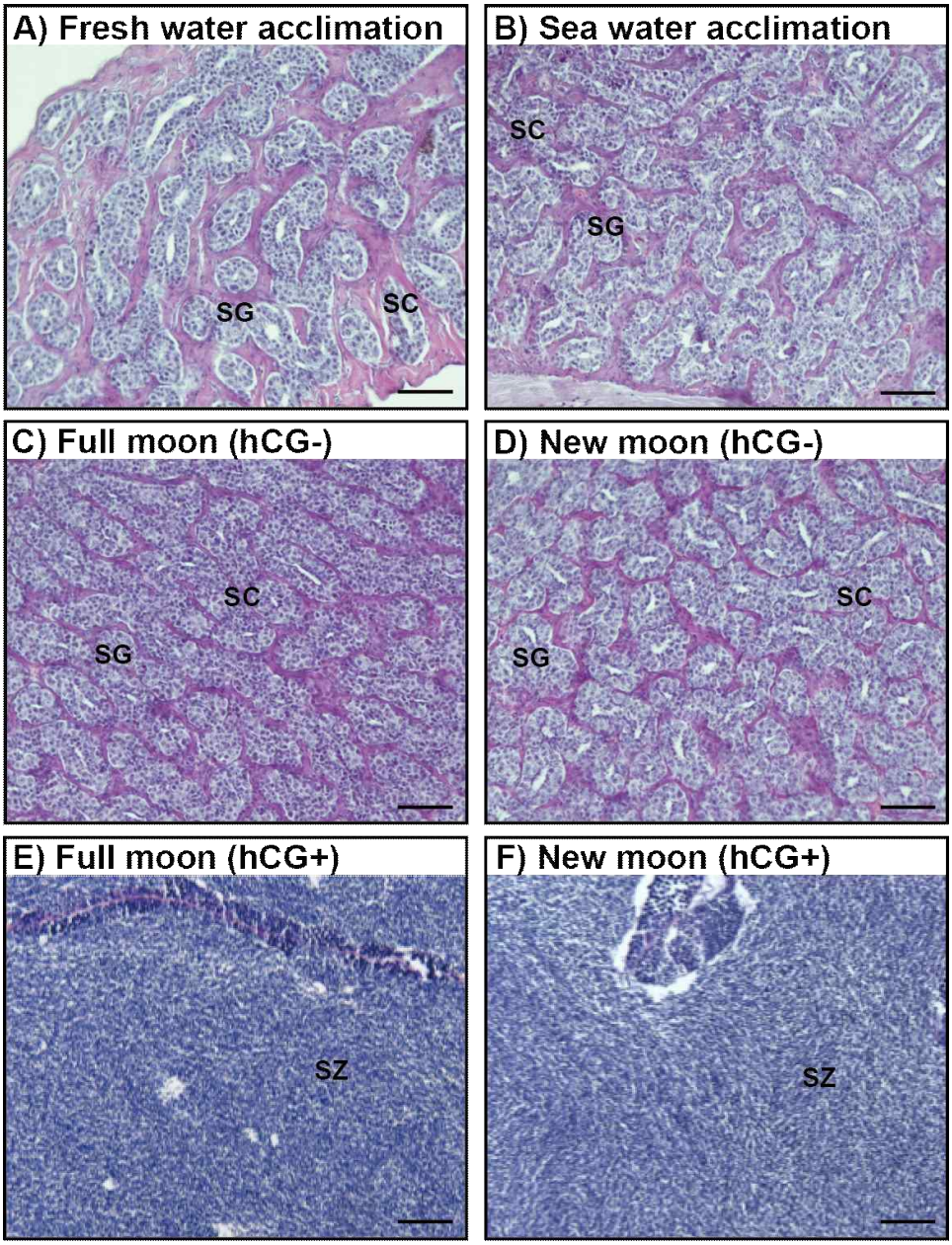

Figure 2.4. Histological observation of the testis development. Light-micrographs images of the testes from the groups acclimated to FW (A) and SW (B). After an 8 weeks treatment with hCG or saline, his- tological observations were performed to examine the testes from the FM (hCG−; C, hCG+; E) and NM (hCG−; D, hCG+; F) groups. The testes were sectioned after paraffin embedding and stained with hema- toxylin and eosin.

3.3.2. Changes in the GSI and EI values during artificially induced testis development

Changes in the GSI and EI values of male Japanese eels are shown in Figure 2.5. The GSI values were low during acclimation to fresh water and sea water. After 8 weeks, no significant differences were observed in the GSI values in the hCG− group at the NM and FM or in the groups acclimated to fresh water (FW) or sea water (SW). The GSI values of the hCG+ group were different in the NM and FM groups (Figure 2.5A) ($P < 0.05$).

The EI values were not significantly different between the FW and SW groups. After 8 weeks, the EI values in the hCG− groups at both NM and FM were higher than those in FW and SW ($P < 0.001$). After 8 weeks, the EI values of the hCG− group at FM and NM were significantly lower than those in the hCG+ group ($P < 0.001$), with no significant difference between the NM and FM conditions (Figure 2.5B).

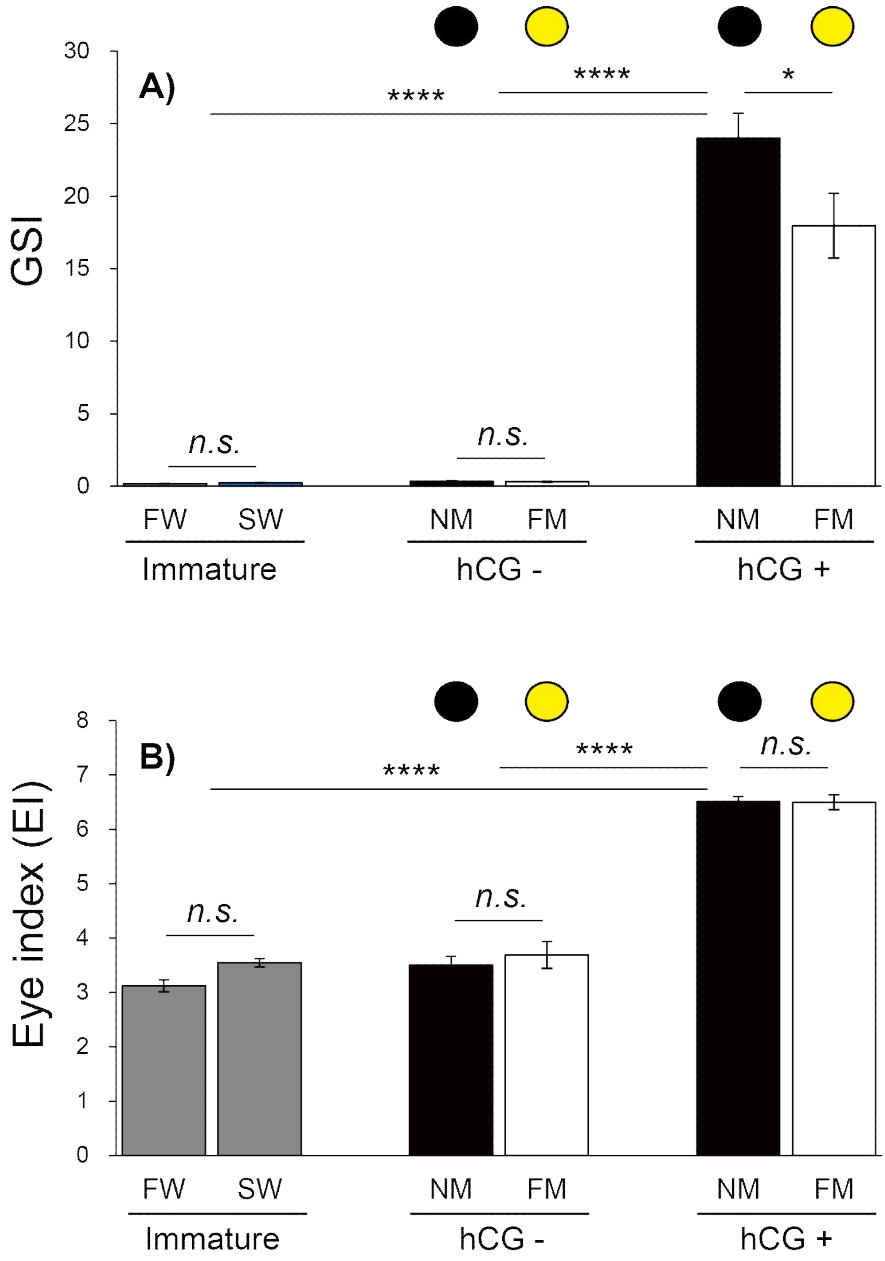

Figure 2.5. Changes of EI and GSI values. The black and yellow circles represent data from the NM and FM groups, respectively. The GSI (A; F = 69.04, df = 45) and EI (B; F = 130.6, df = 45) values shown were determined after FW and SW acclimation, for Japanese eels in the NM and FM groups. In all graphs, the significance levels are as follows: * $P < 0.05$; *** $P < 0.001$; **** $P < 0.0001$. The error bars represent the SEMs (n = 5–9 fish/treatment).

3.3.3. Changes in eye and plasma melatonin levels between the NM and FM, according to testis development

Next, we investigated the effects of moonlight on the eye and plasma melatonin levels, according to the sexual maturity of male Japanese eels (Figure 2.6). After a 1-week acclimation period in SW, the eye melatonin levels were slightly higher than those in FW, although the difference was not statistically significant. There was no significant difference in eye melatonin levels at NM and FM in the hCG⁻ group at 8 weeks, whereas significantly higher melatonin levels were found at the NM than at the FM in the hCG+ group ($P < 0.0001$). The plasma melatonin levels in the SW group were higher than those in the FW group; however, no significant difference was found. In the hCG⁻ group, the plasma melatonin levels in the NM group were slightly higher than those in the FM group, but the difference was not statistically significant. However, the plasma melatonin levels were significantly higher at NM than at FM in the hCG+ group ($P < 0.01$).

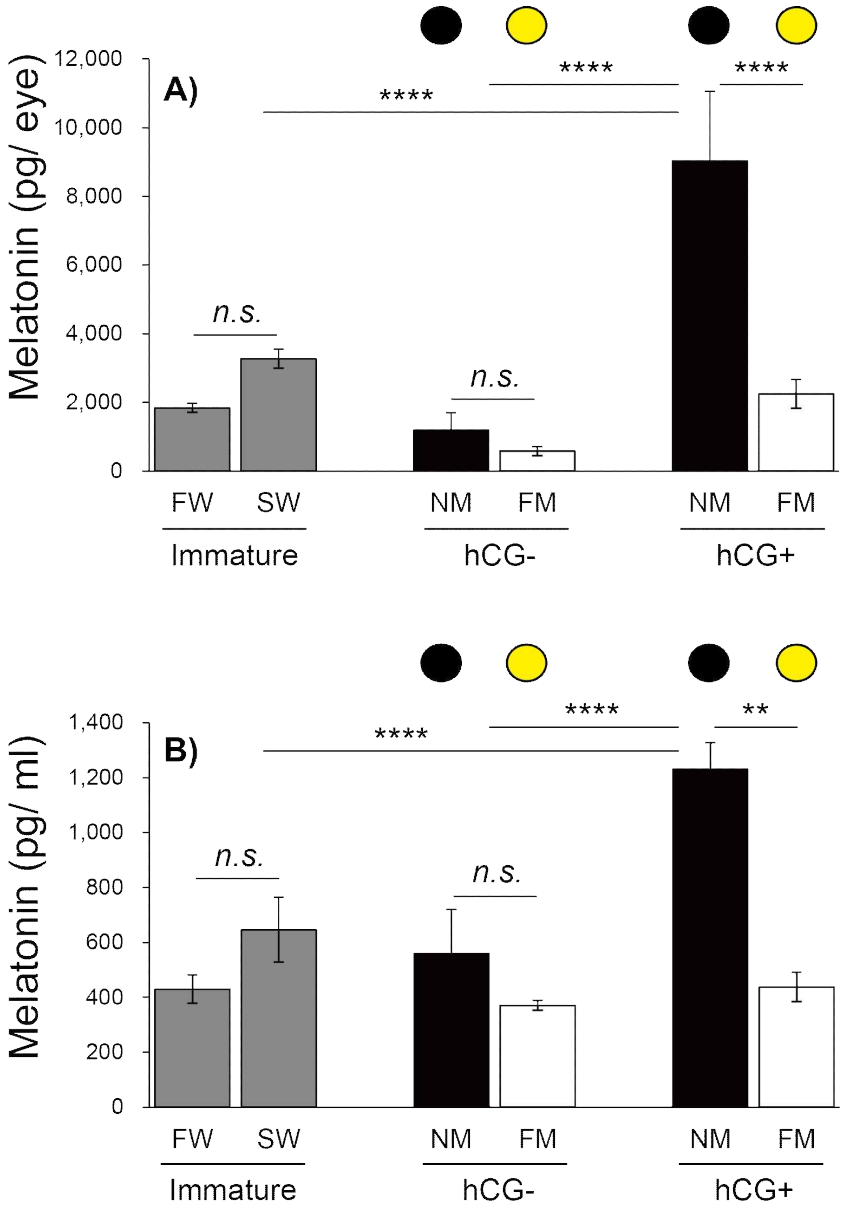

Figure 2.6. Changes in eye and plasma melatonin levels between Japanese eels exposed to an NM or FM, according to testis development. The black and yellow circles represent eels from the NM and FM groups, respectively. The levels of eye (A; F = 14.93, df = 42) and plasma melatonin (B; F = 16.43, df = 43) in hCG+ group after NM exposure were significantly higher than those in the other groups. In all graphs, the significance levels are as follows: ** P < 0.01; **** P < 0.0001. The error bars represent the SEM (n = 5–9 fish/treatment).

4. Discussion

In this study, we showed the plasma melatonin rhythms have similar fluctuation patterns to eye melatonin rhythms. Studies in the sheep *Ovis aries* demonstrated that melatonin produced by the pineal gland was released into the CSF, resulting in approximately 20-fold higher CSF melatonin levels compared with those in the plasma (Skinner & Malpaux, 1999). Although melatonin is also detectable in the retina (Iigo et al., 2007) and in the gastrointestinal tract (Vera et al., 2007), it remains unclear to what extent the melatonin secreted by a non-pineal gland organ contributes to the plasma level. The fluctuation patterns between eye and plasma melatonin in Japanese eel were similar under the 12L12D and DD conditions employed in this study; however, a different fluctuation pattern was observed under the LL condition. These findings imply a partial influence of eye melatonin on plasma melatonin levels, although it is also possible that eye melatonin secreted in the retinas does not directly move to the bloodstream. Unfortunately, this possibility could not be verified in this study because we did not measure melatonin secretion from the pineal gland. Nevertheless, melatonin receptors have been found in the retinas of various vertebrates, including fish, demonstrating a role in dopamine release, horizontal cell sensitivity, and in regulating physiological processes, as detected by electroretinogram findings (Cahill, Grace & Besharse, 1991; Vera et al., 2007). These results certainly suggest that high melatonin concentrations may also play a crucial neuromodulatory role in the retinas in Japanese eels; however, this possibility remains to be verified.

Changes in the amounts of eye melatonin and plasma melatonin were observed in each photoperiod tested in this study. Eye melatonin levels were similar under the 12L12D and SP conditions; however, with a long-photoperiod, the melatonin levels peaked at ZT22. With respect to plasma, different melatonin-secretion patterns were found between the 12L12D condition and other conditions. With a short-photoperiod, melatonin secretion began when the lights were turned off, whereas no difference in

the daily amount of melatonin was found in the LP condition. In a study conducted in turkey (*Meleagris gallopavo*), the production period of retinal and pineal melatonin was found to be significantly longer with a short-photoperiod than with a regular photoperiod (Zawilska et al., 2006; Zawilska et al., 2007). In particular, both tissues displayed amplitudes in melatonin production during the short-photoperiod. These findings imply that melatonin production is correlated with light-exposure time based on the photoperiod. Although it is considered that secretion of high melatonin concentrations by the retinas does not directly affect the plasma concentration—which can explain the different retina and plasma melatonin-fluctuation patterns found with photoperiodic changes—no detailed evidence has been found to support this possibility. Nevertheless, it may be speculated that periodic changes are involved. In general, melatonin signals act collectively as an important endocrine factor in synchronizing the annual reproductive cycle in teleosts (Falcón et al., 2007). However, Japanese eels spawn only once in their lifetime and undergo a photoperiodic change during spawning migration because they migrate from a temperate zone to sub-tropical and tropical zones. Thus, the influence of such photoperiodic changes and/or particular photic signals on eel physiology, and the influence of cumulative changes over the preceding years on synchronizing eel spawning migration should be taken into consideration.

In this study, we investigated changes in melatonin levels under natural moonlight conditions (NM and FM). In the sexually mature, male hCG+ group under an NM, eye melatonin and plasma melatonin levels were significantly higher than those detected in the other treatment groups. These findings imply that the moonlight of the FM partially inhibited melatonin synthesis. A similar pattern of inhibition was found in lunar melatonin rhythms of golden rabbitfish inhabiting a tropical zone based in both *in vivo* and *in vitro* assays (Takemura et al., 2004; Takemura et al., 2006). The plasma melatonin levels of individuals in a tank exposed to the natural light from an FM at midnight were markedly reduced compared with those in a covered tank (Takemura et al., 2004). In numerous previous studies of teleosts, retina melatonin levels exhibited nocturnal patterns that oscillated in a daily/circadian rhythm (Cahill,

1996; Iigo et al., 1997a; Iigo, Tabata & Aida, 1997b; Iigo et al., 2006; Iigo et al., 2007; Rahman et al., 2004; Takeuchi et al., 2014). Similarly, light from an FM led to inhibition of the eye melatonin levels in seagrass rabbitfish (Rahman et al., 2004). These studies in fish that can sense changes in moonlight suggest that FM light can inhibit eye and plasma melatonin. However, in this study, we found no significant difference in eye and plasma melatonin levels between sexually immature eels exposed to an NM or FM.

Anguillids only spawn once in their lifetime. Moreover, sexual maturity occurs only during the spawning migration period. Therefore, the concept of the annual reproductive cycle does not apply for these species. Accordingly, it is likely that eels sense environmental changes that occur repeatedly and use specific environmental signals to initiate reproductive activity without synchronizing their spawning rhythms. In addition, Sébert et al. (2008) revealed that 5-month melatonin implantation increased the mRNA expression of brain tyrosine hydroxylase in sexually immature female European eels and inhibited the synthesis and release of pituitary gonadotropin (follicle-stimulating hormoneβ and luteinizing hormoneβ). These findings raised the possibility that melatonin may have negative effects during the early stages of sexual maturation and puberty. Nonetheless, these results could not confirm the role of melatonin during the spawning period because sexually immature females were used in the experiments. A notable difference in melatonin secretion was found in the present study between sexually mature (hCG+ group) and immature (hCG− group) eels. This finding suggests that changes in melatonin levels due to moonlight may be involved in spawning, at least partially during the spawning period of sexually mature eels, despite the negative or negligible influence of melatonin on the brain–pituitary–gonad axis during the early stages of sexual maturation (puberty). The spawning period of Japanese eels is estimated to occur toward the last days of the lunar month (Tsukamoto et al., 2011), which appears to be correlated with melatonin production. However, it remains unclear whether moonlight directly regulates melatonin, or if moonlight simply has a promoting effect following the activation of other endocrine

factors during sexual maturation.

Japanese eels exhibit diel vertical migration with repetitive rises and falls based on the day–night cycle during spawning migration (nighttime: 100–500 m; daytime: 500–800 m) (Chow et al., 2015; Manabe et al., 2011). This may be attributed to the eel moving deeper into the water to continuously be in relatively dark conditions, which likely helps to increases melatonin secretion during sexual maturation (spawning migration). In addition, previous reports have shown interesting results regarding the locomotor activity of Japanese eels in relation to the lunar cycle. Monitoring eel behavior during spawning migration through short-term tracking with an ultrasonic transmitter revealed that the rise to the upper mesopelagic zone under an NM or a very small moon after sunset was contrasted by the trend to fall deeper as the moon grew in size, followed by another rise to the upper mesopelagic zone toward the moon set (Chow et al., 2015). These findings indicate a direct correlation between the locomotor activities of eels and the sunlight or moonlight, in which eels sense the moonlight through their retinas, while melatonin plays a crucial role in promoting their locomotor activities.

In this study, we examined changes in the eye and plasma melatonin levels in Japanese eels according to changes in moonlight and during the circadian cycle, photoperiod, and spawning period. Our findings suggest that melatonin signaling results from the eels sensing photic cues to regulate the physiology. Furthermore, eels are considered to sense the moonlight during the spawning period and use it as a signal for oviposition (Tesch, 1978). According to Ikegami et al. (2014), fish species in tropical regions reside in a location where temperature or photoperiod changes are relatively less frequent (*i.e.,* a relatively more stable aquatic environment) compared to fish species residing in temperate regions. Consequently, the moonlight signal promotes synchronization during several biological and physiological processes.

The spawning period of Japanese eel is estimated to occur around the NM (Tsukamoto et al., 2003). These results suggest that lunar signals may serve as a key link in regulating endocrine secretion in anguillids. Thus, further studies are need to

evaluate the biological activities of melatonin mediated by photic signals, as well as to identify the basic melatonin- secretion patterns that depend on nocturnal eel behaviors. Anguillids may provide a useful model for addressing even more intriguing topics given the limited knowledge of the endocrinology and ecology of these species, despite presumptions regarding their spawning sites or reports on their spawning ecology (Aoyama et al., 2014; Tsukamoto et al., 2003).

5. References

Aoyama J, Watanabe S, Miller MJ, Mochioka N, Otake T, Yoshinaga T, Tsukamoto K. 2014. Spawning sites of the Japanese eel in relation to oceanographic structure and the West Mariana Ridge. PLOS ONE. 9(2):e88759. DOI 10.1371/journal.pone.0088759.

Besseau L, Benyassi A, Møller M, Coon SL, Weller JL, Boeuf G, Klein DC, Falcón J. 2006. Melatonin pathway: breaking the 'high-at-night' rule in trout retina. Experimental Eye Research. 82:620–627. DOI 10.1016/j.exer.2005.08.025.

Bromage NR, Porter M, Randall C. 2001. The environmental regulation of maturation in farmed finfish with special reference to the role of photoperiod and melatonin. Aquaculture. 197:63–98. DOI 10.1016/S0044-8486(01)00583-X.

Cahill GM. 1996. Circadian regulation of melatonin production in cultured zebrafish pineal and retina. Brain Research. 708:177–181. DOI 10.1016/0006-8993(95) 01365-2.

Cahill GM, Grace MS, Besharse JC. 1991. Rhythmic regulation of retinal melatonin: Metabolic pathways, neurochemical mechanisms, and the ocular circadian clock. Cellular and Molecular Neurobiology. 11(5):529–560. DOI 10.1007/BF00734814.

Chow S, Okazaki M, Watanabe T, Segawa K, Yamamoto T, Kurogi H, Tanaka H, Ai K, Kawai M, Yamamoto S, Mochioka N, Manabe R, Miyaki Y. 2015. Lightsensitive vertical migration of the Japanese eel Anguilla japonica revealed by RealTime Tracking and its utilization for geolocation. PLOS ONE. 10(4):e0121801. DOI 10.1371/journal.pone.0121801.

Dou SZ, Yamada Y, Okamura A, Shinoda A, Tanaka S, Tsukamoto K. 2008. Temperature influence on the spawning performance of artificially-matured Japanese eel, Anguilla japonica, in captivity. Environmental Biology of Fishes. 82:151–164. DOI 10.1007/s10641-007-9268-8.

Ekström P, Meissl H. 1997. The pineal organ of teleost fishes. Reviews in Fish

Biology and Fisheries. 284:199–284.

Falcón J. 1999. Cellular circadian clocks in the pineal. Progress in Neurobiology. 58:121–162. DOI 10.1016/S0301-0082(98)00078-1.

Falcón J, Besseau L, Sauzet S, Boeuf G. 2007. Melatonin effects on the hypothalamo–pituitary axis in fish. Trends in Endocrinology & Metabolism. 18:81–88. DOI 10.1016/j.tem.2007.01.002.

Falcón J, Collin JP. 1991. Pineal-retinal relationships: rhythmic biosynthesis and immunocytochemical localization of melatonin in the retina of the pike (Esox luxius). Cell and Tissue Research. 265(1991):601–609. DOI 10.1007/BF0034 0884.

Falcón J, Migaud H, Muñoz Cueto JA, Carrillo M. 2010. Current knowledge on the melatonin system in teleost fish. General and Comparative Endocrinology. 165(3):469–482. DOI 10.1016/j.ygcen.2009.04.026.

Iigo M, Abe T, Kambayashi S, Oikawa K, Masuda T, Mizusawa K, Kitamura S, Azuma T, Takagi Y, Aida K, Yanagisawa T. 2007. Lack of circadian regulation of in vitro melatonin release from the pineal organ of salmonid teleosts. General and Comparative Endocrinology. 154:91–97. DOI 10.1016/j.ygcen.2007.06.013.

Iigo M, Hara M, Ohtani-Kaneko R, Hirata K, Tabata M, Aida K. 1997a. Photic and circadian regulations of melatonin rhythms in fishes. Biological Signals. 6:225–232. DOI 10.1159/000109132.

Iigo M, Ikeda E, Sato M, Kawasaki S, Noguchi F, Nishi G. 2006. Circadian rhythms of ocular melatonin in the wrasse Halichoeres tenuispinnis, a labrid teleost. General and Comparative Endocrinology. 145:32–38. DOI 10.1016/j.ygcen.2005. 06.010.

Iigo M, Kezuka H, Suzuki T, Tabata M, Aida K. 1994. Melatonin signal transduction in the goldfish, Carassius auratus. Neurosci Biobehavio Reviews. 18(4):563–569. DOI 10.1016/0149-7634(94)90012-4.

Iigo M, Tabata M, Aida K. 1997b. Ocular melatonin rhythms in a cyprinid teleost, oikawa zacco platypus, are driven by light-dark cycles. Zoological Science.

14(2):243−248. DOI 10.2108/zsj.14.243.

Ikegami T, Takeuchi Y, Hur SP, Takemura A. 2014. Impacts of moonlight on fish reproduction. Marine Gensets. 14:59−66. DOI 10.1016/j.margen.2013.11.007.

Klein DC, Coon SL, Roseboom PH, Weller JL, Bernard M, Gastel JA, Zatz M, Iuvone PM, Rodriguez IR, Begay V, Falcón J, Cahill GM, Cassone VM, Baler R. 1997. The melatonin rhythm-generating enzyme: molecular regulation of serotonin N-acetyltransferase in the pineal gland. Recent Progress in Hormone Research. 52:307−356.

Manabe R, Aoyama J, Watanabe K, Kawai M, Miller MJ, Tsukamoto K. 2011. First observations of the oceanic migration of Japanese eel, from pop-up archival transmitting tags. Marine Ecology Progress Series. 437:229−240. DOI 10.3354/meps09266.

Mazurais D, Le Dréan G, Brierley I, Anglade I, Bromage N, Williams LM, Kah O. 2000. Expression of clock gene in the brain of rainbow trout: Comparison with the distribution of melatonin receptors. Journal of Comparative Neurology. 422:612−620. DOI 10.1002/1096-9861(20000710)422:4<612::AID-CNE9>3.0.CO;2-Y.

Migaud H, Taylor JF, Taranger GL, Davie A, Cerda-Reverter JM, Carrillo M, Hansen T, Bromage NR. 2006. A comparative ex vivo and in vivo study of day and night perception in teleosts species using the melatonin rhythm. Journal of Pineal Research. 41:42−52. DOI 10.1111/j.1600-079X.2006.00330.x.

Palstra A, Curiel D, Fekkes M, Bakker M, Székely C, Ginneken V, Van den Thillart GE. 2007. Swimming stimulates oocyte development in European eel. Aquaculture. 270:321−332. DOI 10.1016/j.aquaculture.2007.04.015.

Pankhurst NW. 1982. Relation of visual changes to the onset of sexual maturation in the European eel Anguilla anguilla (L.). Journal of Fish Biology. 21:127−140. DOI 10.1111/j.1095-8649.1982.tb03994.x.

Parmeggiani A, Govoni N, Zannoni A, Di Biase A, Sirri R, Forni M, Mandelli M, Mordenti O. 2015. Effect of photoperiod on endocrine profiles and vitellogenin

expression in European eels Anguilla anguilla during artificially induced ovarian development. Theriogenology. 83:478-484. DOI 10.1016/j.theriogenology.2014.10.008.

Ping Y, Huang H, Zhang XJ, Yang XL. 2008. Melatonin potentiates rod signals to ON type bipolar cells in fish retina. Journal de Physiologie. 586:2683-2694. DOI 10.1113/jphysiol.2008.152959.

Rahman MS, Kim BH, Takemura A, Park CB, Lee YD. 2004. Influence of light-dark and lunar cycles on the ocular melatonin rhythms in the seagrass rabbitfish, a lunar-synchronized spawner. Journal of Pineal Research. 37:122-128. DOI 10.1111/j.1600-079X.2004.00147.x.

Sauzet S, Besseau L, Perez PH, Covès D, Chatain B, Peyric E, Boeuf G, Muñoz-Cueto JA, Falcón J. 2008. Cloning and retinal expression of melatonin receptors in the European sea bass, Dicentrarchus labrax. General and Comparative Endocrinology. 157(2):186-195. DOI 10.1016/j.ygcen.2008.04.008.

Sébert ME, Legros C, Weltzien FA, Malpaux B, Chemineau P, Dufour S. 2008. Melatonin activates brain dopaminergic systems in the eel with an inhibitory impact on reproductive function. Journal of Neuroendocrinology. 20:917-929. DOI 10.1111/j.1365-2826.2008.01744.x.

Siu AW, Maldonado M, Sanchez-Hidalgo M, Tan DX, Reiter RJ. 2006. Protective effects of melatonin in experimental free radical-related ocular diseases. Journal of Pineal Research. 40(2):101-109. DOI 10.1111/j.1600-079X.2005.00304.x.

Skinner DC, Malpaux B. 1999. High melatonin concentrations in third ventricular cerebrospinal fluid are not due to galen vein blood recirculating through the choroid plexus. Endocrinology. 140(10):4399-4405. DOI 10.1210/endo.140.10.7074.

Takemura A, Susilo ES, Rahman MD, Morita M. 2004. Perception and possible utilization of moonlight intensity for reproductive activities in a lunar-synchronized spawner, the golden rabbitfish. Journal of Experimental Zoology Part A Comparative Experimental Biology. 301(10):844-51.

Takemura A, Ueda S, Hiyakawa N, Nikaido Y. 2006. A direct influence of moonlight intensity on changes in melatonin production by cultured pineal glands of the golden rabbitfish, Siganus guttatus. Journal of Pineal Research. 40(3):236–41. DOI 10.1111/j.1600-079X.2005.00306.x.

Takeuchi Y, Imamura S, Sawada Y, Hur SP, Takemura A. 2014. Effects of different colors of light on melatonin suppression and expression analysis of Aanat1 and melanopsin in the eye of a tropical damselfish. General and Comparative Endocrinology. 204:158–165. DOI 10.1016/j.ygcen.2014.05.015.

Tesch FW. 1978. Telemetric observations on the spawning migration of the eel Anguilla anguilla west of the European continental shelf. Environmental Biology of Fishes. 3:203–209. DOI 10.1007/BF00691944.

Tsukamoto K, Chow S, Otake T, Kurogi H, Mochioka N, Miller MJ, Aoyama J, Kimura S, Watanabe S, Yoshinaga T, Shinoda A, Kuroki M, Oya M, Watanabe T, Hata K, Ijiri S, Kazeto Y, Nomura K, Tanaka H. 2011. Oceanic spawning ecology of freshwater eels in the western North Pacific. Nature Communications. 2:179. DOI 10.1038/ncomms1174.

Tsukamoto K, Otake T, Mochioka N, Lee TW, Fricke H, Inagaki T, Aoyama J, Ishikawa S, Kimura S, Miller MJ, Hasumoto H, Oya M, Suzuki Y. 2003. Seamounts, new moon and eel spawning: the search for the spawning site of the Japanese eel. Environmental Biology of Fishes. 66(3):221–229. DOI 10.1023/A:1023926705906.

Vera LM, De Pedro N, Gómez-Milán E, Delgado MJ, Sánchez-Muros MJ, Madrid JA, Sánchez-Vázquez FJ. 2007. Feeding entrainment of locomotor activity rhythms, digestive enzymes and neuroendocrine factors in goldfish. Physiology & Behavior. 90:518–524. DOI 10.1016/j.physbeh.2006.10.017.

Zawilska JB, Lorenc A, Berezińska M, Vivien-Roels B, Pévet P, Skene DJ. 2006. Daily oscillation in melatonin synthesis in the Turkey pineal gland and retina: diurnal and circadian rhythms. Chronobiology International. 23:341–350. DOI 10.1080/07420520500482082.

Zawilska JB, Lorenc A, Berezińska M, Vivien-Roels B, Pévet P, Skene DJ. 2007. Photoperiod-dependent changes in melatonin synthesis in the Turkey pineal gland and retina. Poultry Science. 86:1397–1405. DOI 10.1093/ps/86.7.1397.

Chapter Ⅲ

Clock gene expression in response to photoperiodic changes and absent of moonlight in eel retina and brain

Abstract

Assessment of the clock genes, period (Per) 1, Per2, Per3, and cryptochrome (Cry) 2, Cry3, and Cry4, can help better understand eel spawning ecology. In this study, the circadian rhythm and moonlight effects of these clock genes in the eel retina and brain were analyzed. We examined clock gene expression patterns under 12 h light:12 h darkness (12L12D), constant darkness (DD), and constant light (LL) conditions; under a short photoperiod (SP; 9L15D) and long photoperiod (LP; 15L9D); and under new moon (NM) and full moon (FM) in male eels. Owing to the light signal received by the retina, the secretion of melatonin, a major regulator of the clock genes, increased at scotophase and decreased during the photophase in the retina. Further, Per2 expression increased after sunrise, Cry2 and Cry4 expression increased around sunset, and Per1, Per3, and Cry3 expression increased before sunrise. Under short photoperiod conditions, oscillations of retinal Per3 and Cry4, which did not occur under long photoperiod conditions, were generated. In addition, retinal Cry4 oscillation was generated under NM conditions. These results suggest that the retina of the eel plays a key role in regulating circadian rhythm, and it can be inferred that migration is initiated by the synchronization of clock genes by moonlight, suggesting that photic signals are closely related to the migratory activity of the eel.

1. Introduction

The circadian clock vibrates at a cycle of approximately 24 h, and recognition and synchronization of daily behavior and homeostasis occurs depending on the environmental light and darkness. Most organisms have an internal clock and their circadian rhythms exhibit certain basic features. Predictable environmental changes, such as the light-dark cycle, which is approximately 24 h, are the most important external zeitgebers in the circadian system of vertebrates (Hastings, O'Neill & Maywood, 2007). The circadian rhythm is created and maintained by a transcription-translational feedback loop that is automatically regulated by the interaction of clock genes. This regulation is of two types: transcriptional activation (positive feedback) and repression (negative feedback). The heterodimerization of transcription factors CLOCK (circadian locomotor output cycle kaput) and BMAL1 (brain and muscle arylhydrocarbon receptor nuclear translocator-like protein1), which act as positive regulators, facilitates the binding to the E-box in the promoter of the period (Per) and cryptochrome (Cry) genes, thus stimulate transcription. The regulation of the circadian clock in animals other than mammals is closely linked to the signal of the external light-dark cycle recognized via the optical input pathway and biological clock synchronization via the endogenous optical input pathway. The circadian system in fish is made up of other elements by which light is sensed by the organism and converted into neuronal or endocrine hormonal signals. Therefore, the circadian rhythm regulated by light signal input affects the reproduction and growth rhythm of fish (Falcón et al., 2010).

Cryptochromes are flavoproteins found in bacteria, plants, and animals. CRY has also been reported to act as a photoreceptor that is essential for circadian rhythm activity and is involved in responses to DNA damage, cancer biology, and metabolic signals (Michael et al., 2017). In migratory birds, cry4 has been proposed as a strong candidate magnetoreceptor; a novel isoform of cryptochrome 4 (Cry4b) is

expressed in the retina of a night-migratory songbird. It is hypothesized that Cry-based magnetic field recognition causes electron transfer between highly conserved tryptophan residues of Cry and FAD through the use of short-wavelength photoactivation, resulting in the formation of magnetically sensitive radical pairs (Ritz, Adem & Schulten, 2000; Liedvogel et al., 2007; Solov'yov, Domratcheva & Schulten, 2014).

The teleost group is the largest and most species-diverse group of vertebrates. Teleosts are a result of exposure to various external environments owing to their dynamic performance environment (Bone, 2019). Physiological changes such as lunar phases, reproductive activity by moonlight, expression of clock genes Per and Cry, and changes in melatonin secretion in various marine species can improve our understanding of lunar-biospheric relationships. Eels are migratory fish that migrate long distances at specific times for spawning. It has been reported that the migratory and spawning processes of eels depend on the influence of moonlight (Miyagi et al., 2004; Tesch, 1978; Tsukamoto, 2006). In this study, we focused on the ecology of eels by studying the light dependence of the Per and Cry genes on the core loop to understand the working principle of the little-known endocrine concepts of time, circadian rhythm, and seasonality.

2. Material and Methods

2.1. Animals and maintenance

Japanese yellow eels (n = 234, 2-years-old) used in this study were cultivated males (body weight: 280-405 g) obtained from a commercial source in Gwangju Prefecture, South Korea. The eels were reared in indoor circular tanks (one-metric ton capacity) at 20 ± 1 °C in the Lava-water Aquatic Animals Care Center (Jeju Techno-Park, Jeju, South Korea) with continuously running fresh water under artificial 12L12D condition (LD; light on at 07:00 h and light off at 19:00 h, 600 lx, PPFD = 10.0 μmol $m^{-2}s^{-1}$, λp = 545 nm) with a white light-emitting diode (LED) light (KRGB3, SS Light, Co., Seoul, South Korea). Food was not provided to the eels during the experiment. All experiments were conducted in compliance with the guidelines of the Animal Care and Use Committee of the Korea Institute of Ocean Science and Technology (KIOST 2021-0001).

2.1.1. Experiment 1: Expression of clock genes in the retina and brain under LD, constant light (LL), and constant darkness (DD) conditions

To evaluate daily and circadian fluctuations in clock gene transcript levels in the eye and brain, eels (30 individuals per tank) were housed in three fresh water tanks (one-metric ton capacity) without a fish shelter under the 12L12D condition with a water temperature of 20 ± 1 °C. Following a one-week acclimation period, the eels were reared for three days under the LD or LL condition and a water temperature of 20 ± 1 °C. The light intensity at the water surface was adjusted to approximately 600 lx (10.0 μmol $m^{-2}s^{-1}$, λp = 545 nm). Five eels (per sampling time from one tank) were also kept under DD conditions for comparison. The eels were anesthetized with 150 mg L^{-1} MS-222 (Sigma-Aldrich, St. Louis, MO, USA) and decapitated at 4-h intervals beginning at zeitgeber time (ZT) 2.

2.1.2. Experiment 2: Expression of clock genes in the retina and brain under short- and long-photoperiod conditions

To examine the effects of photoperiodic changes on clock gene transcript levels in the eyes and brain, eels (36 per tank) were housed in two tanks (one-metric ton capacity) under LD condition with a water temperature of 20 ± 1 °C for one week. After the one-week acclimation period, the photoperiod in the tanks was changed to a short photoperiod (SP) condition (9L15D, light on at 06:00 h and light off at 17:00 h) or a long photoperiod (LP) condition (15L9D, light on at 06:00 h and light off at 21:00 h) for one week. Five eels (per sampling time from one tank) were anesthetized and decapitated at 4-h intervals beginning at ZT 2.

2.1.3. Experiment 3: Expression of clock genes in the retina and brain under the new moon (NM) and full moon (FM) conditions

Next, we compared clock gene transcript levels between the NM and FM periods. A total of 25 eels were housed in an indoor tank with recirculating, aerated fresh water under the LD condition at 20 ± 1 °C. Following acclimation for one week in fresh water, the eels were transferred to two outdoor acrylic tanks (three-metric ton capacity). The rearing tanks were maintained under natural photoperiod conditions (approximately 11L13D) with recirculating water (20 ±1 °C) for two weeks, but without a cover on the tank, until the end of the experiment. Samples were collected during the NM (n = 25) and FM (n = 25) periods. On each sampling day, the eels were anesthetized and sacrificed by decapitation in accordance with the guidelines mentioned above at 4-h intervals beginning at 12:00 h. After weighing, the left eyes were immediately collected, frozen in liquid nitrogen, and stored at -80 °C until analysis. All sample collections were carried out under dim-light conditions (1.5 lx, 0.0 μmol $m^{-2}s^{-1}$ at 670 nm) using a red-light LED module.

2.2. Total RNA extraction and cDNA synthesis

Total RNA was extracted from the whole brain and left eye using RNAiso Plus (Takara Bio, Otsu, Japan), according to the manufacturer's instructions. Isolated total RNA (1 μg) was treated with DNase I (Promega, Madison, WI, USA) at 37 °C for 15 min to prevent contamination with genomic DNA. The total RNA quantity was measured using NanoDrop Onec (Thermo Fisher Scientific, Waltham, MA, USA) at 260 and 280 nm, and samples with an A260:A280 ratio of 1.8-2.0 were used for cDNA synthesis. Then, the cDNA was synthesized using the Transcriptor First Strand cDNA Synthesis Kit, according to the manufacturer's protocol (Roche Diagnostics, Indianapolis, IN, USA).

2.3. cDNA library construction and massively parallel sequencing

RNA sequencing (RNA-seq) paired end libraries were prepared using the Illumina TruSeq RNA Sample Preparation Kit v2 (catalog #RS-122-2001; Illumina, San Diego, CA, USA). Total RNA was isolated from the retina and brain. After removal of genomic DNA contamination, RNA quality and quantity were assessed using the 2100 Bioanalyzer RNA 6000 NANO chip (Bio-Rad , Hercules, CA, USA). High-quality total RNA extracted from the retina and brains of 6 individuals was pooled. Starting with the total RNA, mRNA purified using poly (A) selection was chemically fragmented and converted into single-stranded cDNA using random hexamer priming. Next, the second strand was generated to create double-stranded cDNA. Library construction began with the generation of blunt-end cDNA fragments from ds-cDNA. Then, the A-base was added to the blunt end in order to prepare them for ligation of sequencing adapters. After size selection of the ligates, the ligated cDNA fragments containing adapter sequences were enhanced via PCR using adapter-specific primers. The library was quantified using the KAPA library quantification kit (Kapa Biosystems KK4854), following the manufacturer's instructions. Each library was loaded on the Illumina Hiseq2000 platform, and throughput sequencing (read length 2 × 100) was performed to ensure that each sample met the desired average sequencing depth.

2.4. Preprocessing and de novo reconstruction of transcriptome

The bases from the 5' end and 3' ends of each read with low-quality and adapter sequences were trimmed using Trimmomatic (ver. 0.3.6, Bolger, Lohse & Usadel, 2014), and low average quality (Q<25) was removed by PRINSEQ lite (ver. 0.20.4, Schmieder & Edwards, 2011). Cleaned raw reads from the retina and brain RNA were pooled and mapped to the Anguilla japonica draft genome sequence (Ref) using tophat2 (ver.2.1.0, Kim, 2013), and de novo transcriptome reconstruction was performed using genome-guided Trinity (ver. 2.3.2, Grabherr et al., 2011) with the beam mapping results. To remove redundant contigs and create a unigene set, the assembled contigs were clustered and filtered using cd-hit-est with default parameters (CD-HIT package, Li & Godzik, 2006).

2.5. Analysis of the clock DNA sequence

To examine clock genes from the assembled transcriptome sequences of the Japanese eel, the tBlastn program was utilized (E-value < 0.01) on zebrafish opsin protein sequences as queries. The ORF regions of the Japanese eel clock gene candidates were identified using ORF Finder (http://www.ncbi.nlm.nih.gov/gorf/gorf.html), and the presumed protein sequences were aligned with the teleost clock gene family proteins. A phylogenetic tree was constructed using the maximum-likelihood algorithm in RAxML (Stamatakis, 2014). To quantify the expression of the identified clock gene family genes, cleaned reads were mapped onto reconstructed contigs using Bowtie2 (Langmead & Salzberg, 2012), then the expression levels were estimated using Tigar2 (Nariai et al., 2014).

2.6. Real-time quantitative PCR

The expression of each target gene was analyzed using the BioRad CFX96TM Real Time System (BioRad) and SYBR Green premix II (Takara Bio). Primers for qPCR (Table 3.1) were designed using Primer-BLAST (http://www.ncbi.nlm.nih.gov/tools/primer-blast/). Each PCR mix contained 50% SYBR Premix, 0.2 μM of each forward and reverse primer, and 2 μl of cDNA template. The amplification conditions were as follows: initial denaturation for 1 min at 95 °C, 40 cycles of denaturation for 45 s at 95 °C, and annealing and extension for 1 min at 60 °C. The expression of each gene in each sample was normalized to that of the internal control EF1α gene.

Table 3.1. Primer sets for qPCR.

Gene ID	Oligo ID	Sequence	Product size (bp)
EF1–alpha (MH020210)	Forward	5′–TCACCCTGGGAGTAAAGCAG–3′	222
	Reverse	5′–TCCATCCCTTGAACCAGGAC–3′	
Per1 (LC616387)	Forward	5′–GCAGAAGGAGCTGATGAAGG–3′	224
	Reverse	5′–TGATGTTGTCCAGCTCTTCG–3′	
Per2 (LC616388)	Forward	5′–CAAGGCGAAAACTCAGAAGG–3′	232
	Reverse	5′–GTCGATCTCCTCGATGGTGT–3′	
Per3 (LC616389)	Forward	5′–CACGCTGATCCTGCCAGTAA–3′	356
	Reverse	5′–CTGGTCAGGGAGAACACCAC–3′	
Cry2 (LC616385)	Forward	5′–CCCCTCACCTACAAGCGTTT–3′	286
	Reverse	5′–TGGCGTTCATTCTGGGTCTC–3′	
Cry3 (LC616386)	Forward	5′–GGGTCAGCCAGCAGATGTAT–3′	177
	Reverse	5′–TCCAGGTTGTAGAGCGTGTG–3′	
Cry4	Forward	5′–ATTCCAAGCCTGGAGGATCT–3′	159
	Reverse	5′–CGGTAACAGGGAGTTTGGAA–3′	

2.7. Statistical analysis

All statistical analyses were performed using the GraphPad Prism software (version 8.0). The expressions of the clock genes were compared using one-way analysis of variance (ANOVA), followed by Tukey's multiple-comparisons test. The circadian oscillation patterns of the clock gene expression were analyzed using CircWave v1.4 (http://www.euclock.org/results/item/circ-wave.html). CircWave employs a forward linear harmonic regression model to calculate the profile of a 24 h period with alpha set at 0.05. The *P*-values reported are the result of the *F*-test from the software.

3. Results

3.1. RNA-seq

Expression of the clock genes of Japanese eels in the whole brain was investigated using NGS. After adapter trimming and quality filtering, 150,898,925 paired-end reads were used for de novo transcriptome reconstruction. As a result of cd-hit est clustering, 313,671 contigs (N50 = 965) were identified. tBlastn analysis identified two main gene families, periods and cryptochromes, in the whole brain through RNA-seq.

Per1, Per2, and Per3 had 3173, 3657, and 1248 bp, respectively; Per1, Per2, and Per3 carried 1057, 1218, and 416 amino acids, respectively. Comparison of the amino acid sequence homology between the Per genes of the eel and other animal groups revealed that the homology of Per1 was 59-71% in fish, 57% in amphibians (*Xenopust laevis*), and 59-61% in mammals (*Mus musculus*, *Rottus norvericus*, and *Homo sapiens*). low homology was observed in all other animal groups. The amino acid sequence homology of Per2 was 61-73% in fish, which was relatively high compared to other animal groups, but 47% in amphibians (*Xenopust laevis*) and 49-51% in mammals (*Rottus norvericus*, *Mus musculus*, *Homo sapiens*). It showed relatively low homology. The amino acid sequence homology of Per3 was 60-64% in fish and 53-55% in mammals (*Mus musculus*, *Rottus norvericus*, and *Homo sapiens*), indicating low homology in all animal groups (Figure 3.1).

The base sequences of three Cry genes in the brain of eels were also analyzed. Cry2, Cry3, and Cry4 had 1857, 951, and 1002 bp, respectively, and Cry2, Cry3, and Cry4 had 618, 317, and 333 amino acids, respectively. As a result of comparing the amino acid sequence homology of the Cry genes in eels with that in other animal groups, we observed that the homology of Cry2 was 82-91% in fish, 79% in amphibians (*Xenopust laevis*), 80% in birds (*Gallus gallus*), and 81-82% in mammals

(Mus musculus and Homo sapiens), thus showed high homology in all animal groups. The amino acid sequence homology of Cry3 was 84% in zebrafish (*Danio rerio*), indicating relatively high homology. In addition, the amino acid sequences of Cry1 showed relatively high homology (73%) with that of other animal groups (*Gallus gallus*, *Mus musculus*, and *Homo sapiens*). The amino acid sequence homology of Cry4 was 72% in zebrafish (*Danio rerio*), showing relatively high homology, but 65% in amphibians (*Xenopust laevis*) and 65% in birds (*Gallus gallus*), showing relatively low homology (Figure 3.2). Most clock genes identified in this study showed a relatively high identity to that of zebrafish.

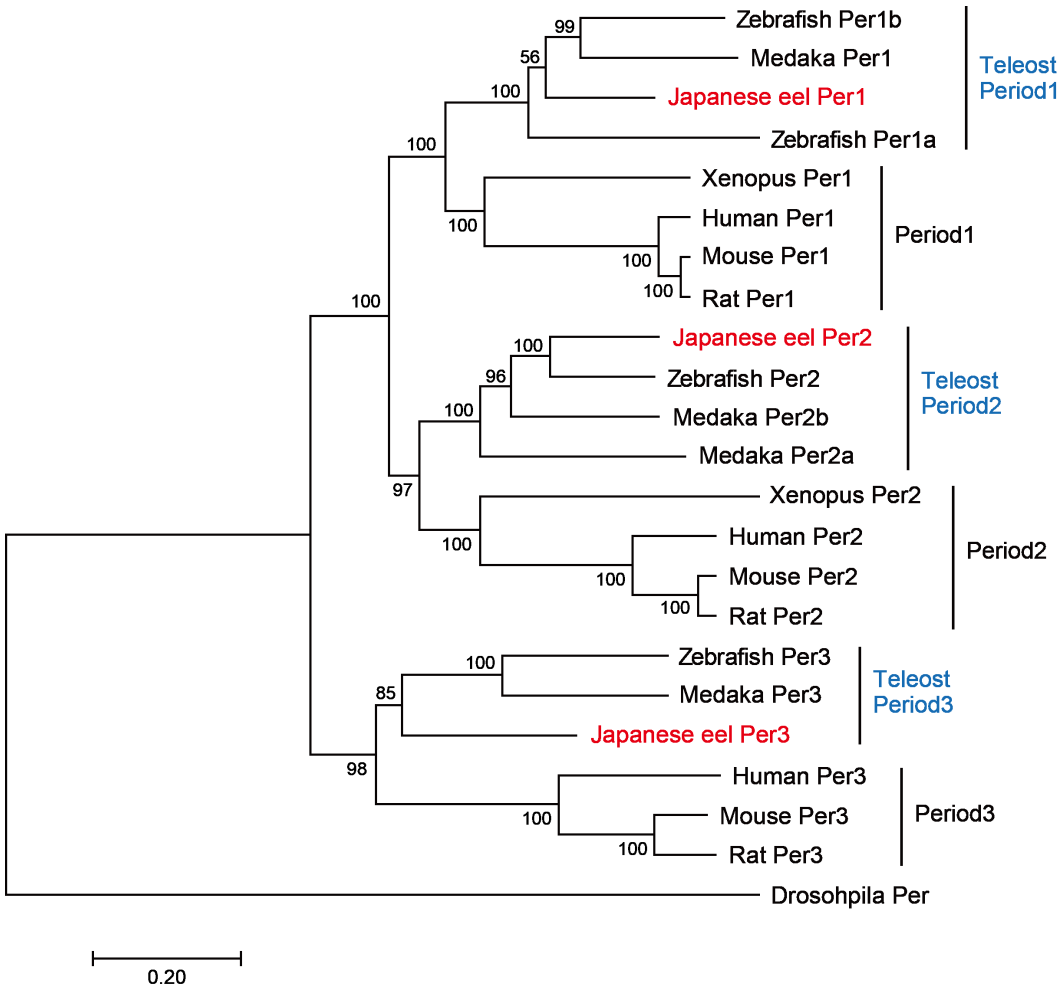

Figure 3.1. Phylogenetic tree of Pers of vertebrate including Japanese eel Pers. One thousand bootstrap repetitions were performed and values are shown at the inner nodes. *Drosophila melanogaster* Per was used as an outgroup. The protein alignment was performed for the phylogenetic analysis by ClustalW program. Bold is indicated the Per1, -2, and -3 of Japanese eel, *A. japonica*.

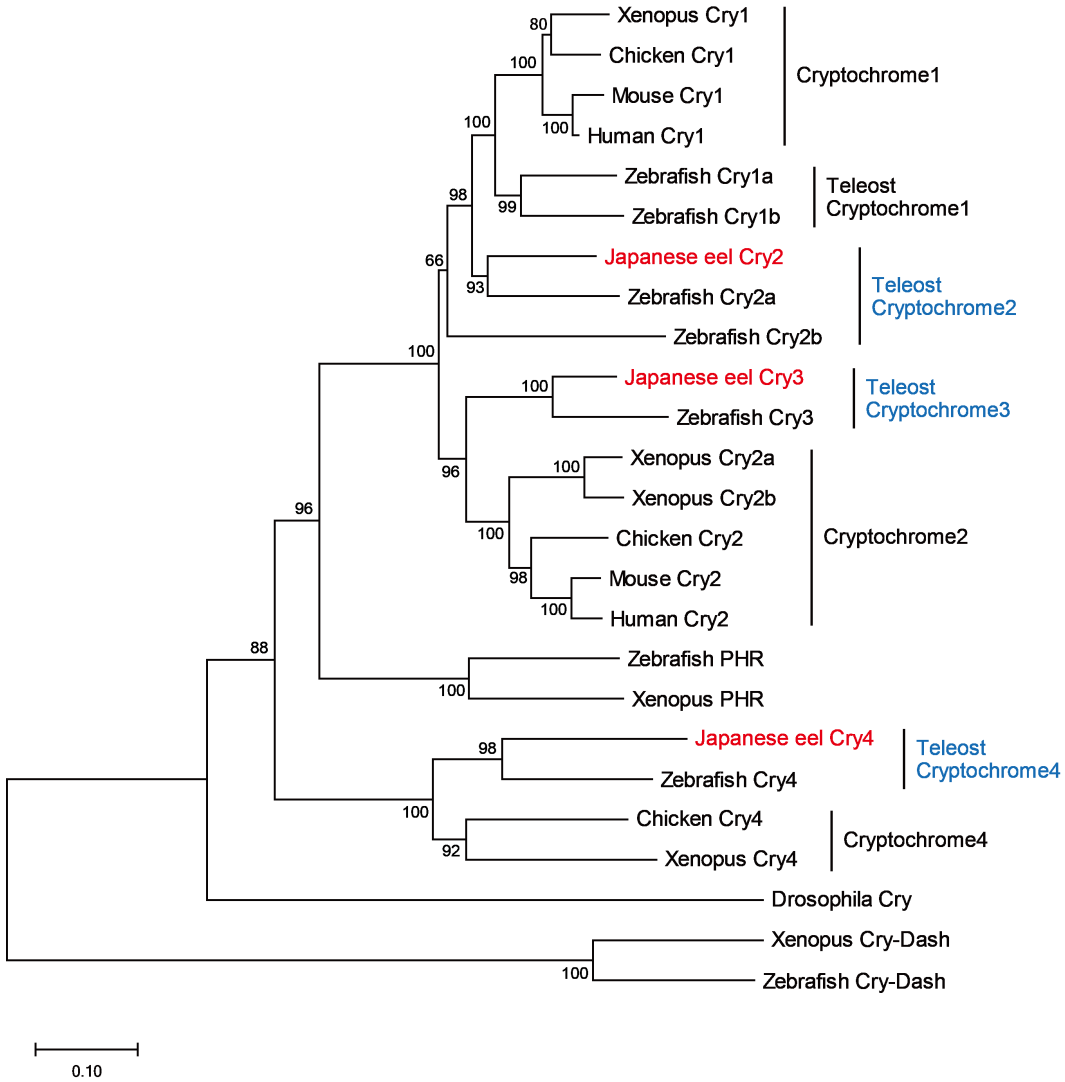

Figure 3.2. Phylogenetic tree of Crysof vertebrate including Japanese eel Crys. One thousand bootstrap repetitions were performed and values are shown at the inner nodes. The protein alignment was performed for the phylogenetic analysis by ClustalW program. Bold is indicated the Cry2, -3, and -4 of Japanese eel, *A. japonica*.

3.2. Experiment 1: Expression of clock genes in the retina and brain under the LD, LL, and DD conditions

The circadian oscillation patterns of clock genes of eels were investigated under LD, DD, and LL conditions. Per1 mRNA expression in the retina showed no circadian oscillation change in the LL condition, but peaked at ZT22 in the LD and DD conditions, and a similar pattern of circadian oscillation change was observed. The brain showed an opposite circadian oscillation pattern under DD and LL conditions and no circadian oscillation changes under LD conditions (Figure 3.3). Retina Per2 mRNA expression showed similar oscillation patterns, with Per2 mRNA expression peaking at ZT6 and ZT2 in the LD and DD conditions, respectively, but no circadian oscillation change was observed in the LL condition. The circadian oscillation of the brain was observed in the DD condition but not in the LD and LL conditions (Figure 3.4). Per3 mRNA expression showed circadian oscillation changes in the retina under LD conditions, but no oscillation changes were observed under DD and LL conditions. Per3 mRNA expression in the brain showed circadian oscillation changes in DD and LL conditions, but did not show circadian oscillation changes in LD conditions (Figure 3.5).

Cry2 mRNA expression in the retina showed a circadian oscillation under LD and LL conditions but no oscillation change under DD conditions. Cry2 mRNA expression showed rhythmic changes in the brain under LD conditions, but no circadian oscillation was observed under DD and LL conditions (Figure 3.6). Cry3 mRNA expression in the retina showed circadian oscillation changes in LD, DD, and LL conditions and peaked at ZT22 under LD and DD conditions. Similar circadian oscillation patterns were observed in LD and DD conditions. Brain Cry3 mRNA expression did not show an oscillation in LD and DD conditions, but showed circadian oscillation changes under LL conditions (Figure 3.7). Cry4 mRNA expression in the retina showed a circadian oscillation change with a peak at ZT14 in LD, DD, and LL conditions, and a similar circadian oscillation pattern was

observed in LD and DD conditions. Cry4 mRNA expression in the brain did not show circadian oscillation changes under LD and LL conditions but showed a circadian oscillation in DD conditions (Figure 3.8). In the retina, the Per1, Per2, Cry3, and Cry4 mRNA expression oscillations showed similar patterns under LD and DD conditions.

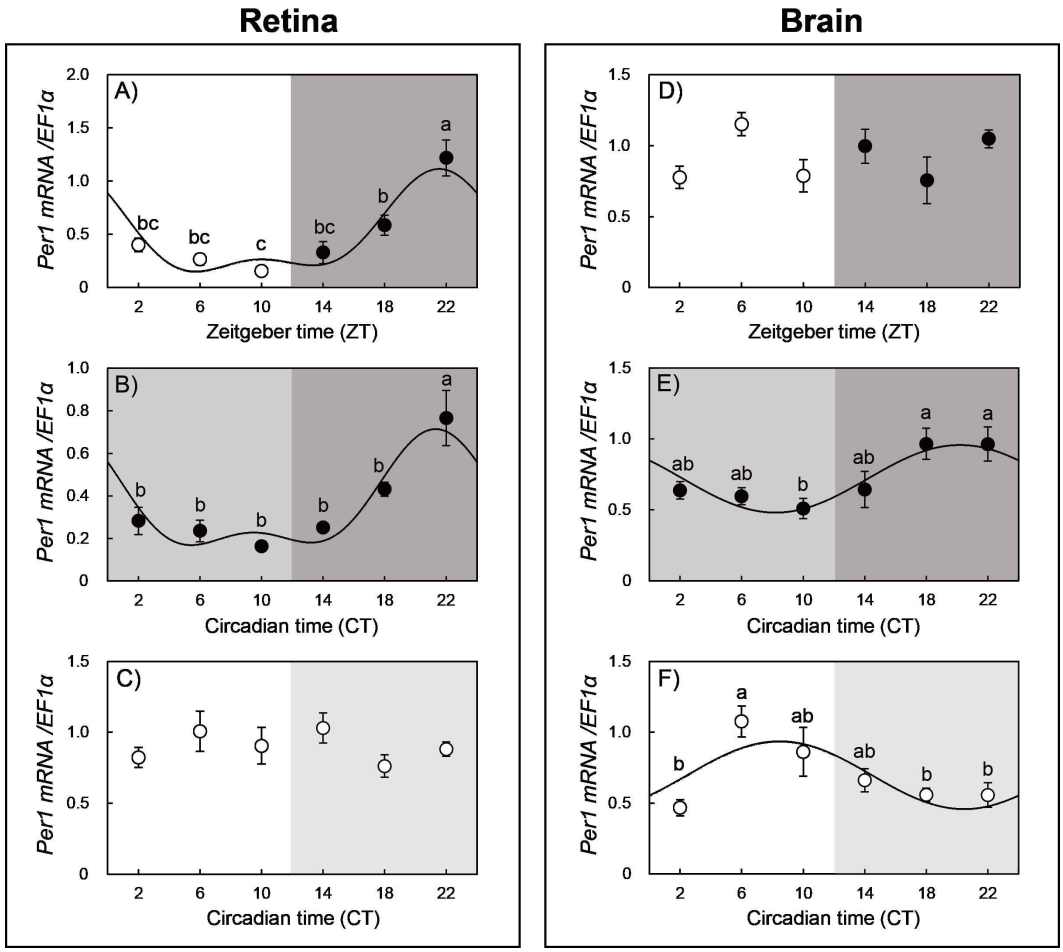

Figure 3.3. Cosinor analyses of Per1 genes expression levels in the retina and brain of the eel for three days during the LD (12L12D), DD and LL. The values are mean ± SEM (n = 5) of the normalized transcript levels of Per1 gene. White and black, represent the light and photophase and scotophase, respectively. Significant differences between the means at each sampling time are indicated by different letters ($P < 0.05$).

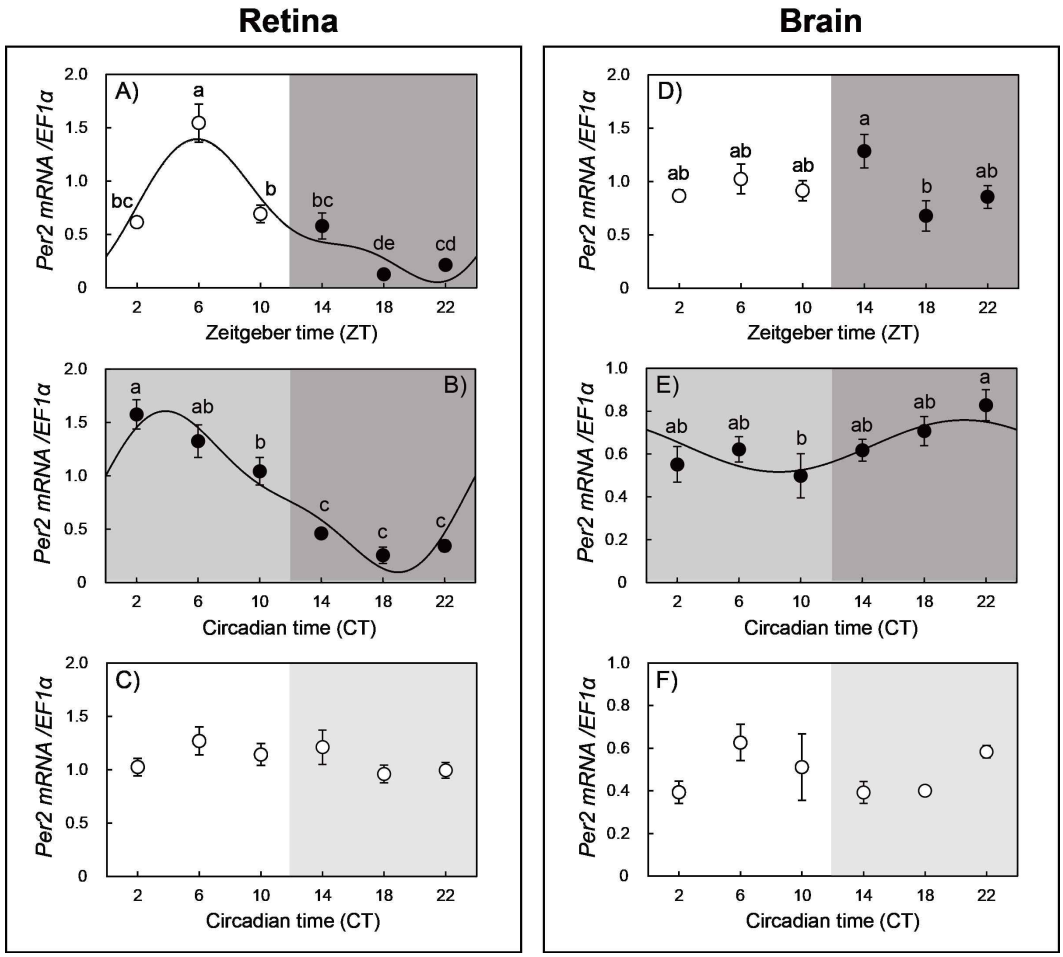

Figure 3.4. Cosinor analyses of Per2 genes expression levels in the retina and brain of the eel for three days during the LD (12L12D), DD and LL. The values are mean ± SEM (n = 5) of the normalized transcript levels of Per2 gene. White and black, represent the photophase and scotophase, respectively. Significant differences between the means at each sampling time are indicated by different letters ($P < 0.05$).

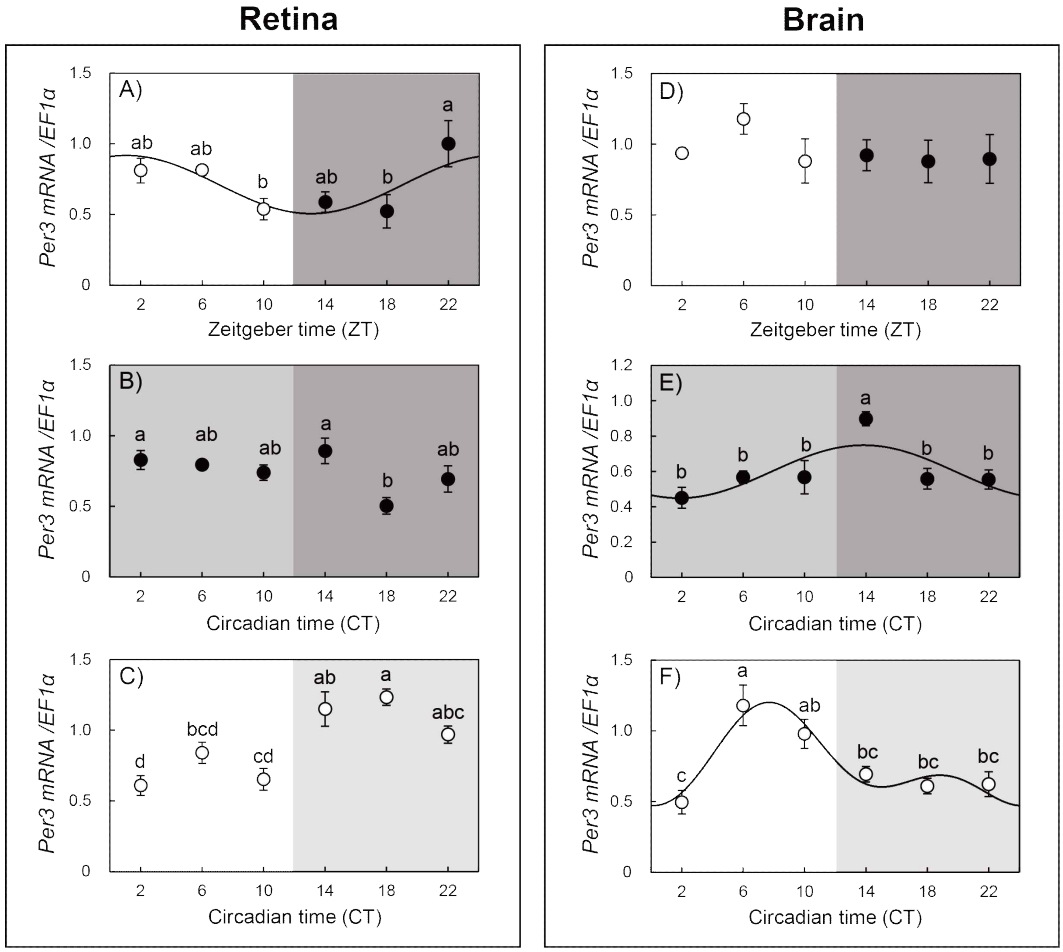

Figure 3.5. Cosinor analyses of Per3 genes expression levels in the retina and brain of the eel for three days during the LD (12L12D), DD and LL. The values are mean ± SEM (n = 5) of the normalized transcript levels of Per3 gene. White and black, represent the photophase and scotophase, respectively. Significant differences between the means at each sampling time are indicated by different letters ($P < 0.05$).

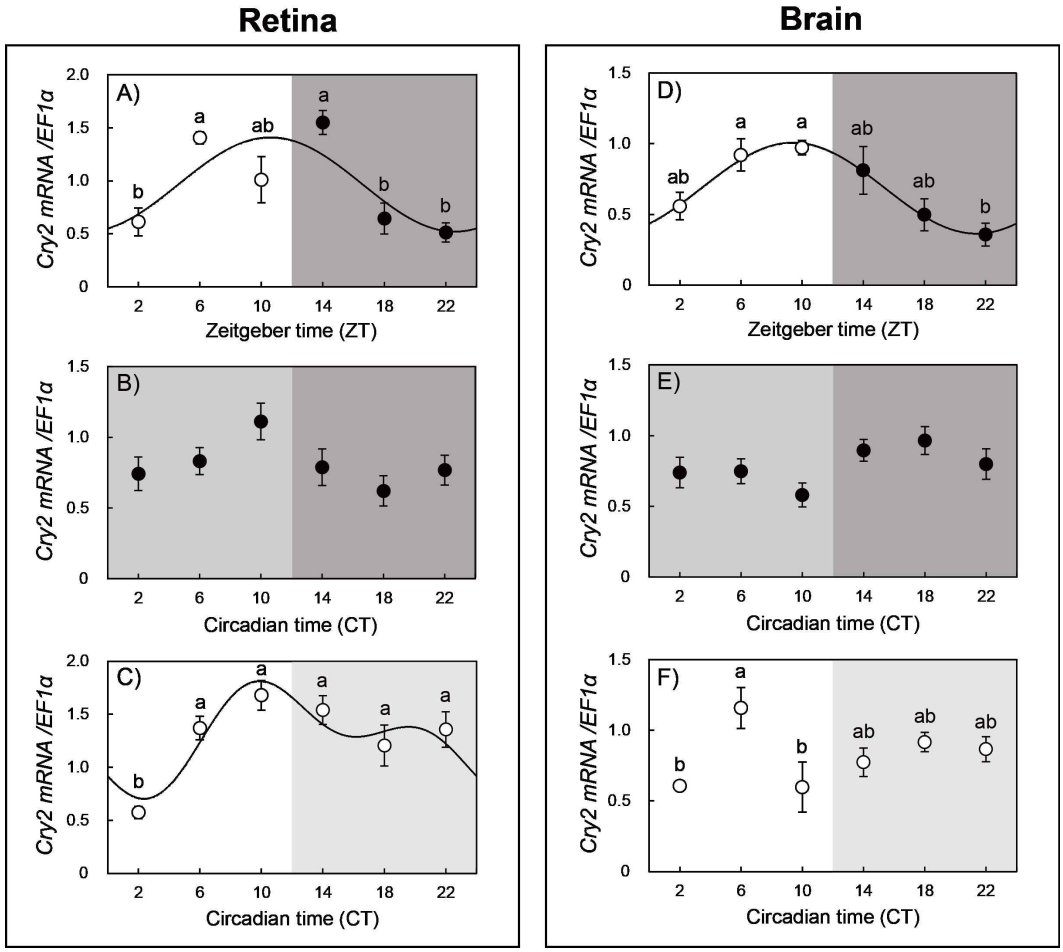

Figure 3.6. Cosinor analyses of Cry2 genes expression levels in the retina and brain of the eel for three days during the LD (12L12D), DD and LL. The values are mean ± SEM (n = 5) of the normalized transcript levels of Cry2 gene. White and black, represent the photophase and scotophase, respectively. Significant differences between the means at each sampling time are indicated by different letters ($P < 0.05$).

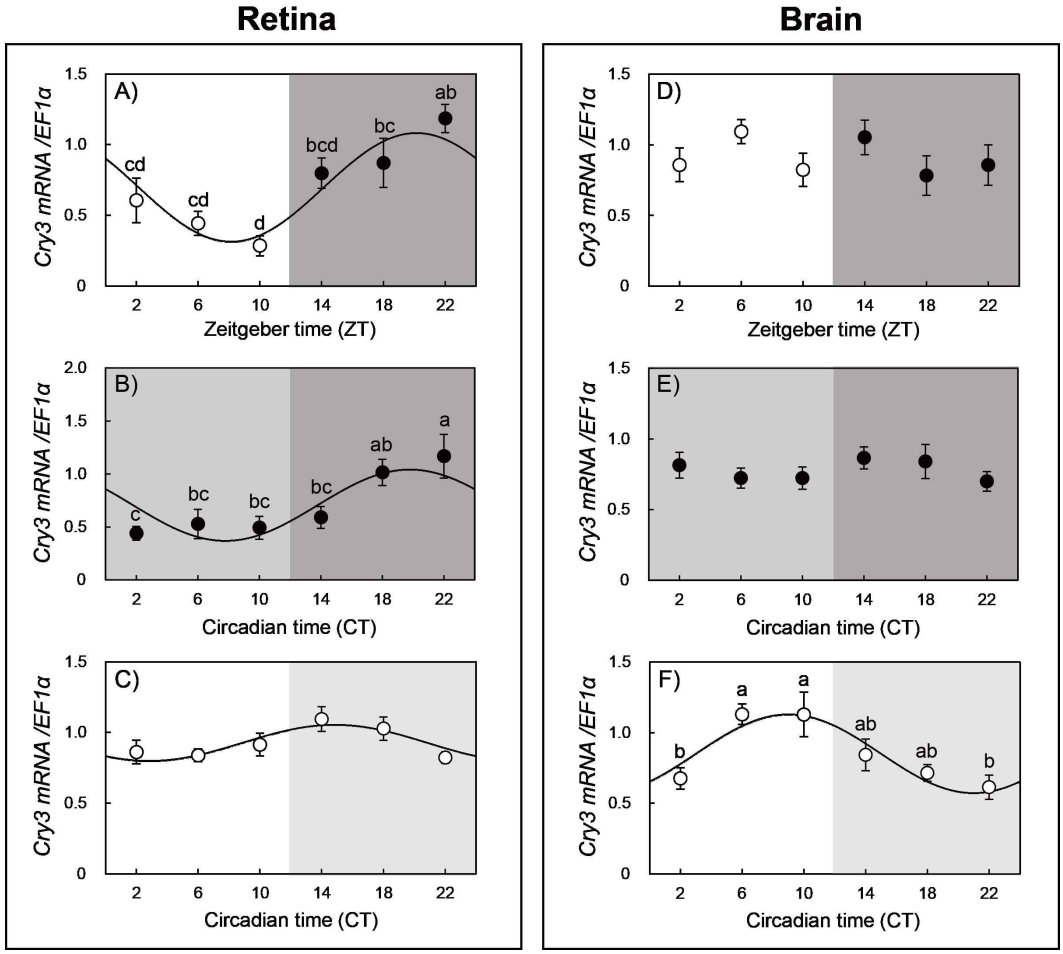

Figure 3.7. Cosinor analyses of Cry3 genes expression levels in the retina and brain of the eel for three days during the LD (12L12D), DD and LL. The values are mean ± SEM (n = 5) of the normalized transcript levels of Cry3 gene. White and black, represent the photophase and scotophase, respectively. Significant differences between the means at each sampling time are indicated by different letters ($P < 0.05$).

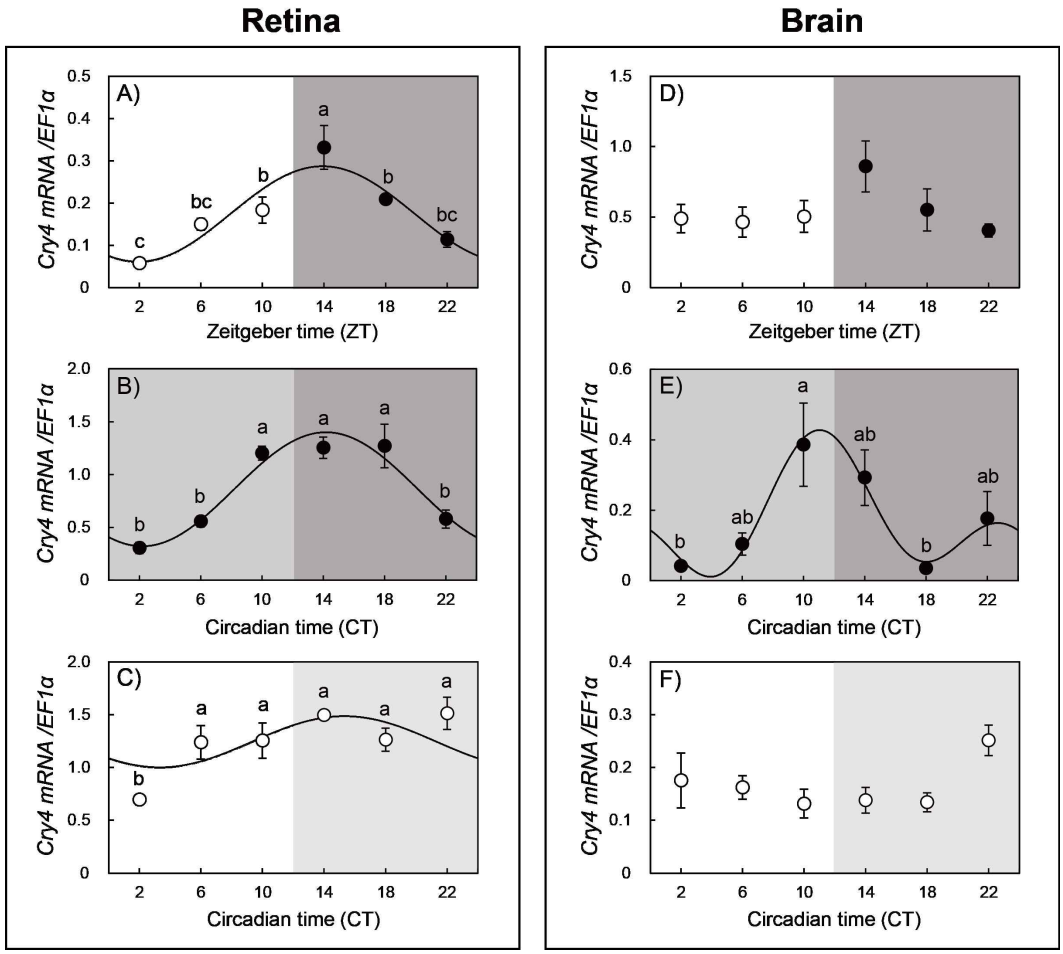

Figure 3.8. Cosinor analyses of Cry4 genes expression levels in the retina and brain of the eel for three days during the LD (12L12D), DD and LL. The values are mean ± SEM (n = 5) of the normalized transcript levels of Cry4 gene. White and black, represent the photophase and scotophase, respectively. Significant differences between the means at each sampling time are indicated by different letters ($P < 0.05$).

3.3. Experiment 2: Expression of clock genes in retina and brain under SP and LP conditions

Circadian rhythms of clock genes were investigated under LP and SP conditions in Japanese eels. Per1 mRNA expression showed an oscillation in the retina in both the LP and SP conditions, but the oscillation was delayed in the LP condition, and the SP condition oscillation showed an oscillation similar to that in the LD condition. Brain Per1 mRNA expression showed an oscillation in the LP condition, but there was no significant difference in the mRNA expression levels in the SP condition in all sections (Figure 3.9). Per2 mRNA expression, in both the LP and SP conditions in the retina, showed an oscillation similar to that in the LD and DD conditions, but peaked at ZT14 in the LP condition and showed a slightly different oscillation pattern. The oscillation pattern in the brain under the SP condition was similar to that in the DD condition and no oscillation was observed in the LP condition (Figure 3.10). Per3 mRNA expression showed an oscillation in the retina only in the SP condition, whereas the brain showed a higher level in all sections in the SP condition than in the LP condition, and an oscillation similar to that in the DD condition (Figure 3.11).

Retinal Cry2 mRNA expression showed oscillation in LP and SP conditions, but showed a significant difference in ZT10 and a different pattern of oscillation. In the brain, Cry2 showed no oscillation in the LP condition and showed oscillation in the SP condition, but showed a significant difference was observed only at ZT6 and ZT22 (Figure 3.12). Cry3 mRNA expression peaked at ZT22 in the SP condition in the retina and showed an oscillation similar to that in the LD condition. The oscillation was delayed in the LP condition, whereas the brain showed an oscillation in all the SP conditions, except for the LP condition and at ZT2. There were no significant differences between the sections (Figure 3.13). Cry4 mRNA expression showed an oscillation with a peak at ZT14 in the SP condition in the retina, but no oscillation in the brain in both the LP and SP conditions (Figure 3.14). In the retina,

the Per1, Per2, Cry3, and Cry4 mRNA expression oscillations showed similar patterns under SP and LD conditions.

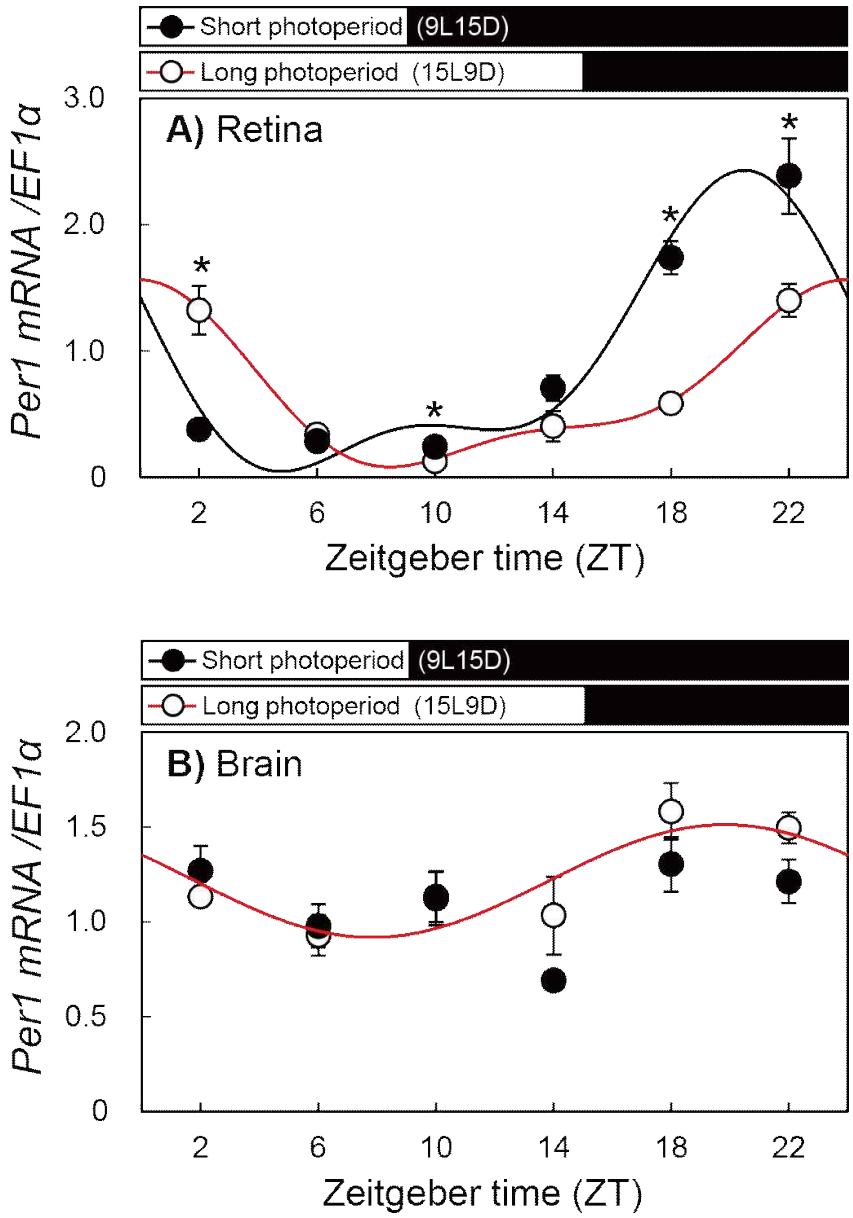

Figure 3.9. Cosinor analyses of Per1 genes expression levels in the retina and brain of the eel for one week during the long-photoperiod (15L9D) and short-photoperiod (9L15D). The values are mean ± SEM (n = 5) of the normalized transcript levels of Per1 gene. White and black, represent the long photoperiod and short photoperiod, respectively. Significant differences between the means at each sampling time are indicated by different letters ($P < 0.05$).

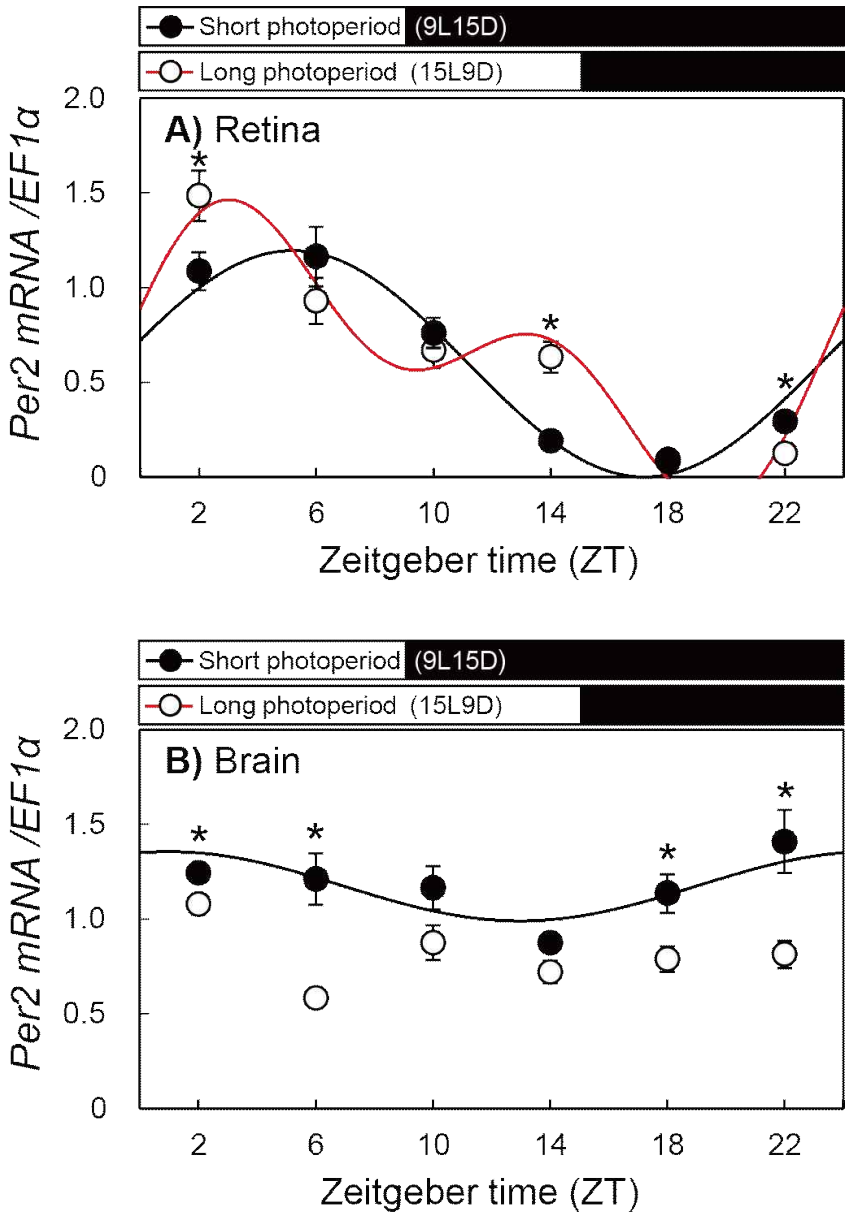

Figure 3.10. Cosinor analyses of Per2 genes expression levels in the retina and brain of the eel for one week during the long-photoperiod (15L9D) and short-photoperiod (9L15D). The values are mean ± SEM (n = 5) of the normalized transcript levels of Per2 gene. White and black, represent the long photoperiod and short photoperiod, respectively. Significant differences between the means at each sampling time are indicated by different letters ($P < 0.05$).

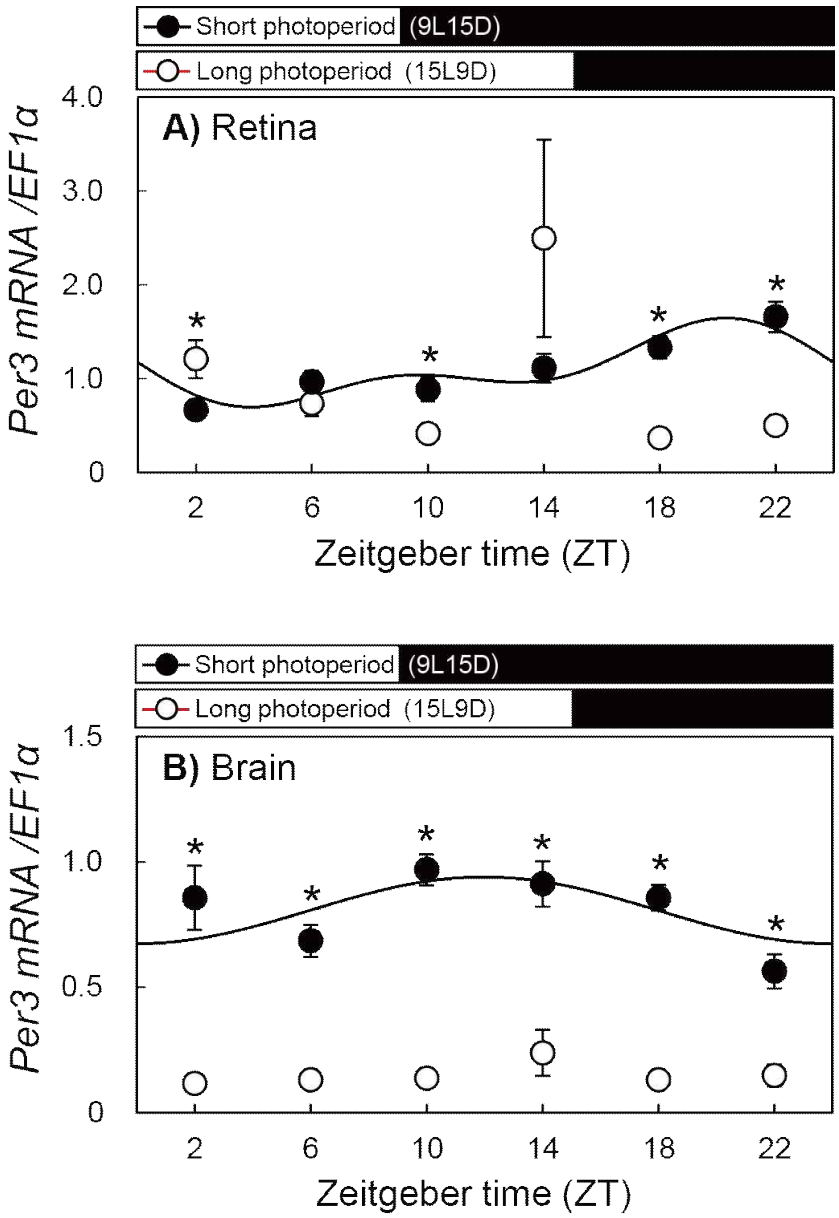

Figure 3.11. Cosinor analyses of Per3 genes expression levels in the retina and brain of the eel for one week during the long-photoperiod (15L9D) and short-photoperiod (9L15D). The values are mean ± SEM (n = 5) of the normalized transcript levels of Per3 gene. White and black, represent the long photoperiod and short photoperiod, respectively. Significant differences between the means at each sampling time are indicated by different letters ($P < 0.05$).

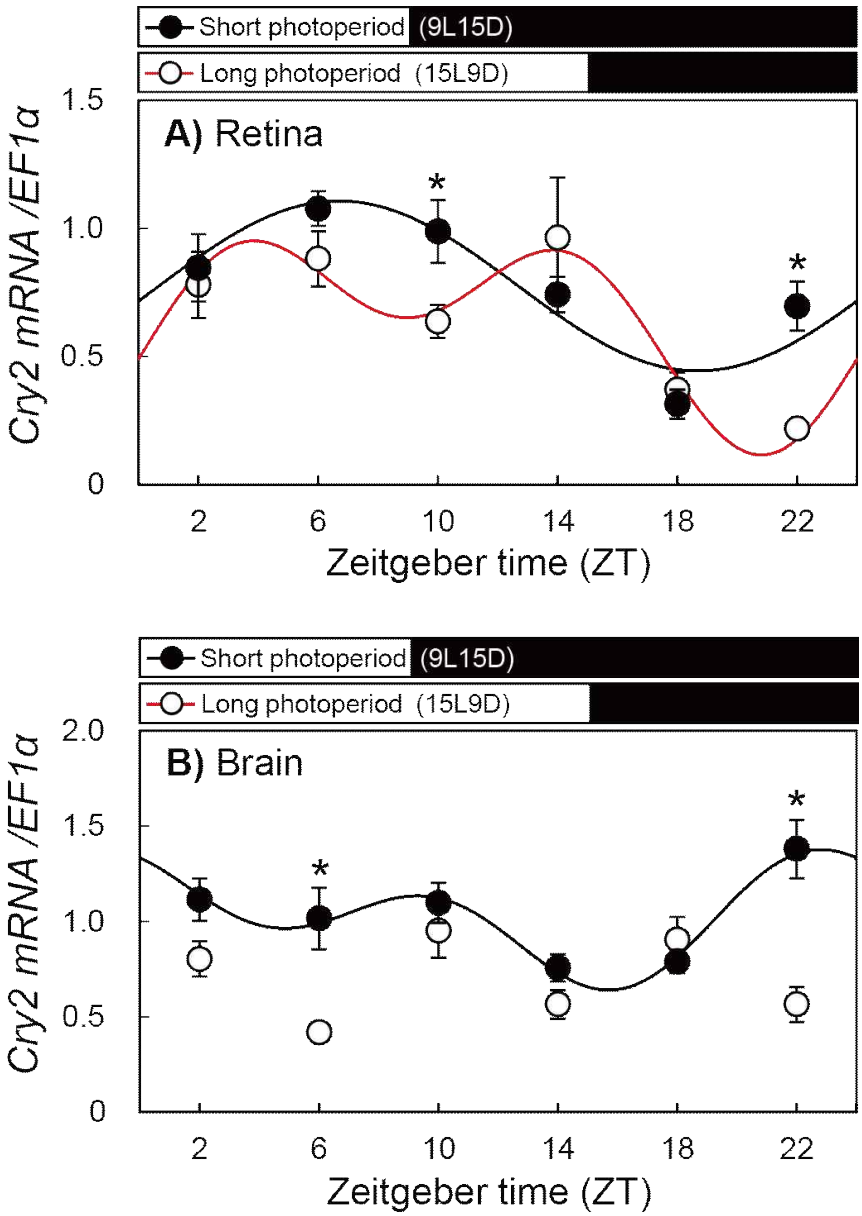

Figure 3.12. Cosinor analyses of Cry2 genes expression levels in the retina and brain of the eel for one week during the long-photoperiod (15L9D) and short-photoperiod (9L15D). The values are mean ± SEM (n = 5) of the normalized transcript levels of Cry2 gene. White and black, represent the long photoperiod and short photoperiod, respectively. Significant differences between the means at each sampling time are indicated by different letters ($P < 0.05$).

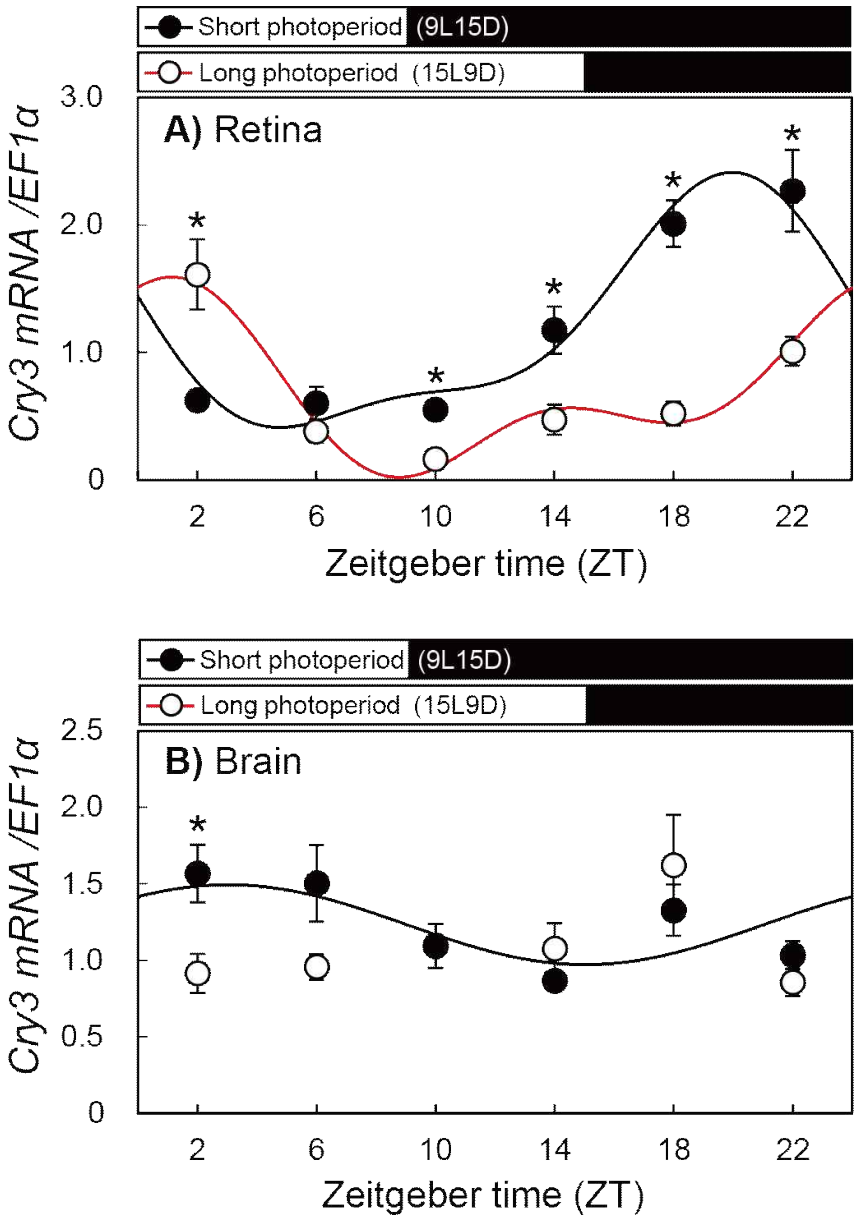

Figure 3.13. Cosinor analyses of Cry3 genes expression levels in the retina and brain of the eel for one week during the long-photoperiod (15L9D) and short-photoperiod (9L15D). The values are mean ± SEM (n = 5) of the normalized transcript levels of Cry3 gene. White and black, represent the long photoperiod and short photoperiod, respectively. Significant differences between the means at each sampling time are indicated by different letters ($P < 0.05$).

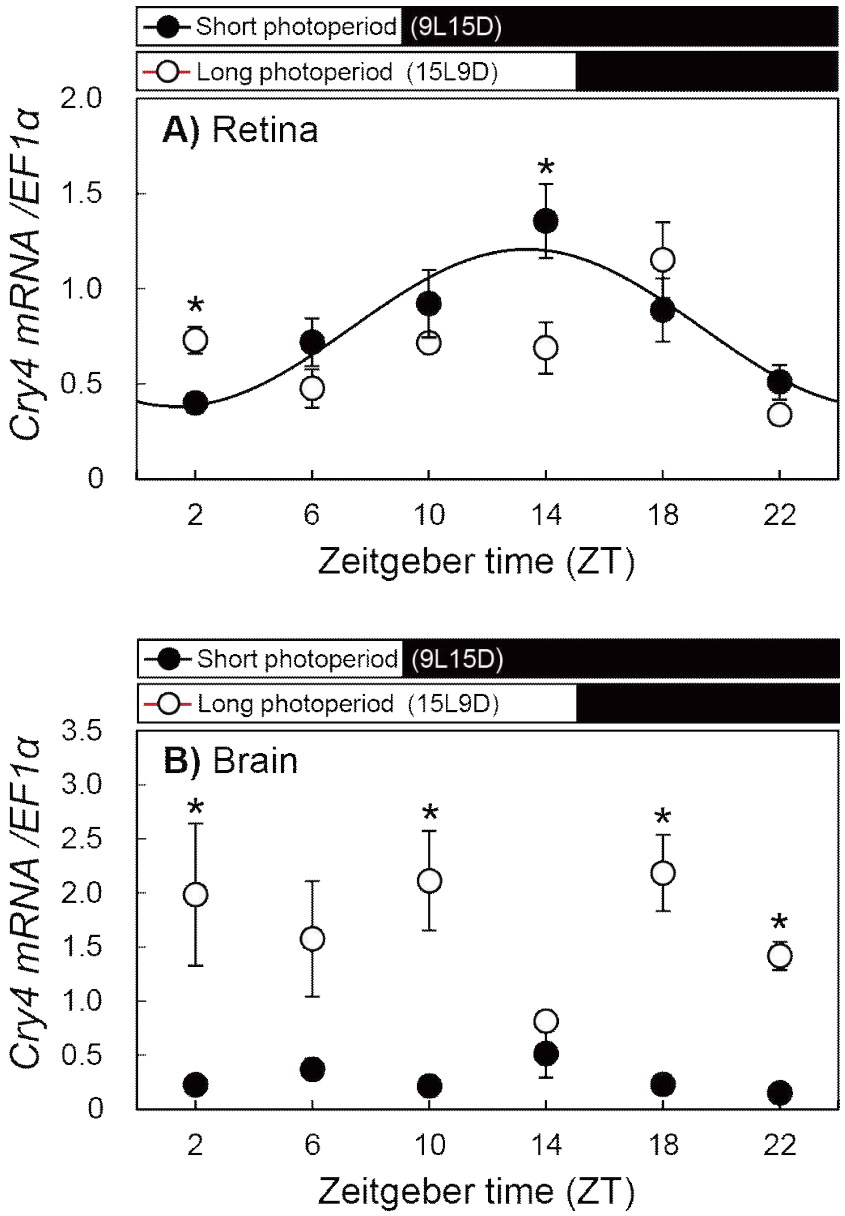

Figure 3.14. Cosinor analyses of Cry4 genes expression levels in the retina and brain of the eel for one week during the long-photoperiod (15L9D) and short-photoperiod (9L15D). The values are mean ± SEM (n = 5) of the normalized transcript levels of Cry4 gene. White and black, represent the long photoperiod and short photoperiod, respectively. Significant differences between the means at each sampling time are indicated by different letters ($P < 0.05$).

3.4. Experiment 3: Expression of clock genes in the retina and brain under NM and FM conditions

Per1 mRNA expression peaked at 4 h in the retina and showed an oscillation in NM and FM, and NM and FM also showed an oscillation in the brain (Figure 3.15). Retinal Per2 mRNA expression was highest at 12 h and lowest at 24 h, showing oscillations similar to those of the LD and DD conditions in both NM and FM. Brain Per2 showed no oscillation in FM but showed a significant difference at 12 h and showed oscillation in NM (Figure 3.16). Per3 had no oscillation in the brain but showed opposite oscillations in the NM and FM conditions in the retina (Figure 3.17).

Cry2 mRNA expression showed similar oscillations in NM and FM in the retina, but showed opposite oscillations in NM and FM in the brain (Figure 3.18). Cry3 mRNA expression showed no oscillation in both NM and FM in the brain but showed the highest level at 4 h in the retina and had an oscillation in NM and FM. This oscillation was similar to the oscillation pattern observed in the LD and DD conditions (Figure 3.19). Brain Cry4 showed no rhythm. Retinal Cry4 showed the highest level at 20 h in NM and showed an oscillation similar to that of the LD and DD conditions (Figure 3.20). In the retina, Per1, Per2, Cry3, and Cry4 mRNA expression oscillations showed similar patterns to those in NM, SP, and LD conditions.

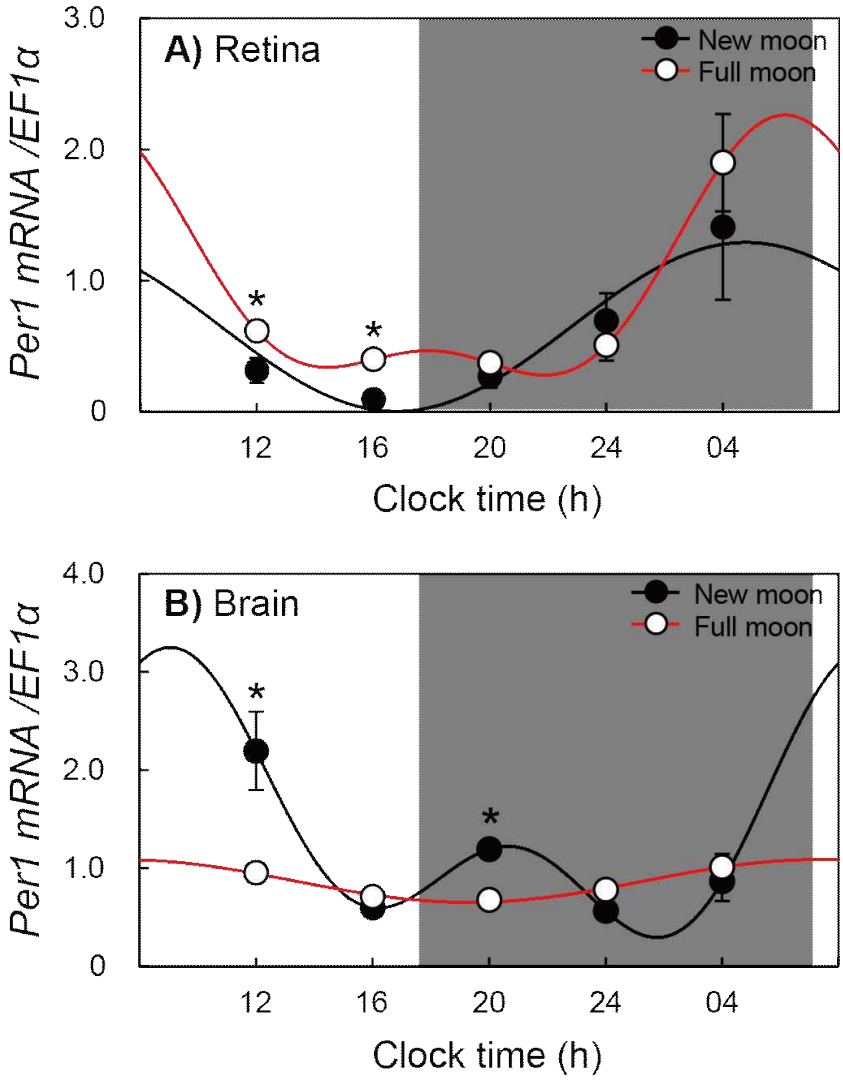

Figure 3.15. Cosinor analyses of Per1 genes expression levels in the retina and brain of the eel during the natural moonlight (NM; new moon, FM; full moon). White (red-line) and black (black-line), represent the NM and FM, respectively. *P < 0.05 at the same time point (Student`s t-test), mean ± SEM (n = 5).

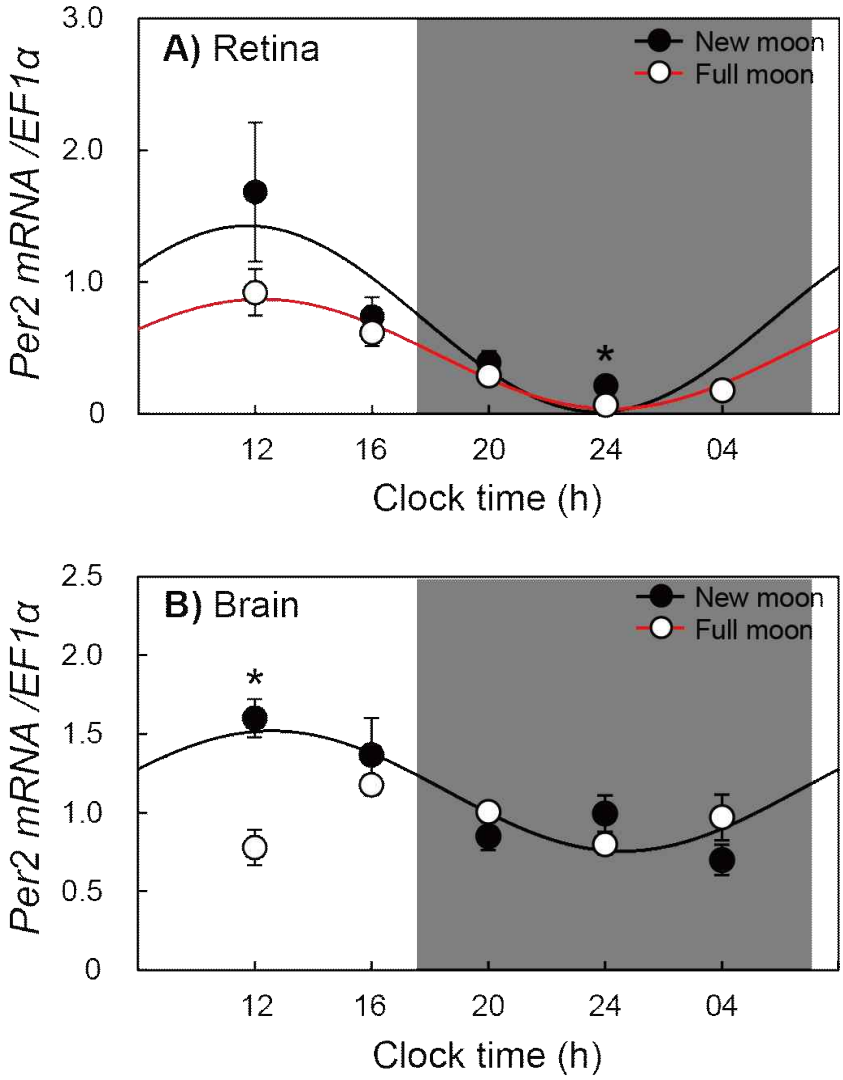

Figure 3.16. Cosinor analyses of Per2 genes expression levels in the retina and brain of the eel during the natural moonlight (NM; new moon, FM; full moon). White (red-line) and black (black-line), represent the NM and FM, respectively. *P < 0.05 at the same time point (Student`s t-test), mean ± SEM (n = 5).

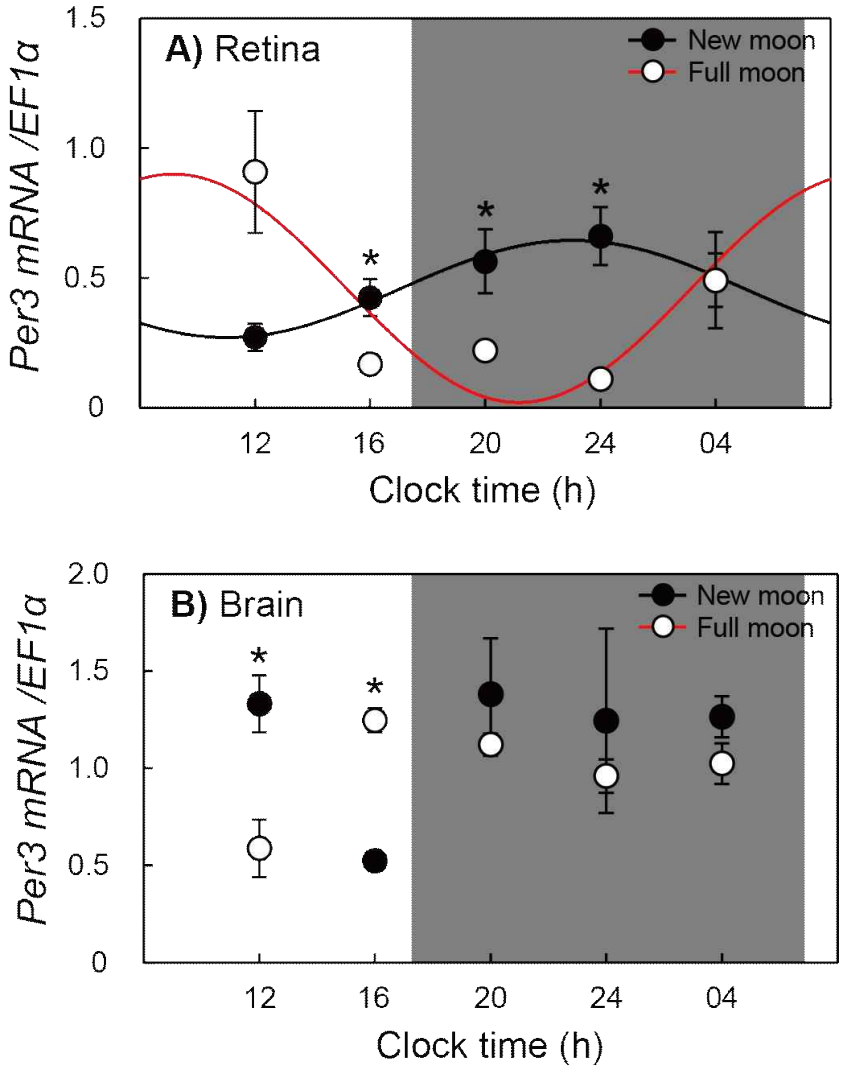

Figure 3.17. Cosinor analyses of Per3 genes expression levels in the retina and brain of the eel during the natural moonlight (NM; new moon, FM; full moon). White (red-line) and black (black-line), represent the NM and FM, respectively. *P < 0.05 at the same time point (Student`s t-test), mean ± SEM (n = 5).

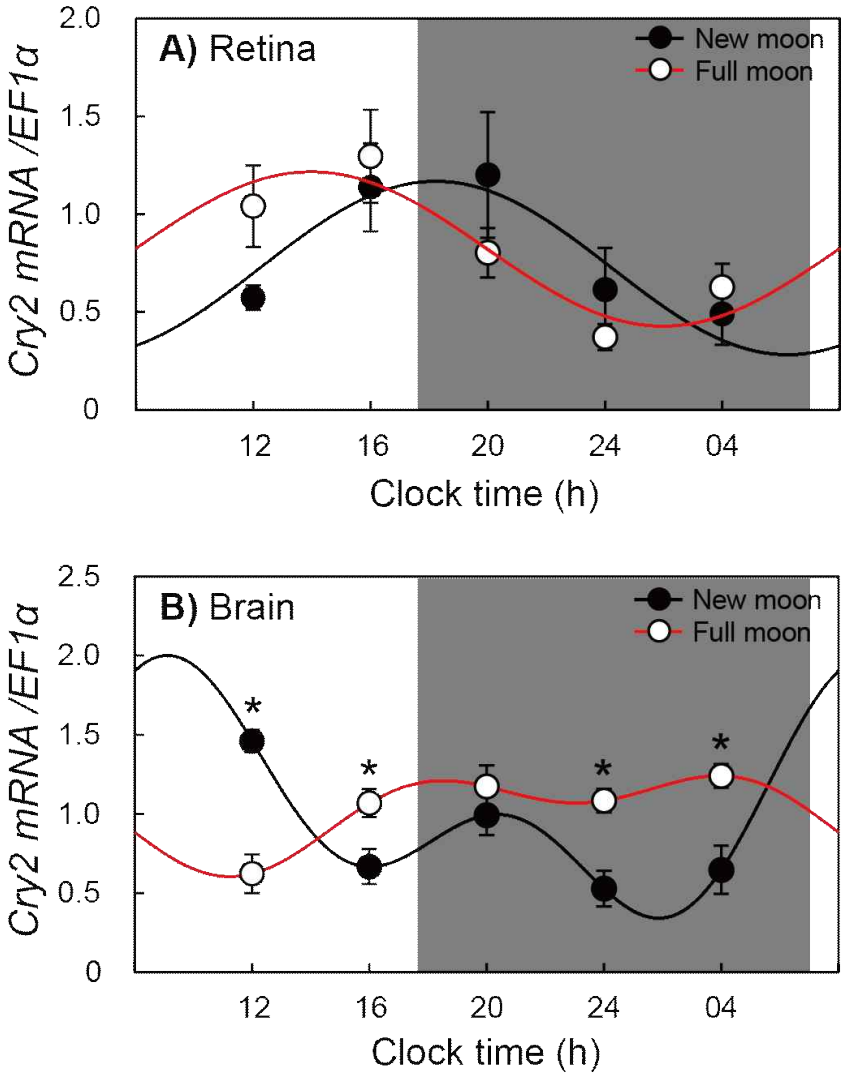

Figure 3.18. Cosinor analyses of Cry2 genes expression levels in the retina and brain of the eel during the natural moonlight (NM; new moon, FM; full moon). White (red-line) and black (black-line), represent the NM and FM, respectively. *P < 0.05 at the same time point (Student`s t-test), mean ± SEM (n = 5).

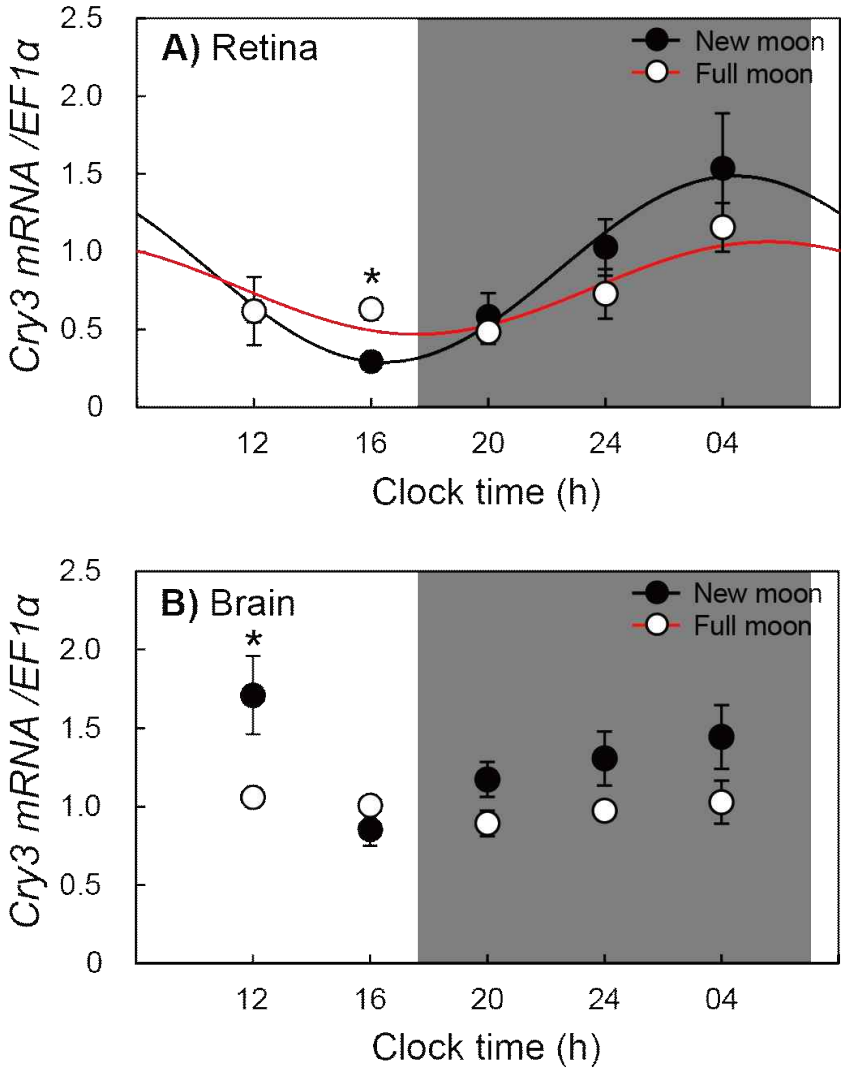

Figure 3.19. Cosinor analyses of Cry3 genes expression levels in the retina and brain of the eel during the natural moonlight (NM; new moon, FM; full moon). White (red-line) and black (black-line), represent the NM and FM, respectively. *P < 0.05 at the same time point (Student`s t-test), mean ± SEM (n = 5).

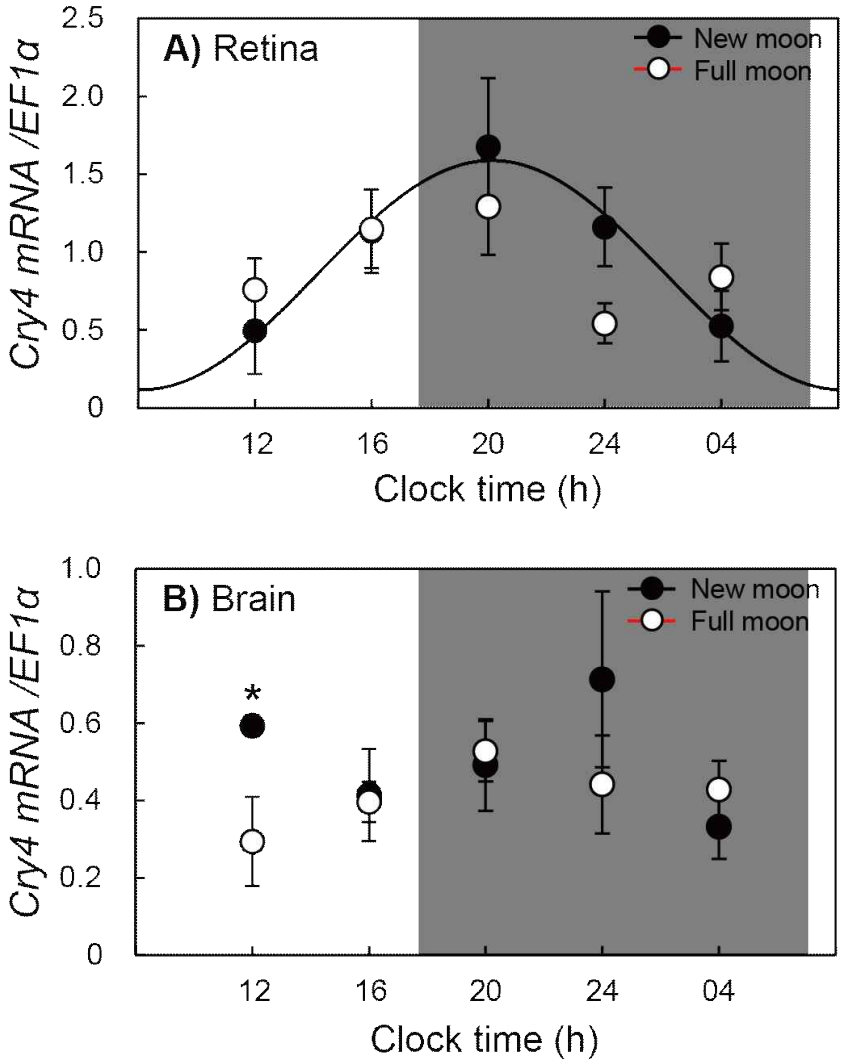

Figure 3.20. Cosinor analyses of Cry4 genes expression levels in the retina and brain of the eel during the natural moonlight (NM; new moon, FM; full moon). White (red-line) and black (black-line), represent the NM and FM, respectively. *P < 0.05 at the same time point (Student`s t-test), mean ± SEM (n = 5).

4. Discussion

In many teleost, reproductive control is synchronized by the photoperiod. However, to date, there is little evidence on the relationship between photoperiod changes and reproduction in eels. In this regard, to elucidate the correlation between changes in the photoperiod and reproduction, factors that synchronize the 24-h cycle and photoperiod clock or light availability information for inputting day/night length information into the photoperiod clock should be analyzed. However, these input factors have not been determined for the eel. We had previously confirmed that melatonin secretion in eels was inhibited by photoperiod change (SP to LP) and the full moon. Therefore, it is speculated that a change in the photoperiod or photostimulation of moonlight could play a key role in synchronizing the eel's biological clock. In this study, we aimed to demonstrate the potential of Per1, -2, -3, and Cry2, -3, -4 as magnetic field receptors on the core loop that are involved in seasonal and lunar responses.

First, using RNA-seq, we identified six core clock genes (Per1, -2, -3, and Cry2, -3, and -4) in eels belonging to the clock gene family (Per and Cry), which are orthologous genes that have been previously reported in zebrafish and other fish species. The phylogenetic relationship of each gene family was confirmed to be consistent with the results for zebrafish and other fish species. It is speculated that this can function as a biological clock gene in a biological process synchronized with previously reported circadian oscillations.

However, little is known about the expression rhythms of clock genes in eels. We first investigated the circadian rhythm of core clock genes in the brain and retina of pubertal male eels. Our results showed that Per1, -2, and -3, according to the circadian cycle, showed more pronounced oscillations in the retina than in the brain. In the retina, Per1 and -2 mRNA expressions showed a similar rhythmic expression that increased just before the photophase in all conditions except the LL condition.

In contrast, in the brain, Per1, -2, and -3 mRNA expression oscillations did not show a clear repeating pattern, and the oscillation amplitude of expression was not large compared to that in the retina. More specifically, in the retina, Per1 mRNA increased just before the photophase, and Per2 mRNA increased during the photophase. This was similar to the mRNA expression patterns of Per1 and Per2 in teleost (goldfish retina; Velarde et al., 2009, *Astatotilapia burtoni*; Song et al., 2017, turbot; Ceinos et al., 2019) and *Xenopus laevis* retinas. This indicates that, in eels, Per1 mRNA is regulated in a circadian manner and Per2 mRNA is regulated by light. These results suggest that Per1 functions as a major regulator of the circadian feedback loop. However, since Per2 mRNA maintains oscillation under DD conditions, Per2 can also act as a regulator in the circadian feedback loop.

The photoperiodic response is determined by a combination of the internal clock signal and the external optical signal. It has long been known that a photoperiodic response is induced when light stimulation occurs within a specific time of the day (Bünning, 1960; Pittendrigh & Minis, 1964; Pittendrigh, 1972). In mammalian Syrian hamsters, the circadian pacemaking system of Per1, -2, and -3 in the (suprachiasmatic nucleus) SCN is tightly regulated according to the photoperiod, showing high levels during the day (Tournier et al., 2003). Moreover, in the pars tuberalis of sheep, the time of expression of Per1 and Per2 vary according to the photoperiod (Lincoln, Andersson & Hazlerigg, 2003). In this study, SP oscillations showed a clear pattern in the brain and retina of the eels. In contrast, the oscillation of retinal Per3 disappeared in the LP condition, but the oscillation was confirmed again in the SP condition. In the retina of birds (Japanese quail: Yoshimura et al., 2000) and fish (goldfish: Velarde et al., 2009, Senegal sole: Martín-Robles et al., 2012), Per3 expression was significantly decreased at the end of the photophase, and oscillation was observed.

In the telencephalon and diencephalon of the Malabar grouper, in the brain of the European sea bass, and in the retina of goldfish and zebrafish, Cry2 mRNA expression peaks at the day-night phase (Yamashina et al., 2019; del Pozo et al.,

2012; Velarde et al., 2009; Kobayashi et al., 2000). A similar expression was observed in pea aphids (Barberà, Collantes-Alegre & Martínez-Torres, 2022) and other insects such as the bean bug and monarch butterfly (Ikeno, Numata, & Goto, 2011; Merlin et al., 2013; Zhang et al., 2017). In fish, Cry2 is a gene possible induced by a light signal (Yamashina et al., 2019), whereas in insects, Cry2 does not respond to light but rather functions as a transcription factor similar to the Per gene (Barberà, Collantes-Alegre & MartMartíneznez-Torres, 2022). In this study, Cry3 showed a similar expression pattern under all conditions and increased with a peak in the scotophase or approximately 10 h after the start of scotophase. In bony fish, Cry3 mRNA expression peaked at midnight in the goldfish retina (Velarde et al., 2009), and oscillations were highest in ZT24 under the 14L10D condition in the whole body and eyes of zebrafish (Kobayashi et al., 2000). In the Japanese eel, the amplitude of Cry3 expression oscillations decreased or the phase shifted in the LL and LP conditions, respectively, when compared to the LD and SP conditions. This may be due to the relatively long photoperiod and exposure to high-intensity light. However, although Cry3 functions as a core clock gene, further research is needed to elucidate the additional function of Cry3 in the Japanese eel because of lack of solid evidence for its ability to recognize light.

In this study, we investigated whether the presence or absence of moonlight is involved in the regulation of clock genes in eels. It is assumed that the lunar cycle or moonlight is directly related to the onset of spawning migration, vertical migration, locomotor activity, and spawning in many previous reports on eels (Tesch, 1978; Miyagi et al., 2004; Tsukamoto, 2006; Chow et al., 2015; Higuchi et al., 2021). In the present study, the amplitude of oscillations of the core clock genes in the NM period was more distinct than that in the FM period. This is presumably because melatonin, a major regulator of clock genes, is mainly synthesized and secreted in the eel retina. We have previously demonstrated that light from the full moon and long-to-short-cycle transitions inhibit melatonin secretion in eels (Hyeon et al., 2021). In particular, level of melatonin in the eye, compared to that in the

blood, increased dramatically during the last month. This indicates that eye melatonin perceives moonlight and is affected by it. Previous studies have also shown that melatonin affects the transcriptional levels of clock genes in mammals (Dardente et al., 2003; Hazlerigg et al., 2004). It has been reported that the disappearance of the melatonin signal in the retina of mice significantly affects the retinal Per1, -2, and Bmal expression patterns (Hiragaki, 2014). This study confirmed that the presence or absence of moonlight and changes in photoperiod are involved in the vibration of the clock gene on the core loop. Overall, the amplitude of vibration decreased in the NM condition compared to the FM condition, and on the contrary, in Cry2 and Cry3, the amplitude decreased in FM rather than NM. In particular, the oscillation of Cry4 in the retina disappeared under FM conditions. This indicates that even in eels, the 24-h retinal core clock gene is not controlled by the endogenous cyclic timer, and that the normal transcription cycle of the retinal clock gene can be disrupted by light exposure time and moonlight.

In this study, for the first time, we investigated the expression rhythm of Cry4 under external light conditions in an eel. According to previous reports on the Cry4 gene, Cry4 does not have a nuclear localization signal (NLS) motif or a protein-protein interaction domain; therefore, it does not function as a circadian function (Liu et al., 2015). Since Cry4 in zebra finches is not affected by the circadian rhythm and there is no rhythm change, it is speculated that it will act as a magnetoreceptor rather than a circadian clock (Pinzon-Rodriguez, Bensch & Muheim, 2018). In addition, strong evidence has suggested that Cry4 does not participate in circadian transcriptional regulation as a circadian clock in zebrafish (Kobayashi et al., 2000; Liu et al., 2015), but it has been suggested that Cry4 may serve as an upstream optical sensor expressing genes required to accompany the circadian clock in UV cones (Cermakian & Sassone-Corsi, 2002; Hirayama et al., 2009; Vatine et al., 2011). In this study, we confirmed that the expression pattern of clock genes in eels was altered by circadian rhythm, photoperiod, and moonlight. In particular, the amplitude of Cry4 mRNA disappeared in the LP and FM. Further research is needed

to determine whether Cry4 acts as an upstream light sensor for driving biological clock gene expression, as in the case of zebrafish, or a magnetic field receptor function according to the initiation of scattering migratory activity around their spawning migratory period (September to October, photoperiod conversion to LP-SP).

Previous studies have suggested that Cry4 mediates light-dependent self-acceptance in various animal groups (Gegear et al., 2010; Bazalova et al., 2016; Foley, Gegear & Reppert, 2011; Wiltschko & Wiltschko, 2005). In particular, in seasonal migratory avians (*Erithacus rubecula*), Cry4 is a magnetoreceptor that acts as a light-dependent magnetic compass (Xu et al., 2021). Although the role of magnetoreceptors in fish is not well known, the existence and function of magnetoreceptors can be inferred because magnetic field recognition behaviors are observed in some fish that migrate (Shcherbakov & Fabian, 2005; Takebe et al., 2012; Krylov et al., 2016; Quinn; 1980; Putman et al., 2013; Cresci et al., 2017a; Cresci et al., 2017b; Putman, 2018; Bottesch et al., 2016; Cresci et al., 2019). Eels also migrate to the Mariana Trench, near the equator, to spawn. However, unlike other migratory animals, sexual maturation begins when they start migrating. We found that Cry4 expression in eels was similar to the melatonin secretion pattern. Based on the rapid increase in melatonin secretion in mature eels in the NM, it is speculated that melatonin is related to sexual maturation (Hyeon et al., 2021).

5. References

Barberà M, Collantes-Alegre JM, Martínez-Torres D. 2022. Mapping and quantification of cryptochrome expression in the brain of the pea aphid *Acyrthosiphon pisum*. Insect Molecular Biology. 31:159-169. DOI 10.1111/imb.12747.

Bazalova O, Kvicalova M, Valkova T, Slaby P, Bartos P, Netusil R, Tomanova K, Braeunig P, Lee HJ, Sauman I, Damulewicz M, Provaznik J, Pokorny R, Dolezel D, Vacha M. 2016. Cryptochrome 2 mediates directional magnetoreception in cockroaches. Proceedings of the National Academy of Sciences of the United States of America. 113:1660-1665. DOI 10.1073/pnas.1518622113.

Bolger AM, Lohse M, Usadel B. 2014. Trimmomatic: a flexible trimmer for Illumina sequence data. Bioinformatics. 30:2114-2120. DOI 10.1093/bioinformatics/btu170.

Bone Q. 2019. Fish: general review. Encyclopedia of Ocean Sciences. 129-137. DOI 10.1016/B978-0-12-409548-9.10779-1

Bottesch M, Gerlach G, Halbach M, Bally A, Kingsford MJ, Mouritsen H. 2016. A magnetic compass that might help coral reef fish larvae return to their natal reef. Current Biology. 26:R1266-R1267. DOI 10.1016/j.cub.2016.10.051.

Bünning E. 1960. Circadian rhythms and the time measurement in photoperiodism. Cold Spring Harbor Symposia on Quantitative Biology. 25:249-256. DOI 10.1101/SQB.1960.025.01.026.

Ceinos RM, Chivite M, López-Patiño MA, Naderi F, Soengas JL, Foulkes NS, Míguez JM. 2019. Differential circadian and light-driven rhythmicity of clock gene expression and behaviour in the turbot, *Scophthalmus maximus*. PLoS ONE. 14:e0219153. DOI 10.1371/journal.pone.0219153.

Cermakian N, Sassone-Corsi P. 2002. Environmental stimulus perception and control of circadian clocks. Current Opinion in Neurobiology. 12:359-365. DOI

10.1016/S0959-4388(02)00347-1.

Chow S, Okazaki M, Watanabe T, Segawa K, Yamamoto T, Kurogi H, Tanaka H, Ai K, Kawai M, Yamamoto S, Mochioka N, Manabe R, Miyake Y. 2015. Light-sensitive vertical migration of the Japanese eel *Anguilla japonica* revealed by real-time tracking and its utilization for geolocation. PLoS ONE. 10:e0121801. DOI 10.1371/journal.pone.0121801.

Cresci A, De Rosa R, Putman NF, Agnosola C. 2017a. Earth-strength magnetic field affects the rheotactic threshold of zebrafish swimming in shoals. Comparative Biochemistry and Physiology A. 204:169-176. DOI 10.1016/j.cbpa.2016.11.019.

Cresci A, Durif CM, Paris CB, Shema SD, Skiftesvik AB, Browman HI. 2019. Glass eels (*Anguilla anguilla*) imprint the magnetic direction of tidal currents from their juvenile estuaries. Communications Biology. 2:366. DOI 10.1038/s42003-019-0619-8.

Cresci A, Paris CB, Durif DMF, Shema S, Bjelland RM, Skiftesvik AB, Browman HI. 2017b. Glass eels (*Anguilla anguilla*) have a magnetic compass linked to the tidal cycle. Science Advances. 3:e1602007. DOI 10.1126/sciadv.1602007.

Dardente H, Menet JS, Poirel VJ, Streicher D, Gauer F, Vivien-Roels B, Klosen P, Pévet P, Masson-Pévet M. 2003. Melatonin induces Cry1 expression in the pars tuberalis of the rat. Molecular Brain Research. 114:101-106. DOI 10.1016/S0169-328X(03)00134-7.

del Pozo A, Vera LM, Sánchez JA, Sánchez-Vázquez FJ. 2012. Molecular cloning, tissue distribution and daily expression of cry1 and cry2 clock genes in European seabass (*Dicentrarchus labrax*). Comparative Biochemistry and Physiology A. 163:364-371. DOI 10.1016/j.cbpa.2012.07.004.

Falcón J, Migaud H, MuMuñozoz Cueto JA, Carrillo M. 2010. Current knowledge on the melatonin system in teleost fish. General and Comparative Endocrinology. 165:469-482. DOI 10.1016/j.ygcen.2009.04.026.

Foley LE, Gegear RJ, Reppert SM. 2011. Human cryptochrome exhibits light-dependent magnetosensitivity. Nature Communication. 2:356. DOI

10.1038/ncomms1364.

Gegear RJ, Foley LE, Casselman A, Reppert SM. 2010. Animal cryptochromes mediate magnetoreception by an unconventional photochemical mechanism. Nature. 463:804-807. DOI 10.1038/nature08719.

Grabherr MG, Haas BJ, Yassour M, Levin JZ, Thompson DA, Amit I, Adiconis X, Fan L, Raychowdhury R, Zeng Q, Chen Z, Mauceli E, Hacohen N, Gnirke A, Rhind N, Palma FD, Birren BW, Nusbaum C, Lindblad-Toh K, Friedman N, Regev A. 2011. Full-length transcriptome assembly from RNA-Seq data without a reference genome. Nature Biotechnology. 29(7):644-652. DOI 10.1038/nbt.1883.

Hastings M, O'Neill JS, Maywood ES. 2007. Circadian clocks: regulators of endocrine and metabolic rhythms. Journal of Endocrinology. 195:187-198. DOI 10.1677/JOE-07-0378.

Hazlerigg DG, Andersson H, Johnston JD, Lincoln G. 2004. Molecular characterization of the long-day response in the soay sheep, a seasonal mammal. Current Biology. 14:334-339. DOI 10.1016/j.cub.2004.01.057.

Higuchi T, Watanabe S, Manabe R, Tanimoto A, Miller MJ, Kojima T, Tsukamoto K. 2021. Horizontal and vertical migration behavior of silver-phase Japanese eels in coastal, pelagic and spawning areas observed by pop-up satellite archival tags. Journal of Experimental Marine Biology and Ecology. 542-543:151587. DOI 10.1016/j.jembe.2021.151587.

Hiragaki S, Baba K, Coulson E, Kunst S, Spessert R, Tosini G. 2014. Melatonin signaling modulates clock genes expression in the mouse retina. PLoS ONE. 9:e106819. DOI 10.1371/journal.pone.0106819.

Hirayama J, Miyamura N, Uchida Y, Asaoka Y, Honda R, Sawanobori K, Todo T, Yamamoto T, Sassone-Corsi P, Nishina H. 2009. Common light signaling pathways controlling DNA repair and circadian clock entrainment in zebrafish. Cell Cycle. 8:2794-2801. DOI 10.4161/cc.8.17.9447.

Hyeon JY, Byun JH, Kim ES, Heo YS, Fukunaga K, Kim SK, Imamura S, Kim SJ,

Takemura A, Hur SP. 2021. Testis development in the Japanese eel is affected by photic signals through melatonin secresion. PeerJ. 9:e12289. DOI 10.7717/peerj.12289.

Ikeno T, Numata G, Goto SG. 2011. Photoperiodic response requires mammalian-type cryptochrome in the bean bug *Riptortus pedestris*. Biochemical and Biophysical Research Communications. 410:394-397. DOI 10.1016/j.bbrc.2011.05.142.

Kim D, Pertea G, Trapnell C, Pimentel H, Kelley R, Salzberg SL. 2013. TopHat2 accurate alignment of transcriptomes in the presence of insertions, deletions and gene fusions. Genome Biology. 14:R36. DOI 10.1186/gb-2013-14-4-r36.

Kobayashi Y, Ishikawa T, Hirayama J, Daiyasu H, Kanai S, Toh H, Fukuda I, Tsujimura T, Terada N, Kamei Y, Yuba S, Iwai S, Todo T. 2000. Molecular analysis of zebrafish photolyase/cryptochrome family: Two types of cryptochromes present in zebrafish. Genes to Cells. 5:725-738. DOI 10.1046/j.1365-2443.2000.00364.x.

Krylov VV, Osipova EA, Pavlova VV, Datrakova AA. 2016. Influence of magnetic field on the spatial orientation in zebrafish (*Danio rerio*) (Cyprinidae) and Roach (*Rutilus rutilus*) (Cyprinidae). Journal of Ichthyology. 56:456-461. DOI 10.1134/S003294521603007

Langmead B, Salzberg SL. 2012. Fast gapped-read alignment with Bowtie 2. Nature Methods. 9:357-359. DOI 10.1038/nmeth.1923.

Li W, Godzik A. 2006. Cd-hit: a fast program for clustering and comparing large sets of protein or nucleotide sequences. Bioinformatics. 22:1658-1659. DOI 10.1093/bioinformatics/btl158.

Liu C, Hu J, Qu C, Wang L, Huang G, Niu P, Zhong Z, Hong F, Wang G, Postlethwait JH, Wang H. 2015. Molecular evolution and functional divergence of zebrafish (*Danio rerio*) cryptochrome genes. 5:8113. DOI 10.1038/srep08113.

Liedvogel M, Maeda K, Henbest K, Schleicher E, Simon T, Timmel CR, Hore PJ, Mouritsen H. 2007. Chemical magnetoreception: bird cryptochrome 1a is excited by blue light and forms long-lived radical-pairs. PLoS ONE. 2:e1106 DOI

10.1371/journal.pone.0001106.

Lincoln GA, Andersson H, Hazlerigg D. 2003. Clock genes and the long-term regulation of prolactin secretion: evidence for a photoperiod/circannual timer in the pars tuberalis. Journal of Neuroendocrinology. 15:390-397. DOI 10.1046/j.1365-2826.2003.00990.x.

Martín-Robles ÁJ, Whitmore D, Sánchez-Vázquez FJ, Pendón C, Muñoz-Cueto JA. 2012. Cloning, tissue expression pattern and daily rhythms of Period1, Period2, and Clock transcripts in the flatfish Senegalese sole, *Solea senegalensis*. Journal of Comparative Physiology B. 182:673-685. DOI 10.1007/s00360-012-0653-z.

Merlin C, Beaver LE, Taylor OR, Wolfe SA, Reppert SM. 2013. Efficient targeted mutagenesis in the monarch butterfly using zinc-finger nucleases. Genome Research. 23:159-1268. DOI 10.1101/gr.145599.112.

Michael AK, Fribourgh JL, Van Gelder RN, Partch CL. 2017. Animal cryptochromes: divergent roles in light perception, circadian timekeeping and beyond. Photochemistry and Photobiology. 93:128-140. DOI 10.1111/php.12677.

Miyagi T, Aoyama J, Sasai S, Inoue JG, Miller MJ, Tsukamoto K. 2004. Ecological aspects of the downstream migration of introduced European eels in the Uono River, Japan. Environmental Biology of Fishes. 71: 105-114. DOI 10.1023/B:EBFI.0000043178.50750.18.

Nariai N, Kojima K, Mimori T, Sato Y, Kawai Y, Yamaguchi-Kabata Y, Nagasaki M. 2014. TIGAR2: sensitive and accurate estimation of transcript isoform expression with longer RNA-Seq reads. BMC Genomics. 15:S5. DOI 10.1186/1471-2164-15-S10-S5.

Pinzon-Rodriguez A, Bensch S, Muheim R. 2018. Expression patterns of cryptochrome genes in avian retina suggest involvement of Cry4 in light-dependent magnetoreception. Journal of the Royal Society Interface. 15:20180058. DOI 10.1098/rsif.2018.0058.

Pittendrigh C.1972. Circadian surfaces and the diversity of possible roles of circadian organization in photoperiodic induction. Proceedings of the National Academy of

Sciences of the United States of America. 69:2734-2737. DOI 10.1073/pnas.69.9.273.

Pittendrigh C, Minis DH. 1964. The entrainment of circadian oscillations by light and their role as photoperiodic clocks. The University of Chicago Press Journals. 98:902.

Putman NF. 2018. Marine migrations. Current Biology. 28:R972-R976. DOI 10.1016/j.cub.2018.07.036.

Putman NF, Lohmann KJ, Putman EM, Quinn TP, Klimley AP, Noakes DLG. 2013. Evidence for geomagnetic imprinting as a homing mechanism in Pacific salmon. Current Biology. 23: 312-316. DOI 10.1016/j.cub.2012.12.041.

Quinn TP. 1980. Evidence for celestial and magnetic compass orientation in lake migrating sockeye salmon fry. Journal of Comparative Physiology. 137:243-248. DOI 10.1007/BF00657119.

Ritz T, Adem S, Schulten K. 2000. A model for photoreceptor-based magnetoreception in birds. Biophysical Journal. 78:707-718. DOI 10.1016/S0006-3495(00)76629-X.

Schmieder R, Edwards R. 2011. Quality control and preprocessing of metagenomic datasets. Bioinformatics. 27:863-864. DOI 10.1093/bioinformatics/btr026.

Shcherbakov VP, Fabian K. 2005. On the determination of magnetic grain-size distributions of superparamagnetic particle ensembles using the frequency dependence of susceptibility at different temperatures. Geophysical Journal International. 162:736-746. DOI 10.1111/j.1365-246X.2005.02603.x.

Solov'yov IA, Domratcheva T, Schulten K. 2014. Separation of photo-induced radical pair in cryptochrome to a functionally critical distance. Scientific Reports. 4:3845. DOI 10.1038/srep03845.

Song H, Wang D, Perez FDJ, Xie R, Liu Z, Chen CC, Yu M, Yuan L, Fernald RD, Zhao S. 2017. Rhythmic expressed clock regulates the transcription of proliferating cellular nuclear antigen in teleost retina. Experimental Eye Research. 160:21-30. DOI 10.1016/j.exer.2017.04.004.

Stamatakis A. 2014. RAxML version 8: a tool for phylogenetic analysis and post-analysis of large phylogenies. Bioinformatics. 30:1312-1313. DOI 10.1093/bioinformatics/btu033.

Takebe A, Furutani T, Wada T, Koinuma M, Kubo Y, Okano K, Okano T. 2012. Zebrafish respond to the geomagnetic field by bimodal and group-dependent orientation. Scientific Reports. 2:727. DOI 10.1038/srep00727.

Tesch FW. 1978. Telemetric observations on the spawning migration of the eel *Anguilla anguilla* west of the European continental shelf. Environmental Biology of Fishes. 3:203-209. DOI 10.1007/BF00691944.

Tournier BB, Menet JS, Dardente H, Poirel VJ, Malan A, Masson-Pévet M, Pévet P, Vuilleza P. 2003. Photoperiod differentially regulates clock genes' expression in the suprachiasmatic nucleus of Syrian hamster. Neuroscience. 118:317-322. DOI 10.1016/S0306-4522(03)00008-3.

Tsukamoto K. 2006. Oceanic biology: spawning of eels near a seamount, Nature. 439:929 DOI 10.1038/439929a.

Vatine G, Vallone D, Gothilf Y, Foulkes NS. 2011. It's time to swim! Zebrafish and the circadian clock. FEBS Letters. 585:1485-1494. DOI 10.1016/j.febslet.2011.04.007.

Velarde E, Haque R, Iuvone PM, Azpeleta C, Alonso-Gómezmez AL, Delgado MJ. 2009. Circadian Clock genes of goldfish, *Carassius auratus*: cdna cloning and rhythmic expression of period and cryptochrome transcripts in retina, liver, and gut. Journal of Biological Rhythms. 24:104-113. DOI 10.1177/0748730408329901.

Wiltschko W, Wiltschko R. 2005. Magnetic orientation and magnetoreception in birds and other animals. Journal of Comparative Physiology A. 191:675-693. DOI 10.1007/s00359-005-0627-7.

Xu J, Jarocha LE, Zollitsch T, Konowalczyk M, Henbest KB, Richert S, Golesworthy MJ, Schmidt J, Déjean V, Sowood DJC, Bassetto M, Luo J, Walton JR, Fleming J, Wei Y, Pitcher TL, Moise G, Herrmann M, Yin H, Wu H, Bartölke

R, Käsehagen SJ, Horst S, Dautaj G, Murton PDF, Gehrckens AS, Chelliah Y, Takahashi JS, Koch KW, Weber S, Solov'yov IA, Xie C, Mackenzie SR, Timmel CR, Mouritsen H, Hore PJ. 2021. Magnetic sensitivity of cryptochrome 4 from a migratory songbird. Nature. 594:535-540. DOI 10.1038/s41586-021-03618-9.

Yamashina F, Takeuchi Y, Fukunage K, Udagawa S, Tan ES, Byun JH, Yamauchi C, Takemura A. 2019. Daily expression of a clock gene in the brain and pituitary of the Malabar grouper (*Epinephelus malabaricus*). General and Comparative Endocrinology. 280:9-14. DOI 10.1016/j.ygcen.2019.03.019.

Yoshimura T, Suzuki Y, Makino E, Suzuki T, Kuroiwa A, Matsuda Y, Namikawa T, Ebihara S. 2000. Molecular analysis of avian circadian clock genes. Molecular Brain Research. 78:207-215. DOI 10.1016/S0169-328X(00)00091-7.

Zhang Y, Markert MJ, Groves SC, Hardin PE, Merlin C. 2017. Vertebrate-like CRYPTOCHROME 2 from monarch regulates circadian transcription via independent repression of CLOCK and BMAL1 activity. Proceedings of the National Academy of Sciences of the United States of America. 114:E7516-7525. DOI 10.1073/pnas.1702014114.

General Conclusion

The Japanese eel which has a catadromous life cycle was used in this study. Japanese eel has a catadromous life cycle. The spawning period is regulated by the lunar cycle at a site close to the West Mariana Ridge where spawning occurs during the last days of the lunar month. Although the induction of sexual maturation in eels has been adopted, the application of reproduction mechanisms of general saltwater fish to eels suffers from drawbacks. Reproductive control of teleosts is synchronized by photoperiod; however, little is known about the relationship between photic signal and reproduction in eels. Therefore, the purpose of this study is to show the possibility of inducing reproduction in eels by controlling artificial environmental factors. Therefore, in this study, the following three studies were conducted to investigate the mechanism of activating reproductive endocrine in eels, particularly how external light signals are connected to reproductive endocrine.

In chapter Ⅰ, thousands of opsins have been identified and are divided into eight groups. The current data set shows the diversity of opsins in the animal kingdom because the whole genome sequence is determined in many animals. However, there has been a lack of information on the physiological functions other than the molecular structure or biochemical signals in the retina. In particular, the study of ecologically unique species such as Japanese eels is considered as very important in terms of evolution. In this study, 18 types of opsins were identified in the brain and retina of Japanese eels of which 14 types were new opsin genes. Expression of opsins mRNA in the brain and retina was variable; SWS2 expression was high in all areas of the brain of the sexually mature eels, and TMT3 expression significantly increased in hind-brain. These results suggest that SWS-related shortwave region is directly related to the maturation of Japanese eels. However, follow-up studies are required to demonstrate the relevance. Japanese eels have very unique ecological

characteristics, as mentioned above. Unlike other fish species, eco-physiological studies on Japanese eels are necessary to induce artificial maturation through environmental control (light, water temperature etc.), and various studies on the photosensitivity should be continuously carried out.

In chapter Ⅱ, both eye and plasma melatonin levels were regulated by daylight cycling and circadian oscillations, and melatonin was inhibited under natural moonlight exposure in sexually mature Japanese male eels. Thus, photic cues from daylight and nocturnal moonlight may correlate with nocturnal behavioral responses, including testis development and spawning during the NM period.

In chapter Ⅲ, the results presented here indicate that the retina may play an important role in the circadian rhythm of core clock genes in eels. In addition, it was confirmed that the photoperiod change from LD to SD in the retinal clock gene induces oscillations of Per3 and Cry4 in the retina, and the absence of moonlight induces oscillations of Cry4 in the retina. This suggests that seasonal photoperiod changes and the presence or absence of moonlight in the sexual maturation of eels affect the onset of spawning migratory eels after puberty and that the retina, the central oscillator, is related to the oscillation of the clock gene as a reproductive activity signal. This may be helpful for understanding the ecophysiological aspects of sexual maturity and spawning migratory eels.

In summary, daylight, photoperiodic changes, and moonlight controlled the nocturnal behavior of eels, regulation of melatonin secretion, and oscillation of the clock genes. Particularly, when the retina experienced a change from a long to a short photoperiod, melatonin secretion was regulated during the new moon, and the Per3 and Cry4 gene oscillations were regenerated. This may be closely related to the establishment of photoperiod conditions during August-October, the new moon period, when nocturnal eels start spawning migration. These results may provide important

clues to decipher the reproductive mechanism in eels.

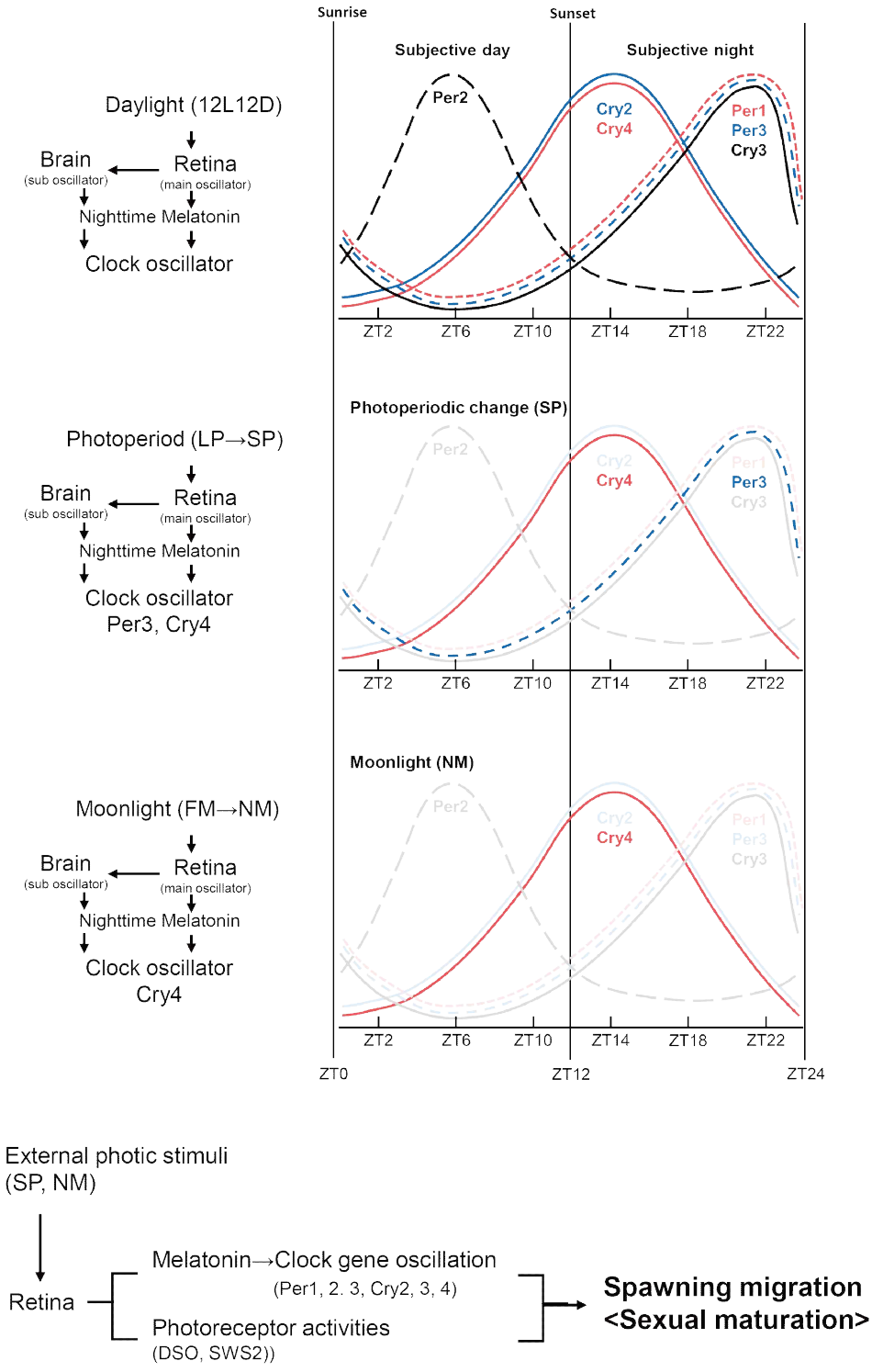

Figure 4.1. Summary in this study. Core clock gene oscillations under different photic stimuli (circadian, photoperiod, moonlight)